MagnoVision™

MG10™

CLINICAL RESULTS

www.**bioretina**.com.tr

General Description of Magnovision MG10:

Magnovision is an electromagnetic / iontophoresis therapy device that creates solutions for retinal and neuroophthalmological disorders. Magnovision acts by sending sinusoidal electromagnetic waves to the nerves in vascular and neurodegenerative retinal/optic nerve diseases. Magnovision device consists of a control unit and a helmet containing 9 coils that generate electromagnetic waves and stimulate the retina, optic nerve and visual pathways. Electromagnetic waves generated by Magnovision cause neuronal depolarization / repolarization and rebalancing in ion channels. The location of the coils on the helmet, the intensity, frequency and duration of the electromagnetic field to be created have been determined as effective and safe by clinical and preclinical studies. Effective and safe parameters cannot be changed by the user or the patient. The device is designed to prevent misuse.

Therapy is initiated after the helmet has been correctly positioned and adjusted on the patient's head under the supervision of a specialist. Magnovision creates a magnetic field of 2000 miligauses with a frequency of 42 Hertz for 30 minutes for each therapy session. These parameters are effective and safe values determined as a result of clinical studies. The magnetic field intensity produced by the device is far below the safety limits recommended by the World Health Organization. The patient completes a therapy session by wearing the helmet in a sitting position for 30 minutes without any effort.

The number of sessions and the frequency of therapy vary according to the disease to be used. The number of sessions and the time between sessions are determined by the relevant specialist according to the clinical condition of the patient and the stage of the disease.

The number of therapy sessions with Magnovision and the time between therapies are summarized below according to clinical research results. However, the physician may change these numbers and frequencies according to the needs of the patient :

- Retinitis Pigmentosa: 24 sessions/One session per week (Follow-up with electroretinography)
- Optic neuropathies 24 sessions/One session per week or 24 sessions / 2 consecutive sessions every day in two weeks (Follow-up with visual evoked potentials)
- Chronic central serous chorioretinopathy : 3 sessions/ every 3 weeks or 10 sessions/ for 10 consecutive days (Follow up with optical coherence tomography – angiography)
- Retinal ischemic diseases: 3 sessions/ every 3 weeks or 10 sessions/ for 10 consecutive days (Follow up with optical coherence tomography – angiography)
- Hereditary retinal dystrophies: 24 sessions/One session per week (Follow-up with electroretinography)
- Glaucoma: 24 sessions/One session per week or 24 sessions / 2 consecutive sessions every day in two weeks (Follow-up with visual evoked potentials, visual field and intraocular pressure)
- Age related macular degeneration: 24 sessions/One session per week (Follow-up with electroretinography, optical coherence tomography – angiography)

⚠ According to the World Health Organization and European Union Standards, the biological safety limit of the electromagnetic field is 3 Tesla (30,000 Gauss). Magnovisio creates a total magnetic field of 2000 milligaus from all coils.

Magnovision MG10 Neuroophthalmologic Therapy device
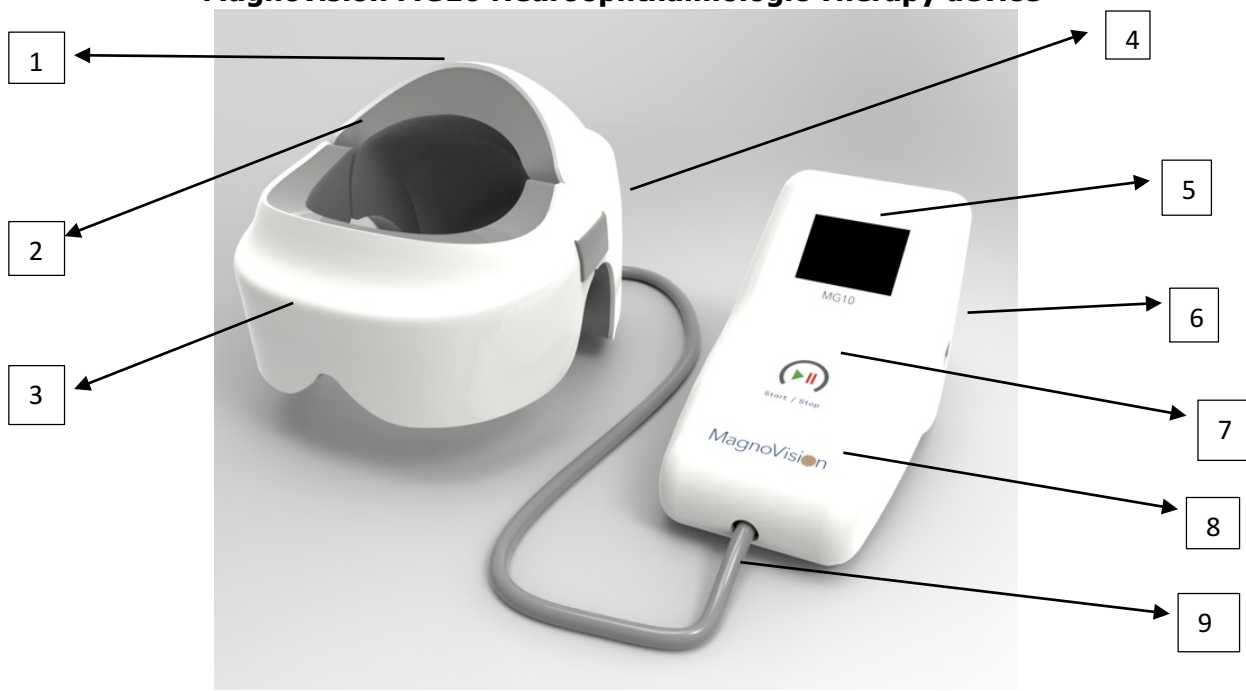
1- The back of the helmet

2- The inner part of the helmet containing 9 coils and covered with sponge and anti-bacterial fabric

3- Front of the helmet

4- Connection and adjustment part of the helmet

5- Control panel screen

6- On / off switch

7- Start / stop button

8- Control panel

9- Helmet and control panel connection cable

Purpose of usage:

Magnovision MG10 electromagnetic stimulation and iontophoresis device is used in the therapy of vascular, ischemic and neurodegenerative diseases of retina and optic nerve.

Indications:

Magnovision has been found to be clinically effective and safe in the following diseases:

- Retinitis Pigmentosa: 24 sessions/One session per week (Follow-up with electroretinography)

- Optic neuropathies 24 sessions/One session per week or 24 sessions / 2 consecutive sessions every day in two weeks (Follow-up with visual evoked potentials)

- Chronic central serous chorioretinopathy : 3 sessions/ every 3 weeks or 10 sessions/ for 10 consecutive days (Follow up with optical coherence tomography – angiography)

- Retinal ischemic diseases: 3 sessions/ every 3 weeks or 10 sessions/ for 10 consecutive days   (Follow up with optical coherence tomography – angiography)

- Hereditary retinal dystrophies: 24 sessions/One session per week (Follow-up with electroretinography)

- Glaucoma: 24 sessions/One session per week or 24 sessions / 2 consecutive sessions every day in two weeks (Follow-up with visual evoked potentials, visual field and intraocular pressure)

- Age releated macular degeneration: 24 sessions/One session per week (Follow-up with electroretinography, optical coherence tomography – angiography)

The number of sessions and the frequency of therapy vary according to the disease to be used. The number of sessions and the time between sessions are determined by the relevant specialist according to the clinical condition of the patient and the stage of the disease.

Other application areas of magnetic stimulation therapy are specified in the general definition section about electromagnetic systems.

It is the responsibility of the physician serving to adapt the treatment method and practices in accordance with the latest developments in medicine within the framework of existing laws and guidelines.

Contraindications:

Contraindications are listed below.

• Magnovision should not be used in the first 3 months of pregnancy (first trimester).

• Magnovision should not be used in epilepsy patients who cannot be controlled with drugs.

• Magnovision should not be used in children under 18 years of age. It can be used in patients under the age of 18 only on the advice of a doctor and under the supervision of a doctor.

• Magnovision should not be used in patients with a cardiac pacemaker.

• Magnovision should not be used in patients with magnetic foreign bodies in the intracranial and orbital areas.

The device is designed for safe and secure use in clinics. It is designed in such a way that the end user can understand it is easy to use, does not allow the operator / doctor to use it incorrectly and does not exceed the safety limits.

What Are the Common Side Effects:

The most common side effect is temporary pain in the area where the treatment is applied. The resulting pain is related to the stimulation of the sensory nerves in the scalp or frequent contraction of the muscles. Mild pain around the eyes has been reported. Pains are short-term and temporary. Changes in color vision perception have been reported. This is again short-term and temporary. No serious side effects that warrant discontinuation of treatment have been encountered.

Lifetime of the Device:

When routine maintenance, calibration and services are carried out due to aging of parts, technical changes and developments, the life of the product is 10 years, after this period it is recommended to renew the product.

Accessories And Spare Parts:

The device does not have any accessories or spare parts.

Device-Related Warnings:

These warnings must be observed in order to use the device correctly.

⚠ It is recommended to use the device at room temperature. ROOM TEMPERATURE SHOULD NOT EXCEED 40 C.

⚠ Only well trained persons can use the device.

⚠ Connect the device to a socket with grounding. If there are fluctuations in the electrical current, use a regulator or uninterruptible power supply.

⚠ The device is designed for clinical use and with patient-specific parameters set; Therefore, it is strictly forbidden to use and use by other people without doctor's permission.

⚠ Do not keep liquid near or near the device while it is in operation.

⚠ Do not use in environments with explosive gas and materials.

⚠ The device should never be used with wet hair.

⚠ Patients with metal or bionic implantation in the head, neck, face and ear region should not use the device before determining the magnetic field compatibility values specified in the implant's user manual.

⚠ The patient with implantation must share this information with the relevant physician.

⚠ The device should not be used near or near electronic devices (mobile phones, hair dryers, televisions, radios, white goods, etc.) that may create magnetic fields.

⚠ Do not use the device while moving or in a vehicle (airplane, car, train, etc.).

⚠ Do not use earphones during therapy.

⚠ During the therapy, there should be no metal-containing parts in the head and neck region that may affect the magnetic field (earrings, necklaces, piercings, glasses, etc.).

⚠ If smoke comes out of the device, unplug the device immediately and contact Bioretina or authorized service immediately.

⚠ Magnetic field scanners may damage the device if the device passes through the control points. The device can go through X-Ray, ultrasound, or infrared scanners.

Magnovision MG10 Specifications

Technical Data of the Device

Electromagnetic Compatibility	EN 60601-1-2
Medical Devices Directive to the human body)	EU 2017/745 Category IIb (Energy sent
Electric Shock Protection	Type BF
Safety Class (according to 60601-1)	II
IP protection degree	IP21
Magnetic Wave	2 gauss
Operating Mode minutes)	Set to single mode (1 session 30
Voltage / Frequency	24 VDC / 2.5A / 60W

Working and Ambient Conditions

Room temperature

    5 ° C - 40 ° C during therapy

Related Humidity

    <80% R.H during therapy.

Atmospheric pressure

86-106 kPa during therapy

Storage and Transport Conditions

Room temperature

During Storage and Transport -20 ° C - 55 ° C

Related Humidity

<80% R.H during Storage and Transport.

Atmospheric pressure

70-106 kPa During Storage and Transport

Max. Capacity

Patient Weight   Not applicable.

ORIGINAL RESEARCH

Management of Deep Retinal Capillary Ischemia by Electromagnetic Stimulation and Platelet-Rich Plasma: Preliminary Clinical Results

Emin Özmert · Umut Arslan

ABSTRACT

Introduction: To investigate the efficacy of retinal electromagnetic stimulation and sub-tenon autologous platelet-rich plasma in the treatment of deep retinal capillary ischemia.

Methods: The study included 28 eyes of 17 patients aged 15–76 years (mean 37.9 years) who had deep retinal capillary ischemia. Patients who had acute-onset paracentral scotoma in the last 1 month were included in the study between January 2018 and January 2019. The diagnosis of deep retinal capillary ischemia was based on clinical history and typical findings of optical coherence tomography angiography. The eyes were divided into three groups: group 1 ($n = 7$ eyes) received electromagnetic stimulation alone; group 2 ($n = 7$ eyes) received electromagnetic stimulation and sub-tenon autologous platelet-rich plasma injection; group 3 had no intervention and served as a control group ($n = 14$ eyes). The patients underwent ten sessions of electromagnetic stimulation in groups 1 and 2. Sub-tenon autologous platelet-rich plasma injection was performed immediately after the first, fifth, and tenth sessions of electromagnetic stimulation in group 2. The deep retinal capillary density and best corrected visual acuity changes were investigated before and after treatment at the first month.

Results: The mean deep retinal capillary density was 52.0% before electromagnetic stimulation and 56.1% after ten sessions of application in group 1; this improvement was statistically significant ($p = 0.01$). In the combined treatment group (group 2), the mean deep retinal capillary density was 46.9% before the treatment and 56.5% after the treatment; this increase was also statistically significant ($p = 0.01$). Statistically significant best corrected visual acuity improvement ($p = 0.01$) could be achieved only in group 2. The combined treatment was significantly superior ($p < 0.01$) to treatment with only electromagnetic stimulation regarding best corrected visual acuity and deep retinal capillary density. In the control group (group 3), there was no statistically significant change ($p = 0.09$) in the mean deep retinal capillary density and best corrected visual acuity.

Conclusion: Treatment of the underlying cause is a priority in the treatment of deep retinal capillary ischemia. However, in the acute period, local ischemia treatment is necessary to prevent permanent retinal damage and

E. Özmert
Department of Ophthalmology, Faculty of Medicine, Ankara University, Ankara, Turkey

U. Arslan (✉)
Ankara University Technopolis, Ankara, Turkey
e-mail: drumutarslan@hotmail.com;
bioretina.net@gmail.com

scotomas. In mild cases, only electromagnetic stimulation, which is non-invasive and easy to use, might have a beneficial effect on deep retinal capillary density. In more severe cases, sub-tenon fresh autologous platelet-rich plasma injection together with electromagnetic stimulation may be more effective in the treatment of local ischemia of the retina in order to augment the response.

INTRODUCTION

Deep retinal capillary ischemia (DRCI) is a recently described entity in patients presenting with an acute-onset paracentral scotoma. Subclinical macular lesions of DRCI were formerly best visualized on near-infrared reflectance imaging. The development of optical coherence tomography angiography (OCTA) has facilitated studies of the retinal capillary structures [1]. The multiplanar superficial capillary plexus is located in the inner plexiform layer (IPL) and contains synapses between bipolar and ganglion cells as well as amacrine cells [2, 3]. The deep capillary plexus (DCP) is located in the outer plexiform layer (OPL), which is thinner than the IPL. The DCP is composed of synapses of photoreceptors, bipolar cells, and horizontal cells [2]. This area is also at the border of the oxygen diffusion from the choroid [4]. It is likely that the oxygen coming from the choroid has been completely consumed by the photoreceptors because of the low partial pressure of oxygen level in the outer nuclear layer (ONL). The DCP supplies both the bipolar cells and the synaptic structure of the OPL and Henle fibers [4].

Deep retinal capillary ischemia is an ischemic event in the middle and deep layers of the retina due to various systemic or local vascular pathologies. It is obvious in the intraretinal hyper-reflective bandlike zone located superior or inferior to the OPL conjointly on a structural cross-sectional B-scan of the spectral domain optical coherence tomography (SD-OCT) examination along with an acute-onset paracentral scotoma and subjective complaints of the patient [5]. Ophthalmologists often face a significant diagnostic challenge because of a lack of noticeable changes in the appearance of the retina.

Deep retinal capillary ischemia has two different appearances on B-scan SD-OCT exams according to the level of the involved DCP. If the hyper-reflective bandlike zone is located on the outer plexiform layer–inner nuclear layer (OPL-INL) junction, then it is termed paracentral acute middle maculopathy (PAMM) or type 1 deep retinal capillary ischemia. If the hyper-reflective band is seen on the OPL–ONL junction, then it is termed type 2 deep retinal capillary ischemia. This might be a new variant of acute macular neuroretinopathy (AMN). These intraretinal hyper-reflective zones are seen as patchy areas of various patterns on en face OCT image, and atrophic areas in the inner and the outer nuclear layer, respectively, are developed in the late stage of the diseases [6–9]. The pathophysiologic features of DCP ischemia are considered to be ischemic hypoxia leading to cell death with swelling of the middle retinal tissues. This may lead to severe vision loss and permanent paracentral scotoma depending on the underlying cause and depth of ischemia [10–17]. It can also be observed by slowing metabolic activity in photoreceptors and neural retina. The metabolic slowdown is defined as a dormant phase in photoreceptors and OFF mode in the neural retina [18–20].

The retinal deep capillary plexus is a single monoplanar capillary plexus located in the OPL. It has the lowest vessel density—this is a significant finding that might be used to evaluate retinal vascular diseases accurately [21]. For this reason, the changes in the percentage of the vessel density in DCP during the follow-up were preferred as an assessment parameter of the treatment modalities used in this prospective clinical study.

Platelets are anucleated cells that contain many types of growth factors including platelet-derived growth factor (PDGF), transforming growth factor beta (TGF-β), vascular endothelial growth factor (VEGF), and epidermal growth factor (EGF) in alpha granules [22–25]. Thus, the supplementation of growth medium with autologous platelet-rich plasma (aPRP) could be desirable for clinical applications and could lead to some functional improvement [26].

High-frequency repetitive electromagnetic stimulation (rEMS) has promising therapeutic potential in ischemic neurological patients. The rationale of rEMS is that it modulates neural excitability and increases neural plasticity; thus, it improves the functional outcome [27–29]. These neuroprotective effects of rEMS are dependent on the increase in the level of brain-derived neurotrophic factor (BDNF), VEGF, and increased tyrosine kinase A, B, and C (TrkA, TrkB, and TrkC) receptor activation [29, 30]. Therefore, high-frequency rEMS might be a promising therapeutic strategy for ischemic retinal disorders such as DRCI [31, 32].

There is no known and proven specific treatment for DRCI to date except for systemic checkups and treatment of the underlying diseases or predisposing factors. The aim of this preliminary clinical study is to investigate the efficacy of high-frequency rEMS alone or in combination with sub-tenon fresh aPRP as a treatment modality in the treatment of DRCI. To the best of our knowledge, this is the first prospective clinical trial on this subject in the ophthalmic literature.

METHODS

Ethics committee approval for the transcranial electromagnetic stimulation study was obtained from the Ankara University Faculty of Medicine Clinical Research Ethics Committee (17-1177-18) as well as and Review Board of the Drug and Medical Device Department within the Turkish Ministry of Health (2018-136). These committees had already approved the aPRP work (12-595-16 and 16-AKD-30). The study was performed in accordance with the tenets of the 1964 Declaration of Helsinki. Written informed consent was obtained from the patients prior to enrollment.

This prospective, open-label preliminary clinical trial was conducted between January 2018 and January 2019 at Ankara University Faculty of Medicine, Department of Ophthalmology. The study included 28 eyes of 17 patients who had either type 1 or type 2 DRCI with some coexisting relevant ocular symptoms. The preliminary diagnosis was based on the clinical history, patients' complaints, and typical appearance of hyper-reflective band on the structural cross-sectional B-scan SD-OCT. All patients enrolled in this study underwent a complete routine ophthalmic examination including best-corrected visual acuity (BCVA) measurement with the ETDRS chart (Topcon CC 100 XP, Japan). The patients were further evaluated with OCTA to confirm the diagnosis of DRCI (RTVue XR "Avanti", Optovue, Fremont, CA, USA), which provides a typical multimodal imaging platform. The vessel densities (in percent) of deep capillary plexus before and after the treatments or in the control group at baseline and last examination were measured with the "AngioAnalytic" feature of the OCTA device. To compare the percentage of the vessel densities precisely during follow-up, the "Link-B Scans" button on the screen was activated so that the exact same segmentation planes of the DCP could be compared. The OCTA device automatically calculated and displayed the vessel density maps as follow-up sequences (Angio Retina multiscan view) and trend analysis.

Subjects

We enrolled patients complaining of blurred vision and/or acute-onset paracentral scotoma during the last month without any visible fundus change along with typical SD-OCT and OCTA findings.

Patients were excluded from the study if one of the following was found:

– The presence of noticeable changes in the fundus examination
– Any optic media opacity that may cause artifacts on OCTA images and interfere with

quantitative measurements of the DCP vessel density

– Complaining of paracentral scotoma lasting more than 1 month (in order to exclude chronic changes in the retinal tissue)

– Presence of atrophic changes in INL or ONL on cross-sectional B-scan SD-OCT

The total number of 28 eyes (17 patients) with DRCI were enrolled into three groups according to the BCVA and treatment approach(s):

Group 1: Comprised patients having fairly good BCVA (92 or better letters, ETDRS) and acute-onset paracentral scotoma(s). Because of non-invasive and easy-to-use features, only rEMS was preferred as the initial step. It was applied to 7 eyes on 10 consecutive days with a specifically designed helmet producing and applying electromagnetic stimulation to the retina without touching the scalp or the eyelids.

Group 2: Comprised patients having decreased BCVA (89 or worse letters, ETDRS) and acute-onset paracentral scotoma(s). In those seriously affected patients, in order to augment the effect of the rEMS, sub-tenon aPRP injection was added. rEMS was applied to 7 eyes on 10 consecutive days. In addition, the eyes were injected with sub-tenon fresh aPRP on days 1, 5, and 10.

Group 3: Comprised patients who refused to receive either rEMS or aPRP therapies with various BCVA and acute-onset paracentral scotoma(s). These eight patients' 14 eyes served as control group, and existing systemic disorder(s) were consulted and treated accordingly.

In all of the three groups, BCVA and vessel density measurements were done at baseline and on the first month. In the treatment groups, at baseline, therapies were given just after the measurements. There was an observation period without any intervention between day 10 and the first month.

Preparation and Injection of Autologous Platelet-Rich Plasma

We used the single-spin protocol for preparing aPRP. About 20 ml of blood was drawn from the patient's antecubital vein and inserted into two 10-ml Vacutainer tubes that contain trisodium citrate (T-LAB PRP Kit, T-Biyoteknoloji, Bursa, Turkey). These tubes were placed in a refrigerated (+ 4 °C) centrifuge (Nüve NF 1200R, Nüve Laboratuar Teknolojileri, Ankara, Turkey) and spun at 2500 rpm ($580 \times g$) for 8 min within 30 min of collection. Three different layers formed in the tubes: red blood cells at the bottom, platelet-rich plasma in the middle, and platelet-poor plasma in the top layer. A total of 1.5 ml of the middle layer (which mainly contained platelets) was withdrawn by syringe and immediately injected into the sub-tenon space of each eye after topical anesthesia with proparacaine hydrochloride (Alcaine, Alcon, USA) drops.

The preparation and injection of the PRP were performed by the same ophthalmologist (UA) under topical anesthesia and sterile conditions. The subjects were asked to look in an inferonasal direction, and the 1.5-ml injection of aPRP was performed under the tenon space in the superotemporal quadrant using a 25-gauge needle. This site was preferred for injection because of its easy access and relatively wide absorption area [26].

Retinal Electromagnetic Stimulation

A high-frequency rEMS protocol has been defined in the literature [31, 32] and was applied in groups 1 and 2 via a novel device developed specifically for ophthalmic usage (Magnovision™, Bioretina Biyoteknoloji AŞ, Ankara,Turkey). The patients underwent ten consecutive sessions of rEMS application. Parameters for the treatment were 42 Hz frequency, 30 min of duration, and mild operating cycle. The power of the electromagnetic field was 2000 mG, which is a very low dose and

Table 1 General characteristics of the groups according to the interventions (n = 28 eyes of 17 patients)

	Intervention	Gender (female/male)	Mean age (years) (range)	Follow-up (months)
Group 1 (n = 7)	rEMS	4/3	34.1 (15–74)	1
Group 2 (n = 7)	rEMS + aPRP	4/3	40.8 (15–76)	1
Group 3 (n = 14)	No ocular treatment[a]	4/4	38.8 (17–75)	1

rEMS repetitive electromagnetic stimulation of the retina, *aPRP* autologous platelet-rich plasma injection into sub-tenon space immediately after first, fifth, and tenth sessions of rEMS application in group 2

[a] There is no local or regional treatment. If any underlying systemic disease was detected, then it was treated accordingly

within the safety limits of World Health Organization [33, 34]. In group 2, sub-tenon aPRP injections were also performed immediately after the first, fifth, and tenth sessions of rEMS application.

Statistical Analysis

The changes in deep retinal capillary density (DRCD) and BCVA before and after the interventions were compared. Statistical analysis was performed using SPSS for Windows (v.22, IBM Corp., Armonk, NY, USA). The results were presented as the mean ± standard deviation. The differences in the vessel density and BCVA in each group were analyzed using the Wilcoxon signed rank test. A Mann–Whitney U test analysis was also performed to determine the vessel density and BCVA changes between the groups. In this study, p values smaller than 0.05 were considered to be statistically significant.

The primary outcome measure of the study is to assess the therapeutic effect of the electromagnetic stimulation alone or combined with sub-tenon aPRP in cases with DRCI via a comparison of the BCVAs and vessel densities of DCPs. The secondary outcome measure is to assess whether a combined application of rEMS and aPRP has a better outcome versus the application of rEMS alone.

RESULTS

Of the 17 patients, 9 were male and 8 were female: their mean age was 37.9 years (range 15–76 years). The mean age was 34.1 (15–74) in group 1, 40.8 (15–76) in group 2, and 38.8 (17–75) in group 3 (Table 1). Gender ratios and age ranges were comparable in the three groups.

DRCDs (%) and BCVAs before and after the treatment modalities were displayed in Table 2 according to demographic characteristics and medical status in group 1 and group 2 (total 14 eyes of 9 patients). The demographic characteristics, medical status, and initial and last values of BCVAs and DRCDs (%) without any ocular treatment in group 3 (control group) are listed in Table 3. The distribution of the 17 patients and 28 eyes according to the applied treatments was as follows:

- 5 patients: received rEMS in one eye, rEMS + aPRP in the other eye (total ten eyes)
- 2 patients: received rEMS in one eye (total two eyes)
- 2 patients: received rEMS + aPRP in one eye (total two eyes)
- 8 patients: 14 eyes served as control group without any ocular treatment

The mean DRCD was 52.0% before rEMS and 56.1% after ten sessions of application in group 1; this improvement was statistically significant (p = 0.01) (Fig. 1). In the combined treatment group (group 2), the mean DRCD was 46.9% before the treatment and 56.5% after the treatment; this increase was also statistically significant (p = 0.01) (Fig. 2). Statistically significant BCVA improvement (p = 0.01) could be achieved only in group 2 (Table 4).

In the control group (group 3), the mean DRCD was 52.7% before the treatment and 50.3% after the treatment; this change was statistically not significant (p = 0.09) (Fig. 3). BCVA changes (p = 0.99) were statistically not significant in group 3 (Table 4).

Table 2 Demographic characteristics and medical status of the treated patients, treatment modalities, and evaluated parameters

Patient no.	Age/gender	Medical status	Eye (*n* = 14)	Treatment	DRCD		BCVA	
					Before	After	Before	After
1	21 F	Pernicious anemia	R	PRP + rEMS	51.0	61.0	65	105
			L	rEMS	48.6	52.3	65	100
2	40 M	Renal hypertension	R	rEMS	55.0	58.4	95	100
3	15 F	Atrial septal defect	R	rEMS	53.3	55.5	65	95
			L	PRP + rEMS	45.0	55.6	50	95
4	33 M	Thoracic trauma	R	rEMS	53.8	58.2	105	105
			L	PRP + rEMS	51.1	59.6	100	105
5	20 F	Oral contraceptive	R	PRP + rEMS	52.1	61.6	100	105
			L	rEMS	53.9	61.1	105	105
6	74 F	Cardiac arrhythmia	R	rEMS	42.2	44.8	95	95
			L	PRP + rEMS	42.8	49.2	89	95
7	36 M	Head trauma	R	rEMS	57.2	62.3	105	105
8	47 M	Retinal detachment surgery	L	PRP + rEMS	39.7	52.3	50	70
9	76 M	Retinal detachment surgery	R	PRP + rEMS	46.9	55.9	50	65

Follow-up 1 month. Treatment group composed of groups 1 and 2, 14 eyes of 9 patients
DRCD deep retinal capillary density (%), *BCVA* best corrected visual acuity (ETDRS letters)

The combined treatment with rEMS and aPRP was significantly superior ($p < 0.01$) to treatment with only rEMS regarding BCVAs and DRCDs improvements.

There were no adverse events or complaints related to application of either electromagnetic stimulation or aPRP.

DISCUSSION

Deep retinal capillary ischemia can occur concomitantly with vascular occlusive events including cardiac arrhythmia, embolus, thrombus, inflammatory or traumatic vessel wall damage, and vasospasm [8–13]. Additional possible associations have been described such as dengue fever, anemia, ulcerative colitis, thrombocytopenia, lupus, and leukemia [14–17]. Deep retinal capillary ischemia may be acute or acute exacerbations of a chronic process such as severe anemia, chronic hypertension, arteriovenous malformations, vitamin B_{12}, or vitamin D deficiency [9]. In both acute and acute exacerbations of chronic conditions, the patient describes a sudden onset of paracentral scotoma and a deterioration in visual quality. This can lead to infarcts in the neural or sensory retina [6]. In some cases, visual acuity measurements may be complete, but the patient can complain of visual disturbances with a normal appearing fundus. Therefore, correct and early diagnosis might be challenging in many cases. In these suspected cases, careful B-scan SD-OCT assessment is necessary to see if there is a hyper-reflective bandlike zone above or below the OPL. We can detect the pathognomonic findings in the deep capillary plexus slab of the OCTA.

In retinal large vessel obstruction, capillary reperfusion may never occur, causing severe acute impairment of flow within the DCP. But

Table 3 Demographic characteristics and medical status of the control group (group 3) and evaluated parameters (composed of 14 eyes from 8 patients)

Patient no.	Age/gender	Medical status	Eye (n = 14)	DRCD		BCVA	
				Initial	Last	Initial	Last
1	17 F	Talassemia minor	R	49.1	47.3	80	80
			L	48.2	47.6	80	80
2	39 M	Cardiac arrhythmia	R	48.6	47.3	105	105
			L	47.8	46.8	105	105
3	21 F	Oral contraceptive	R	56.1	47.9	74	74
			L	55.3	49.8	74	74
4	75 F	Hypertensive attack	R	50.6	43.1	100	100
			L	51.8	49.0	100	100
5	42 M	Uncontrolled hypertension	R	57.9	57.6	105	105
			L	57.9	57.6	105	105
6	37 M	Head trauma	L	59.8	58.7	105	105
7	71 M	Uncontrolled hypertension	R	47.9	47.6	105	105
8	24 F	Oral contraceptive	R	52.8	51.4	105	105
			L	53.7	52.6	105	105

Follow-up 1 month. Control group did not receive any local/regional therapy, only systemic disorder was treated
DRCD deep retinal capillary density (%), *BCVA* best corrected visual acuity (ETDRS letters)

in cases with DRCI, the pathogenesis may be related to ischemia–reperfusion injury. Ischemia disappears with persistent capillary flow in some focal acute lesions, and reperfusion occurs together with low grade inflammation damaging the retina. With time, hyper-reflective band-dlike zone disappears, and subsequent atrophy of middle retinal layers associated with permanent loss of the DCP is seen [13, 35].

When nutritional and microenvironmental balance is disrupted, retinal neurons and photoreceptors develop a condition called dormant phase or OFF mode. At this stage, the cells are viable but dysfunctional. If local ischemia and unstable microenvironment persist for a long time, oncosis occurs. Oncosis is the swelling and permanent death of cells by taking up fluid. Regulation of the local ischemia and inflammatory cytokines before the development of oncosis allows the cells in dormant phase (sleep mode) to switch to the active phase (ON mode) [18–20].

In the case of DRCI, the underlying systemic risk factors should be investigated and treated urgently to prevent the development of permanent scotomas and vital systemic events. There is no proven treatment for DRCI yet except for treating and/or controlling the underlying systemic cause(s). We hypothesized that in mild cases with rEMS, in more severe cases with combined therapy (in order to augment the therapeutic effect of the rEMS, the aPRP therapy was added), it might be possible to increase the capillary flow and suppress and regulate the associated inflamation. Indeed, our favorable findings in terms of DRCD and BCVA supported our hypothesis significantly.

The preclinical and clinical use of aPRP in ophthalmology has encouraged practitioners to use it through sub-tenon injection in the treatment of some retinal diseases [26]. Platelets are
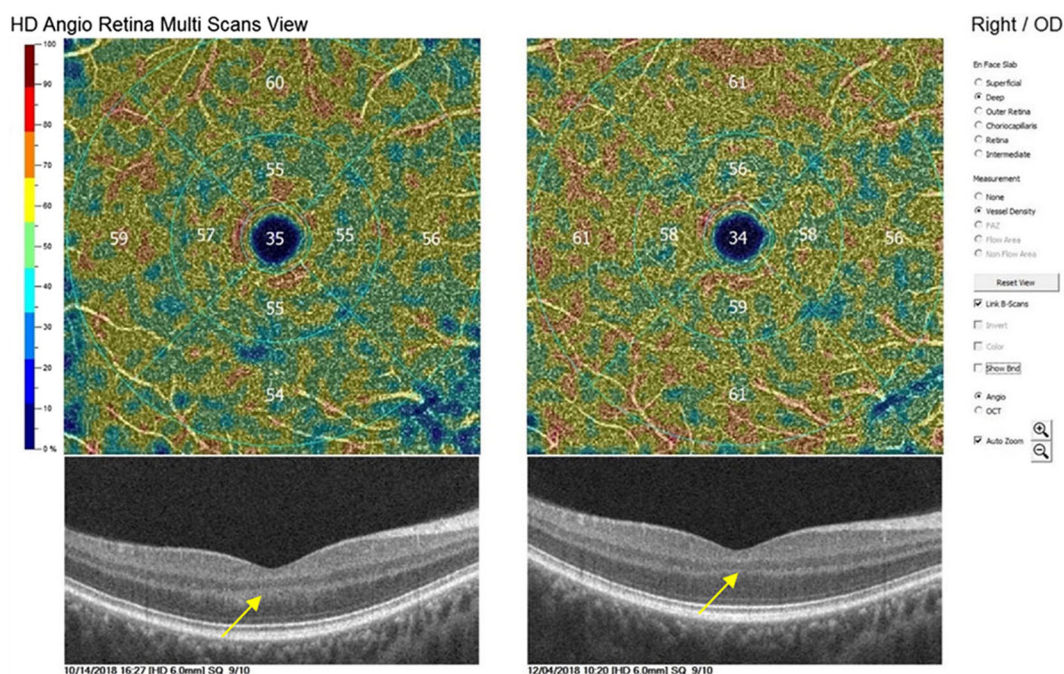
Fig. 1 DRCD and BCVA changes before and after only Magnovision therapy. Hyper-reflective band in ONL connected with OPL disappeared after the therapy without any atrophy (arrows) (Table 2—Patient 2, DRCD 55% to 58.4%/BCVA 95 to 100 ETDRS letters)

part of the blood and contain more than 5000 proteins. About 300 of the contained proteins—especially growth factors and cytokines—are released upon activation [23–25]. Through the sub-tenon injection of aPRP, the release of cytokines, chemokines, and growth factors induces proliferation and activation of reparative cells [23–26]. The level of neurotrophic growth factors may be increased in the microenvironment around the photoreceptors to potentially reactivate photoreceptors that are in sleep mode [26].

It is known that growth factors can pass through the sclera via activation of tyrosine kinase (Trk) receptors, which are commonly found around the limbus, uveoscleral tract, muscle insertions, and optic nerve [36–39]. Molecules smaller than 75 kDa can pass passively through the sclera to the subretinal space. Larger proteins can pass through the sclera by changing the electrical charges by means of the electrical/electromagnetic iontophoresis. These various molecules in the subretinal space activate the cells in the dormant phase [40–44].

The effects of rEMS on local ischemia include increased tissue perfusion, synthesis of growth factors, and enhanced Trk receptor activities [27–32]. The synthesis and affinity of Trk receptors also increase with EMS [29]. Repetitive magnetic stimulation has been used in neurological studies for more than 30 years and magnetotherapy for eye diseases for more than 20 years. The two main effects of this treatment modality make it efficient in the treatment of these disease. The first effect is that it increases the capillary blood flow in the neural tissues. The second effect is that it increases the affinity and activity of growth factor-tyrosine kinase receptors; and it accelerates the effect of growth factors responsible for tissue reparation [31, 32, 45–49]. Electromagnetic stimulation alone or together with aPRP applications might be used in cases with DRCI similar to the treatment of ischemic neurologic conditions [29, 30]. Here, we used the Magnovision™ for electromagnetic stimulation of the retina, optic nerve, and visual pathways similar to the ischemic neurologic diseases. This is a novel device designed specifically for ophthalmic
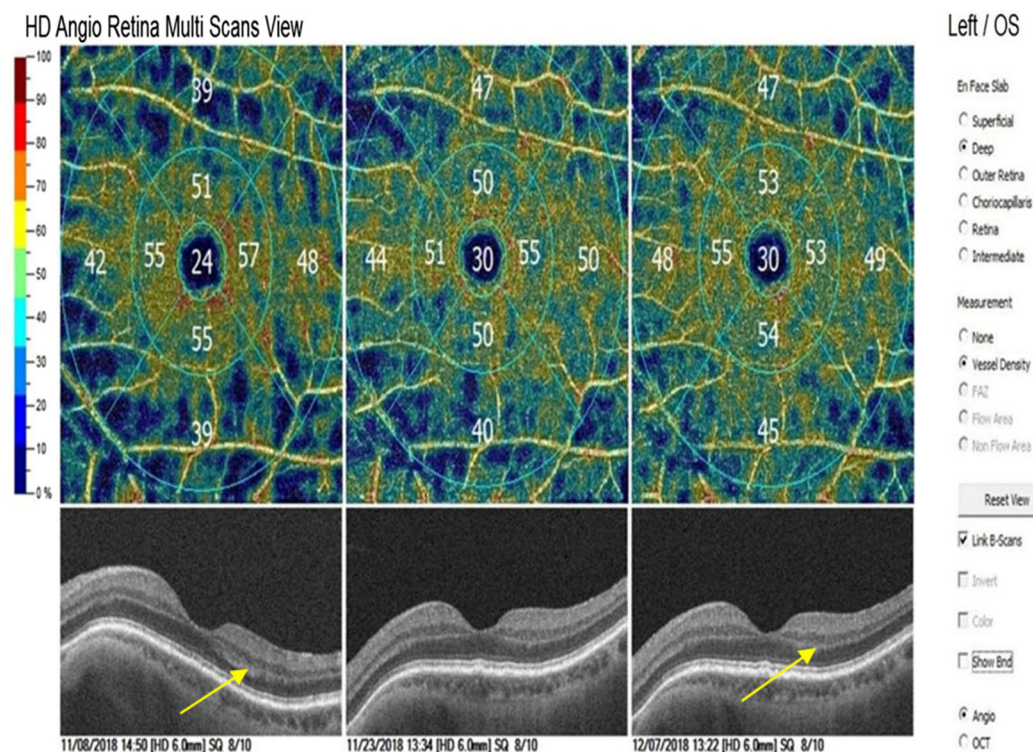
Fig. 2 DRCD and BCVA changes before and after combined sub-tenon PRP + Magnovision therapy. Hyperr-eflective band in OPL disappeared after the therapy without any atrophy (arrows) (Table 2—Patient 6, DRCD 42.8% to 49.2%/BCVA 89 to 95 ETDRS letters)

Table 4 Deep retinal capillary density and best corrected visual acuity changes in three groups ($n = 28$ eyes of 17 patients)

Group	DRCD		p	BCVA		p
	Initial	Last		Initial	Last	
1 rEMS alone ($n = 7$)	52.0 ± 5.5	**56.1 ± 6.0**	**0.01***	90.7 ± 4.13	100.7 ± 4.5	0.14
2 rEMS + aPRP ($n = 7$)	46.9 ± 4.7	**56.5 ± 4.6**	**0.01***	72.0 ± 13.6	**93.6 ± 13.4**	**0.01***
3 Control ($n = 14$)	52.7 ± 4.2	50.3 ± 4.7	0.09	96.3 ± 12.9	96.3 ± 12.9	0.99

Follow-up 1 month. Control group did not receive any local/regional therapy; only systemic disorder was treated
DRCD deep retinal capillary density (%), *BCVA* best corrected visual acuity (ETDRS letters), *rEMS* repetitive electromagnetic stimulation, *aPRP* autologous platelet-rich plasma
*Statistically significant changes displayed as bold

applications. It is a safe, non-invasive, and easy-to-use treatment without any adverse effects. The coils that yield electromagnetic fields are mounted in the helmet without any points touching the head skin or face. The electromagnetic field at the tissue level is significantly below the safety limit specified by the World Health Organization [33, 34].

Deep retinal capillary density has become a reliable and important follow-up parameter with improved image resolution, software, and artifact-removal programs in OCTA devices. We preferred to use the DRCD percentage together with visual acuity measurement with ETDRS logMAR chart for the assessment of the treatment efficacy over control groups in this trial.
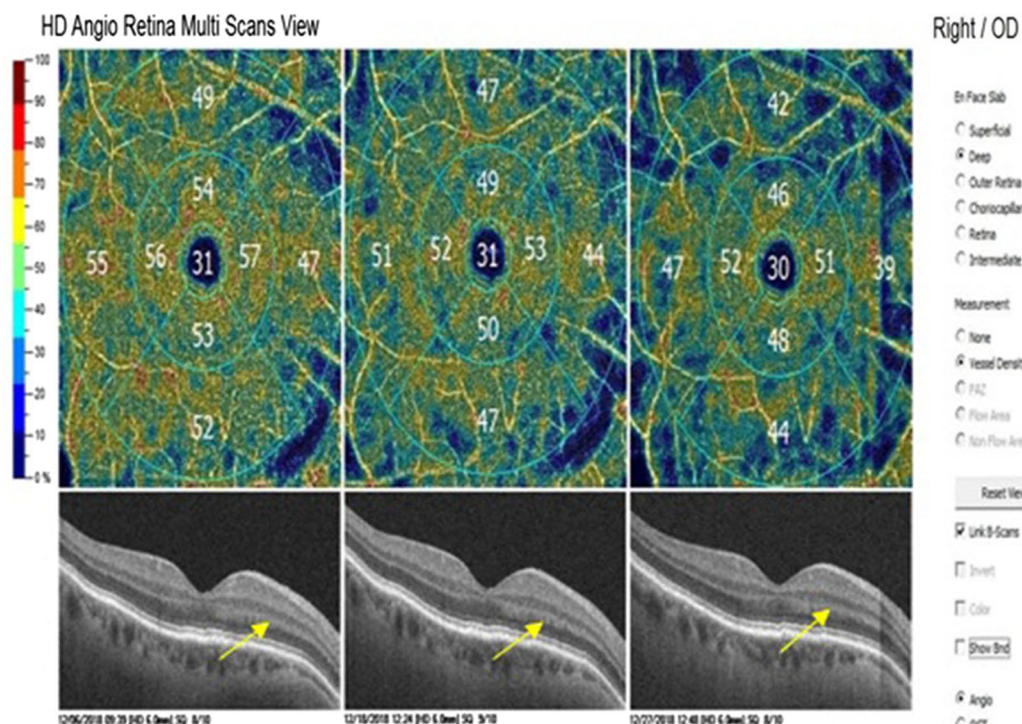
Fig. 3 Patient did not receive any ocular therapy, and only a systemic disorder was treated. Hyper-reflective bandlike zone persisted during the follow-up (arrows). There was no any improvement in DRCD and BCVA (Table 3—Patient 4, DRCD 50.6% to 43.1%/BCVA 100 to 100 ETDRS letters)

Because these are the most reliable and sensitive methods for comparing follow-up parameters [21, 50].

Here, BCVA could be significantly increased with combined therapy of rEMS and aPRP in group 2 versus only application of rEMS in group 1. The PDGFβ/PDGFRβ pathway is critically important for the expansion of the pericyte migration along growing vessels, and various signaling pathways are also involved in angiogenesis [23–25]. In our study, the percentage of DRCDs increased significantly after the treatment modalities in groups 1 and 2. After stimulating these pathways and increasing the various growth factors in the microenvironment by just rEMS or combined with aPRP. However, significant improvement in BCVA could be achieved only with combined treatment (rEMS + aPRP). Regarding the efficacy of the treatment modalities (only rEMS versus rEMS + aPRP) on the BCVA and vessel density of DCP, the combined treatment approach was significantly superior to treatment with only rEMS. There was no significant improvement in DRCD and BCVA in patients who had no intervention. In this group, only the systemic treatments for the underlying cause were initiated by the relevant experts. During this study, we did not encounter any adverse effects, patient complaint, or discomfort with noise or heating.

This prospective preliminary clinical trial has several limitations. The control group of the study comprised the patients with various BCVA who refused to receive either rEMS or aPRP therapies. Since DRCI is a recently described entity, it was difficult to establish a more homogenous control group. We did not differentiate between type 1 and type 2 deep retinal capillary ischemia; both types were included. The follow-up period was 1 month; therefore, other studies are needed to investigate the long-term results and establish the optimal treatment protocol. In cases with cataract and/or other

optic media opacities, the measurement of the vessel density in DCP might be affected leading to an inaccurate result. We did not study the visual field involvement and its changes with the treatment modalities because it was not possible to show the visual field changes for comparison in every case. We could not evaluate the different treatment parameters of the new Magnovision device; these are subject to another trial.

CONCLUSION

Improved diagnosis of deep retinal capillary plexus ischemia can be achieved by considering the presence of acute-onset visual symptoms without visible fundus changes as well as hyper-reflective bands around the OPL. With systemic checkup, it is possible to detect the serious systemic diseases that may cause vital events. In mild cases, only rEMS (which is non-invasive and easy-to-use) might have beneficial effects on deep retinal capillary density. In more severe cases, sub-tenon fresh aPRP injection together with rEMS may be more effective in the treatment of local ischemia of the retina in order to augment the response and prevent permanent retinal damage and scotomas.

ACKNOWLEDGEMENTS

We thank the participants of the study.

Authorship. All named authors meet the International Committee of Medical Journal Editors (ICMJE) criteria for authorship for this article, take responsibility for the integrity of the work as a whole, and have given their approval for this version to be published.

Medical Writing Assistance. Medical writing and editorial assistance was provided by Ali Hariri from the American Manuscript Editors Company, which was funded by the authors.

Compliance with Ethics Guidelines. Ethics committee approval for the transcranial electromagnetic stimulation study was obtained from the Ankara University Faculty of Medicine Clinical Research Ethics Committee (17-1177-18) as well as and Review Board of the Drug and Medical Device Department within the Turkish Ministry of Health (2018-136). These committees had already approved the aPRP work (12-595-16 and 16-AKD-30). The study was performed in accordance with the tenets of the 1964 Declaration of Helsinki. Written informed consent was obtained from the patients prior to enrollment.

Disclosures. Emin Özmert and Umut Arslan have nothing to declare.

Data Availability. The datasets generated during and/or analysed during the study are available from the corresponding author on reasonable request.

REFERENCES

1. Campbell JP, Zhang M, Hwang TS, et al. Detailed vascular anatomy of the human retina by projection-resolved optical coherence tomography angiography. Scientific Rep. 2017. https://doi.org/10.1038/srep42201.

2. Tan PEZ, Yu PK, Balaratnasingam C, et al. Quantitative confocal imaging of the retinal microvasculature in the human retina. Investig Opthalmol Vis Sci. 2012;53(9):5728. https://doi.org/10.1167/iovs.12-10017.

3. Park JJ, Soetikno BT, Fawzi AA. Characterization of the middle capillary plexus using optical coherence tomography angiography in healthy and diabetic eyes. Retina. 2016;36:2039–50.

4. Linsenmeier RA, Zhang HF. Retinal oxygen: from animals to humans. Prog Retin Eye Res. 2017;58:115–51.

5. Rahimy E, Sarraf D. Paracentral acute middle maculopathy: spectral domain optical coherence tomography feature of deep capillary ischemia. Curr Opin Ophthalmol. 2014;25:207.

6. Sarraf D, Rahimy E, Fawzi AA, et al. Paracentral acute middle maculopathy. JAMA Ophthalmol. 2013;131(10):1275. https://doi.org/10.1001/jamaophthalmol.2013.4056.

7. Niyousha MR, Hassanpoor N, Eftekhari A, Mousvi F. Simultaneous paracentral acute middle maculopathy and Purtscher-like retinopathy after acute febrile illness. Can J Ophthalmol. 2018;53(5):e184–6. https://doi.org/10.1016/j.jcjo.2017.11.020.

8. Nemiroff J, Phasukkijwatana N, Sarraf D. Optical coherence tomography angiography of deep capillary ischemia. Dev Ophthalmol. 2016;56:139–45.

9. Kulikov AN, Maltsev DS, Leongardt TA. Retinal microvasculature alteration in paracentral acute middle maculopathy and acute macular neuroretinopathy. Retin Cases Br Rep. 2018. https://doi.org/10.1097/icb.0000000000000709.

10. Nakashima H, Iwama Y, Tanioka K, Emi K. Paracentral acute middle maculopathy following vitrectomy for proliferative diabetic retinopathy. Ophthalmology. 2018. https://doi.org/10.1016/j.ophtha.2018.07.006.

11. McLeod D. En face optical coherence tomography analysis to assess the spectrum of perivenular ischemia and paracentral acute middle maculopathy in retinal vein occlusion. Am J Ophthalmol. 2017;182:203–4.

12. Rahimy E, Kuehlewein L, Sadda SR, Sarraf D. Paracentral acute middle maculopathy. Retina. 2015;35:1921–30.

13. Nemiroff J, Kuehlewein L, Rahimy E, et al. Assessing deep retinal capillary ischemia in paracentral acute middle maculopathy by optical coherence tomography angiography. Am J Ophthalmol. 2016;162:121–32.

14. Bhavsar KV, Lin S, Rahimy E, et al. Acute macular neuroretinopathy: a comprehensive review of the literature. Surv Ophthalmol. 2016;61(5):538–65. https://doi.org/10.1016/j.survophthal.2016.03.003.

15. Introini U, Casalino G, Querques G, Bagini M, Bandello F. Acute macular neuroretinopathy following intranasal use of cocaine. Acta Ophthalmol. 2015;93(3):e239–40.

16. Munk MR, Jampol LM, Cunha Souza E, et al. New associations of classic acute macular neuroretinopathy. Br J Ophthalmol. 2015;100(3):389–94. https://doi.org/10.1136/bjophthalmol-2015-306845.

17. Li M, Zhang X, Ji Y, Ye B, Wen F. Acute macular neuroretinopathy in dengue fever: short-term prospectively followed up case series. JAMA Ophthalmol. 2015;133(11):1329–33.

18. Koenekoop RK. Why some photoreceptors die while others remain dormant: lessons from RPE65 and LRAT associated retinal dystrophies. Ophthalmic Genet. 2011;32(2):126–8.

19. Wang W, Lee SJ, Scott PA, et al. Two-step reactivation of dormant cones in retinitis pigmentosa. Cell Rep. 2016;15(2):372–85.

20. Sabharwala J, Seilheimera RL, Taoc X, Cowanc CS, Frankfortb BJ, Wub SM. Elevated IOP alters the space/time profiles in the center and surround of both ON and OFF RGCs in mouse. PNAS. 2017;114(33):8859–64.

21. Lavia C, Bonnin S, Maule M, Erginay A, Tadayoni R, Gaudric A. Vessel density of superficial, intermediate, and deep capillary plexuses using optical coherence tomography angiography. Retina. 2019;39(2):247–58. https://doi.org/10.1097/iae.000000000000241.

22. Notodihardjo SC, Morimoto N, Kakudo N, et al. Comparison of the efficacy of cryopreserved human platelet lysate and refrigerated lyophilized human platelet lysate for wound healing. Regen Ther. 2019;10:1–9. https://doi.org/10.1016/j.reth.2018.10.003.

23. Zahn J, Loibl M, Sprecher C, et al. Platelet-rich plasma as an autologous and proangiogenic cell delivery system. Mediat Inflamm. 2017;2017:1–14. https://doi.org/10.1155/2017/1075975.

24. Armulik A. Endothelial/pericyte interactions. Circ Res. 2005;97(6):512–23. https://doi.org/10.1161/01.res.0000182903.16652.d7.

25. Benjamin LE, Hemo I, Keshet E. A plasticity window for blood vessel remodelling is defined by pericyte coverage of the preformed endothelial network and is regulated by PDGF-B and VEGF. Development. 1998;125:1591–8.

26. Arslan U, Özmert E, Demirel S, Örnek F, Şermet F. Effects of subtenon-injected autologous platelet-rich plasma on visual functions in eyes with retinitis pigmentosa: preliminary clinical results. Graefes Arch Clin Exp Ophthalmol. 2018;256(5):893–908. https://doi.org/10.1007/s00417-018-3953-5.

27. Klomjai W, Katz R, Lackmy-Vallée A. Basic principles of transcranial magnetic stimulation (TMS) and

repetitive TMS (rTMS). Ann Phys Rehabil Med. 2015;58(4):208–13. https://doi.org/10.1016/j.rehab.2015.05.005.

28. Zhang N, Xing M, Wang Y, Tao H, Cheng Y. Repetitive transcranial magnetic stimulation enhances spatial learning and synaptic plasticity via the VEGF and BDNF–NMDAR pathways in a rat model of vascular dementia. Neuroscience. 2015;311:284–91. https://doi.org/10.1016/j.neuroscience.2015.10.038.

29. Luo J, Zheng H, Zhang L, et al. High-frequency repetitive transcranial magnetic stimulation (rTMS) improves functional recovery by enhancing neurogenesis and activating BDNF/TrkB signaling in ischemic rats. Int J Mol Sci. 2017;18(2):455. https://doi.org/10.3390/ijms18020455.

30. Wang F, Zhang C, Hou S, Geng X. Synergistic effects of mesenchymal stem cell transplantation and repetitive transcranial magnetic stimulation on promoting autophagy and synaptic plasticity in vascular dementia. J Gerontol Ser A. 2018. https://doi.org/10.1093/gerona/gly221.

31. Webster K, Ro T. Retinal and visual cortex distance from transcranial magnetic stimulation of the vertex affects phosphene perception. Exp Brain Res. 2017;235(9):2857–66. https://doi.org/10.1007/s00221-017-5022-4.

32. Nikolaeva NV, Bolotova NV, Kamenskikh TG, Raĭgorodskiĭ IuM, Kolbenev IO, Luk'ianov VF. Transcranial magnetotherapy for the correction of initial manifestations of diabetic retinopathy in children. Vopr Kurortol Fizioter Lech Fiz Kult. 2009;3:25–8.

33. Chandra T, Chavhan GB, Sze RW, et al. Practical considerations for establishing and maintaining a magnetic resonance imaging safety program in a pediatric practice. Pediatr Radiol. 2019;49(4):458–68. https://doi.org/10.1007/s00247-019-04359-8.

34. Heintz PH, Sandoval DJ, Chambers GD, Adolphi NL. Biological effects of magnetic resonance imaging. In: Kelsey CA, Heintz PH, Sandoval MS, et al., editors. Radiation biology of medical imaging. Hoboken: Wiley; 2018. p. 281–95.

35. Sridhar J, Shahlaee A, Rahimy E, et al. Optical coherence tomography angiography and en face optical coherence tomography features of paracentral acute middle maculopathy. Am J Ophthalmol. 2015;160(6):1259–1268.e2. https://doi.org/10.1016/j.ajo.2015.09.016.

36. Colafrancesco V, Coassin M, Rossi S, Aloe L. Effect of eye NGF administration on two animal models of retinal ganglion cells degeneration. Ann 1st Super Sanita. 2011;47:284–9.

37. Lambiase A, Aloe L, Centofanti M, et al. Experimental and clinical evidence of neuroprotection by nerve growth factor eye drops: implications for glaucoma. Proc Natl Acad Sci USA. 2009;106:13469–74.

38. Lambiase A, Mantelli F, Sacchetti M, Rossi S, Aloe L, Bonini S. Clinical applications of NGF in ocular diseases. Arch Ital Biol. 2011;149:283–92.

39. Mysona BA, Zhao J, Bollinger KE. Role of BDNF/TrkB pathway in the visual system: therapeutic implications for glaucoma. Expert Rev Ophthalmol. 2017;12(1):69–81.

40. Giannos SA, Kraft ER, Zhao ZY, Merkley KH, Cai J. Photokinetic drug delivery: near infrared (NIR) induced permeation enhancement of bevacizumab, ranibizumab and aflibercept through human sclera. Pharm Res. 2018;35(6):1. https://doi.org/10.1007/s11095-018-2392-7.

41. Demetriades AM, Deering T, Liu H, et al. Transscleral delivery of antiangiogenic proteins. J Ocul Pharmacol Ther. 2008;24(1):70–9. https://doi.org/10.1089/jop.2007.0061.

42. Meng T, Kulkarni V, Simmers R, Brar V, Xu Q. Therapeutic implications of nanomedicine for ocular drug delivery. Drug Discov Today. 2019. https://doi.org/10.1016/j.drudis.2019.05.00.

43. Li SK, Hao J. Transscleral passive and iontophoretic transport: theory and analysis. Expert Opin Drug Deliv. 2017;15(3):283–99. https://doi.org/10.1080/17425247.2018.1406918.

44. Joseph RR, Tan DWN, Ramon MRM, et al. Characterization of liposomal carriers for the trans-scleral transport of ranibizumab. Scientific Rep. 2017;7(1):1. https://doi.org/10.1038/s41598-017-16791-7.

45. Marg E. Magnetostimulation of vision: direct non-invasive stimulation of the retina and the visual brain. Optom Vis Sci. 1991;68(6):427–40.

46. Bagattini C, Mazzi C, Savazzi S. Waves of awareness for occipital and parietal phosphenes perception. Neuropsychologia. 2015;70:114–25. https://doi.org/10.1016/j.neuropsychologia.2015.02.

47. Kammer T, Beck S. Phosphene thresholds evoked by transcranial magnetic stimulation are insensitive to short-lasting variations in ambient light. Exp Brain Res. 2002;145(3):407–10. https://doi.org/10.1007/s00221-002-1160-3.

48. Marzi CA, Mancini F, Savazzi S. Interhemispheric transfer of phosphenes generated by occipital versus parietal transcranial magnetic stimulation. Exp Brain Res. 2008;192(3):431–41. https://doi.org/10.1007/s00221-008-1496-4.

49. Drakon AK, Elfimov MA, Illarionov VE, Ivanova II, Portnov VV. Contemporary potential of nonmedical treatment in ophthalmology. Med Tr Prom Ekol. 2016;2:6–11.

50. Lim LA, Frost NA, Powell RJ, Hewson P. Comparison of the ETDRS logMAR, "compact reduced logMAR" and Snellen charts in routine clinical practice. Eye (Lond). 2010;24(4):673–7.

Management of Retinitis Pigmentosa via Platelet-Rich Plasma or Combination with Electromagnetic Stimulation: Retrospective Analysis of 1-Year Results

Umut Arslan · Emin Özmert

ABSTRACT

Purpose: To investigate whether the natural progression rate of retinitis pigmentosa can be decreased by subtenon autologous platelet-rich plasma application alone or combination with retinal electromagnetic stimulation.

Methods: The study includes retrospective analysis of 60 patients with retinitis pigmentosa. Patients constitute three groups with similar demographic characteristics: the combined management group (group 1) consists of 20 patients with retinitis pigmentosa (40 eyes) who received combined retinal electromagnetic stimulation and subtenon platelet-rich plasma; the subtenon platelet-rich plasma-only group (group 2) consisted of 20 patients with retinitis pigmentosa (40 eyes); the natural course (control) group (group 3) consists of 20 patients with retinitis pigmentosa (40 eyes) who did not receive any treatment. Horizontal and vertical ellipsoid zone width, fundus perimetry deviation index, and best corrected visual acuity changes were compared within and between groups after a 1-year follow-up period.

Results: Detected horizontal ellipsoid zone percentage changes were $+ 1\%$ in group 1, $- 2.85\%$ in group 2, and $- 9.36\%$ in group 3 (Δp $1 > 2 > 3$). Detected vertical ellipsoid zone percentage changes were $+ 0.34\%$ in group 1, $- 3.05\%$ in group 2, and $- 9.09\%$ in group 3 (Δp $1 > 2 > 3$). Detected fundus perimetry deviation index percentage changes were $+ 0.05\%$ in group 1, $- 2.68\%$ in group 2, and $- 8.78\%$ in group 3 (Δp $1 > 2 > 3$).

Conclusion: Platelet-rich plasma is a good source of growth factors, but its half-life is 4–6 months. Subtenon autologous platelet-rich plasma might more effectively slow down photoreceptor loss when repeated as booster injections and combined with retinal electromagnetic stimulation.

Trial Registration: ClinicalTrials.gov identifier, NCT04252534.

U. Arslan (✉)
Ankara University Technopolis, Ankara, Turkey
e-mail: drumutarslan@hotmail.com;
bioretina.net@gmail.com

E. Özmert
Department of Ophthalmology, Faculty of Medicine, Ankara University, Ankara, Turkey

△ Adis

Key Summary Points

Why carry out this study?

To investigate whether the natural progression rate of retinitis pigmentosa can be decreased by subtenon autologous platelet-rich plasma application alone or combination with retinal electromagnetic stimulation.

The retina pigment epithelium is the unit center where the synthesized peptide growth factors (GFs) regulate photochemical reactions.

The growth factors, peptides, and fragments required for these functions are encoded by over 260 genes in retinal pigment epithelium (RPE). Mutations in any of these genes leads to progressive vision loss and progressive degeneration of the sensorial unit.

This research attempts to answer the following question: is it possible for the growth factors applied into the subtenon region to reach the suprachoroidal area through the scleral pores and stop apoptosis or reactivate the photoreceptors in dormant phase?

The hypothesis is based on the fact that repetitive electromagnetic stimulation (rEMS) increases the affinity and synthesis of Trk growth factor receptors on neural tissues. rEMS also provides an electromagnetic iontophoresis effect by changing the electrical charges of the scleral pores and the peptides.

What was learned from the study?

The results of the study confirmed our hypothesis without any adverse effect.

The ellipsoid zone width and visual field remain statistically significantly stable with combined treatment of electromagnetic stimulation and platelet-rich plasma when compared with control group at 1-year follow-up.

INTRODUCTION

Retinitis pigmentosa (RP) is a progressive outer retinal degeneration resulting from any of the 260 genetic mutations found in the photoreceptor (PR) or retinal pigment epithelium (RPE) [1]. The progression rate and findings of the disease are heterogeneous according to genetic mutation and heredity type. The initial symptom of the disease is usually night blindness (nyctalopia) beginning in childhood or adolescence. Narrowing of the visual field and legal blindness develops as the disease progresses [2–4]. If low grade inflammation is added, then the disease is complicated by cataracts, an epiretinal membrane, and macular edema [5]. In the fundus examination, the appearance of midperipheral bone spicule pigmentation is usually sufficient for diagnosis [1]. Developments in spectral domain optical coherence tomography (SD-OCT) enable detailed imaging of the sensorial retina and the ellipsoid zone. Ellipsoid zone (EZ) is an OCT image of the inner and outer segments of photoreceptor cells. Loss of EZ is the gold standard in the diagnosis and follow-up of RP [6, 7]. Visual field (VF) monitoring and electroretinography (ERG) are indirect signs of EZ loss and correlated with EZ width (EZW) [6]. Mutations in PR or RPE disrupt the synthesis of some vital peptides and growth factors for photoreceptors [1].

Autologous platelet-rich plasma (aPRP) is a good source of growth factors. Platelets have more than 30 growth factors and cytokines in α-granules. These peptides regulate the energy cycle at the cellular level. They also control local capillary blood flow, neurogenesis, and cellular metabolism [8, 9]. Subtenon aPRP application in the management of patients with RP has been shown to be clinically effective [10].

Repetitive electromagnetic stimulation (rEMS) increases binding affinity and the synthesis of growth factor receptors on neural tissues [11–14]. It provides electromagnetic iontophoresis by changing the electrical charges of scleral pores and tyrosine kinase receptors (Trk) [15–17]. rEMS forms hyperpolarization–depolarization waves in neurons, thereby

increasing neurotransmission and capillary blood flow [18]. Trk receptors are commonly found around limbus, extraocular muscle insertions, and the optic nerve [19]. Molecules smaller than 75 kDa can passively move from the sclera to the suprachoroidal space. Electrical or electromagnetic iontophoresis is required for molecules larger than 75 kDa such as brain-derived neurotrophic factor (BDNF) and insulin-like growth factor (IGF) to pass through the sclera into the subretinal space [15–17]. The clinical efficacy of rEMS alone or in combination with subtenon aPRP has also been shown [11].

The aim of this study is to investigate whether the natural progression rate of RP can be decreased by subtenon aPRP application alone or combination with rEMS. Ethics committee approval for the transcranial electromagnetic stimulation study was obtained from the Ankara University Faculty of Medicine Clinical Research Ethics Committee (17-1177-18). This committee had already approved the GFs work (19-1293-18). The study was performed in accordance with the tenets of the 2013 Declaration of Helsinki. Written informed consent was obtained from the patients prior to enrollment.

METHODS

The study includes retrospective analysis of 60 patients with RP who were followed up at Ankara University Faculty of Medicine between 2017 and 2019. The best corrected visual acuity (BCVA) was recorded as letters on the Early Treatment Diabetic Retinopathy Study (ETDRS) chart (Topcon CC 100 XP, Japan). The ellipsoid zone width (EZW) shows healthy photoreceptors and was measured horizontally and vertically on cross-sectional structural SD-OCT (RTVue XR "Avanti'', Optovue, Fremont, CA, USA). A manual segmentation program was used for the measurement of EZW. Fundus perimetry deviation index (FPDI) records were examined in the 24/2 visual field of computerized perimetry records (Compass, CenterVue, Padova, Italy). The FPDI offers data explaining how many of the 100 flashing points can be

seen correctly by the patient and what percentage of the visual field can be seen.

Patients with RP were included in this study if they satisfied all of the following criteria: BCVA from 50 to 110 ETDRS letters, any phenotypic variation of RP, 18 years of age or older. Patients with RP were excluded from the study if they satisfied any of the following criteria: the presence of dense cataracts or the habit of smoking. The retrospective study was designed as comparative and open label. The 60 patients with RP constitute three groups with similar demographic characteristics:

Group 1 The combined management group consists of 20 patients with RP (40 eyes) who received combined rEMS and aPRP. The rEMS was applied with a custom-designed helmet for 30 min just before the subtenon aPRP injection. These combined applications were repeated three times a month with a 2-week interval (loading dose). Then, two additional booster doses were applied with 6-month intervals. The course of the disease was evaluated by comparing the BCVA, EZW, and FPDI parameters recorded before the first application and within 3 months after the last application.

Group 2 The aPRP-only group consisted of 20 patients with RP (40 eyes) who received only subtenon aPRP injections. The aPRP applications were repeated three times a month with a 2-week interval (loading dose). Then, two additional booster doses were applied with 6-month intervals. The course of the disease was evaluated by comparing the BCVA, EZW, and FPDI parameters recorded before the first application and within 3 months after the last application.

Group 3 The natural course (control) group consists of 20 patients with RP (40 eyes) who did not receive any treatment and were followed. The natural course of the disease was

evaluated by comparing the BCVA, EZW, and FPDI parameters recorded at the beginning and at the end of the first year.

Preparation of Autologous PRP and Its Application

A 20-ml aliquot of blood was taken from the antecubital veins of the patients. It was transferred sterile to two 10-ml citrated PRP tubes (T-LAB PRP Kit, T-Biyoteknoloji, Bursa, Turkey). The plasma was separated in a refrigerated centrifuge (1200 NF Nüve, Nüve Technology Laboratory, Ankara, Turkey) at + 4.0 °C for 8 min at 2500 rpm centrifugation. The bottom 1/3 of the upper plasma was drawn into a 2.5-ml sterile syringe as a section rich in growth factors. The 1.5 ml PRP solution was then injected into the subtenon space under topical anesthesia. The injections were made under sterile conditions at the upper-temporal quadrant with a 26-G needle tip.

Retinal Repetitive Electromagnetic Stimulation (rEMS)

The rEMS helmet (Magnovision™, Bioretina Biotechnology, Ankara, Turkey) stimulated the retina and visual pathways with an electromagnetic field strength of 2000 milligauss, frequency of 42 Hz, and duration 30 min. The field was applied just before the PRP application. These values were previously determined to be effective for other clinical and preclinical studies.

The primary outcome measurements are the horizontal and vertical ellipsoid zone widths that directly show the structural changes in the photoreceptors. The secondary outcome measure is a change in micrometry FPDI values.

Statistical Analysis of Data

Descriptive statistics are presented with frequency, percentage, mean, and standard deviation values. A paired t test was used to examine whether the pre- and post-measurement values are different within groups. A Sidak binary comparison test examined the measurement difference between groups. An analysis of variance (ANOVA) test was performed to examine whether the groups are different by age. Here, p values less than 0.05 were considered statistically significant ($\alpha = 0.05$). Analyses were made with SPSS 22.0 package program. The effect of interventional procedures on the natural course of retinitis pigmentosa was evaluated by comparing quantitative data from groups 1, 2, and 3.

RESULTS

The mean age was 33.0 (22–51 years) in group 1, 32.6 (20–56 years) in group 2, and 31.7 (20–-57 years) in group 3. The mean follow-up time between the first measurements and the last measurements in all three groups was 13 months (12–15 months). There were no statistical differences between the groups in terms of age and follow-up times ($p = 0.81$).

Mean Horizontal Ellipsoid Zone Width (m-HEZW)

The m-HEZW in group 1 was 3.46 mm before combined management and 3.50 mm after the procedures. During the mean 13-month follow-up, this positive change was 1.0% on average ($p = 0.10$). In group 2, the m-HEZW was 3.32 mm at the first measurement and 3.26 mm after the PRP injections. During the mean 13-month follow-up, the change was found to be − 2.9% on average ($p = 0.01$). In group 3, the m-HEZW was 3.32 mm at the initial examination and 3.03 mm at the last examination. Over the 13-month follow-up, this negative change was found to be − 9.4% on average ($p = 0.01$) (Tables 1, 2, 3, 4; Figs. 1, 2, 3).

Mean Vertical Ellipsoid Zone Width (m-VEZW)

The m-VEZW was 3.32 mm in group 1 before the combined application and 3.33 mm after the procedures. During the mean 13-month

Table 1 Demographic characteristics and follow-up parameters of group 1 (management with aPRP + rEMS)

Patient no.	Age	Sex	Eye	Horizontal EZW			Vertical EZW			Visual field FPDI			BCVA	
				Before	After	%Difference	Before	After	%Difference	Before	After	Difference	Before	After
1	29	F	R	3.56	3.83	+ 7.6	4.62	4.84	+ 4.8	45	52	+ 7	110	110
			L	4.21	4.34	+ 3.1	3.36	3.41	+ 1.5	43	45	+ 2	110	110
2	37	M	R	6.87	6.90	+ 0.4	6.74	6.79	+ 0.7	57	60	+ 3	110	110
			L	3.97	4.14	+ 4.2	2.57	2.74	+ 6.6	57	60	+ 3	110	110
3	45	F	R	2.58	2.84	+ 10.1	1.90	2.06	+ 8.4	39	42	+ 3	100	100
			L	2.32	3.02	+ 30.2	2.17	2.30	+ 6.0	37	43	+ 6	100	100
4	38	M	R	3.43	3.43	0	2.52	2.70	+ 7.1	26	27	+ 1	100	100
			L	3.64	3.65	+ 0.3	2.75	2.82	+ 2.5	28	29	+ 1	100	100
5	32	M	R	4.01	4.00	− 0.3	3.92	3.89	− 0.8	48	46	− 2	110	110
			L	3.96	3.90	− 1.5	3.88	3.82	− 1.5	44	43	− 1	100	100
6	36	F	R	4.87	4.87	0	4.71	4.70	− 0.2	49	49	0	110	110
			L	4.91	4.90	− 0.2	4.70	4.68	− 0.4	50	49	− 1	110	110
7	38	F	R	7.01	7.16	+ 2.1	7.10	7.12	+ 0.3	65	67	+ 2	110	110
			L	7.03	7.20	+ 2.4	7.13	7.21	+ 1.1	66	70	+ 4	110	110
8	27	M	R	2.21	2.20	− 0.5	2.17	2.15	− 0.9	38	36	− 2	89	80
			L	2.17	2.16	− 0.5	2.14	2.12	− 0.9	37	36	− 1	75	75
9	24	F	R	2.76	2.71	− 2.0	2.74	2.71	− 1.1	41	39	− 2	85	85
			L	2.66	2.63	− 1.1	2.69	2.61	− 2.6	40	39	− 1	85	85
10	28	F	R	2.61	2.60	− 0.4	2.70	2.70	0	27	27	0	80	80
			L	2.59	2.58	− 1.2	2.34	2.31	− 1.3	26	25	− 1	80	80
11	31	M	R	2.43	2.40	− 1.2	2.38	2.37	− 0.4	32	30	− 2	75	75
			L	2.40	2.40	0	2.38	2.37	− 0.4	30	30	0	75	75

Table 1 continued

Patient no.	Age	Sex	Eye	Horizontal EZW			Vertical EZW			Visual field FPDI			BCVA	
				Before	After	%Difference	Before	After	%Difference	Before	After	Difference	Before	After
12	26	M	R	1.24	1.20	− 3.2	1.36	1.29	− 5.1	38	36	− 2	70	70
			L	1.19	1.16	− 2.5	1.20	1.18	− 1.7	35	33	− 2	70	70
13	20	F	R	6.71	6.69	− 0.3	6.70	6.68	− 0.3	76	74	− 2	110	100
			L	6.56	6.56	0	6.49	6.48	− 0.2	72	71	− 1	110	100
14	23	F	R	1.64	1.64	0	1.49	1.49	0	25	25	0	70	70
			L	1.66	1.65	− 0.6	1.38	1.37	− 0.7	27	26	− 1	70	70
15	49	M	R	5.84	5.78	− 1.1	5.91	5.89	− 0.3	76	74	− 2	110	110
			L	5.77	5.73	− 0.7	5.79	5.76	− 0.5	72	70	− 2	110	110
16	51	F	R	4.98	4.96	− 0.4	3.98	3.96	− 0.5	68	67	− 1	110	110
			L	4.78	4.76	− 0.4	4.00	3.98	− 0.5	66	64	− 2	110	110
17	30	M	R	2.63	2.60	− 1.1	2.46	2.44	− 0.8	39	37	− 2	85	85
			L	1.99	1.94	− 2.5	1.87	1.84	− 1.6	34	32	− 2	80	80
18	47	F	R	0.95	0.95	0	1.02	1.00	− 2.0	20	20	0	50	50
			L	1.01	0.99	− 2.0	1.12	1.10	− 1.8	22	21	− 1	65	65
19	22	F	R	2.36	2.33	− 1.3	1.98	1.96	− 1.0	36	34	− 2	89	89
			L	1.90	1.88	− 1.1	1.87	1.85	− 1.1	32	31	− 1	75	75
20	25	F	R	1.56	1.53	− 1.9	1.77	1.74	− 1.7	30	29	− 1	65	65
			L	1.74	1.71	− 1.7	1.82	1.79	− 1.7	30	29	− 1	65	65

aPRP autologous platelet-rich plasma, *rEMS* repetitive electromagnetic stimulation, *EZW* ellipsoid zone width (mm), *FPDI* fundus perimetry deviation index (%), *BCVA* best corrected visual acuity

Table 2 Demographic characteristics and follow-up parameters of group 2 (management with only aPRP)

Patient no.	Age	Sex	Eye	Horizontal EZW			Vertical EZW			Visual field FPDI			BCVA	
				Before	After	%Difference	Before	After	%Difference	Before	After	Difference	Before	After
1	39	M	R	2.89	2.94	+ 1.7	2.10	2.21	+ 5.2	26	28	+ 2	80	80
			L	2.23	2.51	+ 12.0	2.29	2.32	+ 1.3	24	28	+ 4	80	80
2	37	M	R	6.36	6.47	+ 1.7	6.32	6.47	+ 2.4	64	64	0	110	110
			L	7.03	7.21	+ 2.4	7.13	7.20	+ 1.0	71	72	+ 1	110	110
3	47	F	R	7.77	8.30	+ 6.8	7.47	7.65	+ 2.4	75	77	+ 2	110	110
			L	7.95	7.97	+ 0.3	6.91	7.09	+ 1.4	76	77	+ 1	110	110
4	28	F	R	4.87	4.62	− 5.1	3.82	3.56	− 6.9	45	40	− 5	100	100
			L	4.92	4.84	− 1.6	3.73	3.71	− 0.5	43	40	− 3	100	100
5	26	F	R	3.76	3.61	− 4.0	2.63	2.58	− 1.9	64	60	− 4	100	100
			L	4.14	3.97	− 4.1	2.59	2.57	− 0.8	63	60	− 3	100	100
6	40	M	R	2.77	2.63	− 5.1	2.37	2.18	− 8.0	42	36	− 6	75	70
			L	2.48	2.32	− 6.5	2.16	2.10	− 2.8	35	30	− 5	75	70
7	30	F	R	1.98	1.89	− 5.5	1.92	1.83	− 4.7	32	28	− 4	65	65
			L	2.01	1.89	− 5.9	1.97	1.87	− 5.1	33	28	− 5	65	65
8	20	F	R	2.77	2.64	− 4.7	1.96	1.84	− 6.1	60	54	− 6	80	75
			L	3.00	2.87	− 4.3	2.08	1.97	− 5.3	59	55	− 4	80	75
9	23	M	R	3.89	3.70	− 4.9	3.71	3.46	− 6.7	53	50	− 3	89	89
			L	3.76	3.41	− 9.3	3.63	3.42	− 5.8	50	45	− 5	85	80
10	28	M	R	2.71	2.60	− 4.0	2.84	2.70	− 4.9	41	38	− 3	89	89
			L	2.96	2.81	− 5.1	2.73	2.59	− 5.1	41	38	− 3	89	89
11	29	F	R	3.73	3.61	− 3.2	3.37	3.23	− 4.2	55	52	− 3	95	95
			L	3.90	3.77	− 3.3	4.11	3.89	− 5.4	60	56	− 4	95	95

Table 2 continued

Patient no.	Age	Sex	Eye	Horizontal EZW			Vertical EZW			Visual field FPDI			BCVA	
				Before	After	%Difference	Before	After	%Difference	Before	After	Difference	Before	After
12	24	F	R	2.86	2.71	− 5.2	2.77	2.61	− 5.8	40	36	− 4	85	85
			L	2.76	2.63	− 4.7	2.65	2.50	− 5.7	40	36	− 4	85	85
13	50	F	R	2.22	2.09	− 5.9	2.86	2.72	− 4.9	44	39	− 5	100	100
			L	2.61	2.47	− 5.4	3.11	2.96	− 4.8	47	44	− 3	110	110
14	32	M	R	2.53	2.51	− 0.8	2.48	2.47	− 0.4	34	34	0	75	75
			L	2.50	2.49	− 0.4	2.48	2.47	− 0.4	33	33	0	75	75
15	56	F	R	5.08	4.96	− 2.4	4.98	4.86	− 2.4	70	67	− 3	110	110
			L	4.98	4.86	− 2.4	4.71	4.58	− 2.8	69	66	− 3	110	110
16	31	M	R	1.34	1.26	− 6.0	1.38	1.30	− 5.8	38	34	− 4	70	70
			L	1.29	1.21	− 6.2	1.30	1.23	− 5.4	36	32	− 4	70	70
17	23	F	R	2.33	2.24	− 3.9	2.00	1.96	− 2.0	35	32	− 3	89	89
			L	1.97	1.91	− 3.0	1.89	1.82	− 3.7	31	28	− 3	75	75
18	32	F	R	1.77	1.68	− 5.1	1.53	1.45	− 5.2	30	25	− 5	80	80
			L	1.54	1.49	− 3.2	1.70	1.62	− 4.7	27	24	− 3	74	74
19	28	M	R	1.88	1.80	− 4.3	1.88	1.81	− 3.7	48	44	− 4	85	85
			L	2.05	1.98	− 3.4	2.49	2.40	− 3.6	56	53	− 3	92	92
20	29	F	R	2.70	2.70	0	2.76	2.76	0	28	28	0	80	80
			L	2.69	2.69	0	2.64	2.64	0	27	27	0	80	80

aPRP autologous platelet-rich plasma, *rEMS* repetitive electromagnetic stimulation, *EZW* ellipsoid zone width (mm), *FPDI* fundus perimetry deviation index (%), *BCVA* best corrected visual acuity

Table 3 Demographic characteristics and follow-up parameters of group 3 (natural course)

Patient no.	Age	Sex	Eye	Horizontal EZW			Vertical EZW			Visual field FPDI			BCVA	
				Before	After	%Difference	Before	After	%Difference	Before	After	Difference	Before	After
1	48	M	R	8.30	7.77	− 6.4	7.77	7.27	− 6.4	78	67	− 11	110	100
			L	8.30	7.95	− 4.2	7.97	7.09	− 11.1	73	64	− 9	110	110
2	50	M	R	2.12	1.78	− 12.5	2.76	2.50	− 9.4	46	34	− 12	100	95
			L	2.71	2.49	− 8.2	3.01	2.63	− 12.6	49	40	− 9	95	95
3	32	F	R	7.45	7.01	− 5.9	5.68	5.15	− 8.8	85	78	− 7	100	100
			L	8.24	7.80	− 5.3	7.98	7.00	− 12.2	88	80	− 8	100	100
4	29	F	R	3.73	3.10	− 16.8	2.87	2.70	− 6.9	72	63	− 9	95	95
			L	3.79	3.23	− 14.7	3.68	3.29	− 10.5	84	73	− 11	100	100
5	30	F	R	1.92	1.68	− 12.5	1.82	1.72	− 5.6	36	28	− 8	70	70
			L	1.60	1.50	− 6.3	1.55	1.39	− 10.3	32	25	− 7	70	70
6	46	M	R	3.11	2.78	− 10.6	3.50	3.02	− 13.7	55	46	− 9	110	100
			L	3.02	2.90	− 4.0	3.41	3.22	− 5.6	53	45	− 8	110	110
7	31	F	R	1.57	1.42	− 9.5	1.33	1.21	− 9.0	30	22	− 8	80	80
			L	1.34	1.21	− 9.7	1.63	1.51	− 7.3	27	19	− 8	74	74
8	27	F	R	1.80	1.65	− 8.3	1.78	1.60	− 10.1	48	39	− 9	85	85
			L	2.15	1.97	− 8.4	2.39	2.20	− 7.9	56	48	− 8	92	92
9	57	M	R	1.36	1.20	− 11.8	1.46	1.31	− 10.3	17	9	− 8	65	65
			L	1.12	0.98	− 12.5	1.24	1.10	− 11.3	9	4	− 5	65	50
10	22	M	R	5.75	5.16	− 10.3	5.01	4.54	− 9.4	51	40	− 11	110	110
			L	5.69	5.13	− 9.8	5.22	4.84	− 7.3	50	41	− 9	110	110
11	26	F	R	2.40	2.10	− 12.5	2.40	2.12	− 11.6	55	39	− 11	74	74
			L	2.70	2.50	− 7.4	2.60	2.35	− 9.6	59	47	− 12	80	74

Table 3 continued

Patient no.	Age	Sex	Eye	Horizontal EZW			Vertical EZW			Visual field FPDI			BCVA	
				Before	After	%Difference	Before	After	%Difference	Before	After	Difference	Before	After
12	30	F	R	1.90	1.80	− 5.2	1.80	1.70	− 5.5	49	43	− 6	80	80
			L	2.00	1.80	− 10.0	1.90	1.70	− 10.5	52	43	− 9	85	80
13	27	F	R	4.09	3.67	− 10.3	3.44	3.07	− 10.8	68	56	− 12	89	89
			L	4.09	3.79	− 7.3	3.76	3.68	− 2.2	69	63	− 6	89	89
14	29	M	R	3.71	3.39	− 8.6	3.30	3.00	− 9.1	56	48	− 8	95	95
			L	4.01	3.57	− 11.0	4.14	3.59	− 13.3	61	51	− 10	100	100
15	20	F	R	3.60	3.40	− 5.5	4.60	4.30	− 6.5	71	65	− 6	95	95
			L	4.84	4.60	− 4.9	3.70	3.50	− 5.4	72	67	− 4	95	95
16	23	M	R	3.45	3.09	− 10.4	3.74	3.34	− 10.7	52	44	− 8	100	100
			L	3.27	2.97	− 9.2	3.61	3.30	− 8.6	50	40	− 10	100	95
17	25	F	R	1.65	1.50	− 9.1	2.08	1.93	− 7.2	45	37	− 8	74	74
			L	1.10	0.97	− 11.8	1.83	1.71	− 6.5	40	33	− 7	70	70
18	20	F	R	1.70	1.55	− 8.8	1.90	1.75	− 7.9	50	41	− 9	80	80
			L	2.10	1.90	− 9.5	3.20	3.00	− 6.3	58	51	− 7	85	85
19	33	M	R	3.43	3.06	− 10.8	3.19	2.78	− 12.9	57	47	− 10	100	100
			L	3.40	3.01	− 11.5	3.33	2.97	− 10.8	58	47	− 11	100	100
20	28	F	R	2.16	1.90	− 12.0	2.14	1.92	− 10.2	56	45	− 11	74	74
			L	2.13	1.90	− 10.8	2.26	1.98	− 12.3	55	43	− 12	74	74

aPRP autologous platelet-rich plasma, *rEMS* repetitive electromagnetic stimulation, *EZW* ellipsoid zone width (mm), *FPDI* fundus perimetry deviation index (%), *BCVA* best corrected visual acuity

Table 4 Comparison of assessment parameters before the treatments and at the end of the 1-year follow-up period between three groups

Group 1 ($n = 40$) $X \pm SD$	Group 2 ($n = 40$) $X \pm SD$	Group 3 ($n = 40$) $X \pm SD$	p	Difference**
Horizontal EZW %difference				
1 ± 2.4	$- 2.85 \pm 2.8$	$- 9.36 \pm 2.8$	0.01*	$1 > 2 > 3$
Vertical EZW %difference				
0.34 ± 2.8	$- 3.05 \pm 2.7$	$- 9.09 \pm 2.6$	0.01*	$1 > 2 > 3$
Visual field FPDI difference				
0.05 ± 2.5	$- 2.68 \pm 2.3$	$- 8.78 \pm 2.0$	0.01*	$1 > 2 > 3$

aPRP autologous platelet-rich plasma, *rEMS* repetitive electromagnetic stimulation, *EZW* ellipsoid zone width (mm), *FPDI* fundus perimetry deviation index (%), *BCVA* best corrected visual acuity
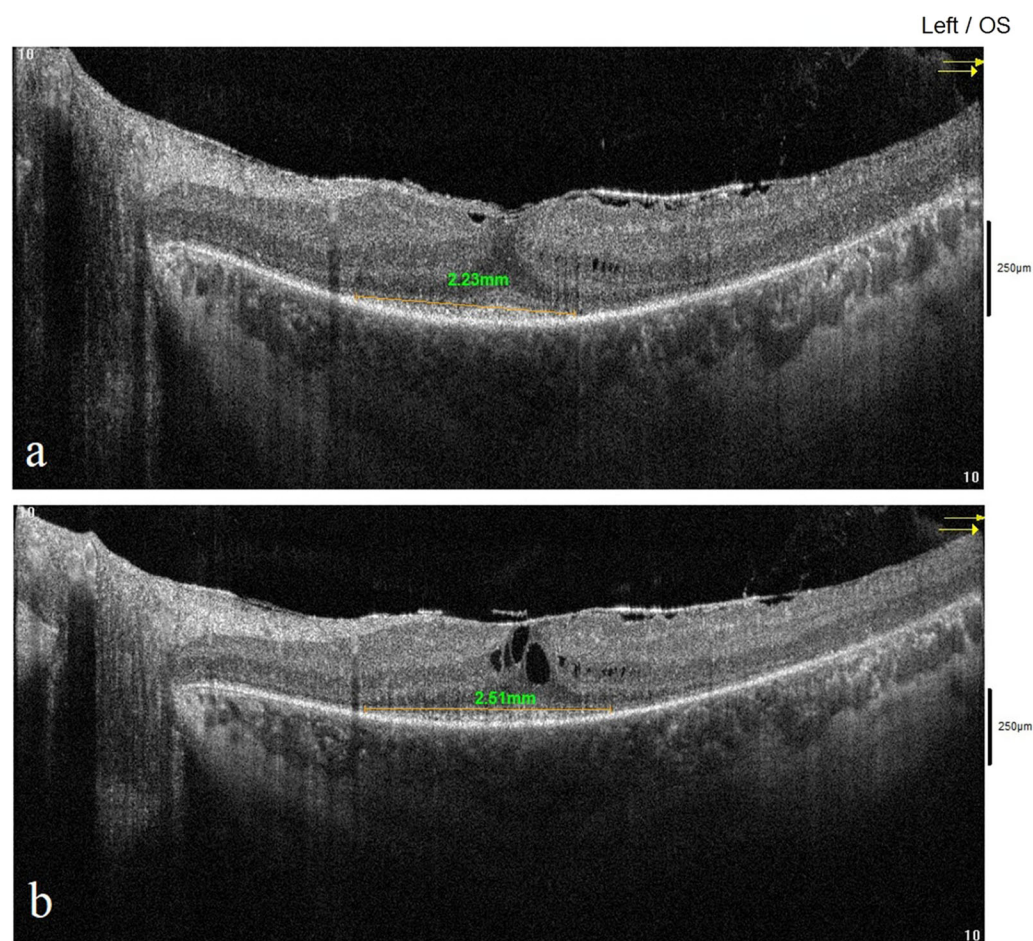**Sidak binary comparison test

Fig. 1 Horizontal EZWs of a patient with retinitis pigmentosa receiving aPRP + rEMS (Table 1, patient no. 1). **a** Before treatment, 3.56 mm. **b** The 13th month of follow-up post-treatment, 3.83 mm
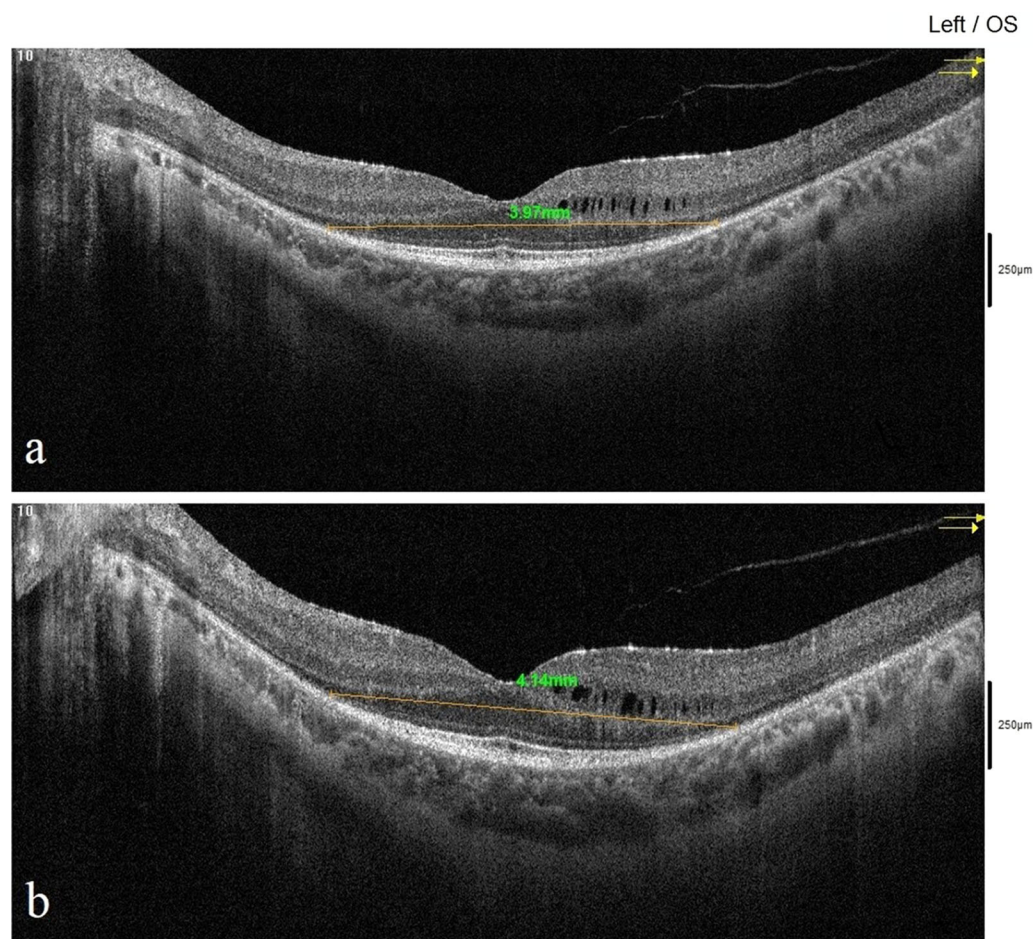
Fig. 2 Horizontal EZWs of a patient with retinitis pigmentosa receiving aPRP + rEMS (Table 1, patient no. 2). **a** Before treatment, 3.97 mm. **b** The 13th month of follow-up post-treatment, 4.14 mm

follow-up, the change was 0.3% on average ($p = 0.19$). In group 2, the m-VEZW was 3.09 mm at the first measurement and 3.02 mm after PRP injections. The change was -3.1% on average during the mean 13-month follow-up ($p = 0.01$). In group 3, the m-VEZW was 3.27 mm at the initial examination and 2.97 mm at the last examination. The change was found to be -9.1% on average during the mean 13-month follow-up ($p = 0.01$) (Tables 1, 2, 3, 4; Figs. 4, 5).

Mean Fundus Perimetry Deviation Index (m-FPDI)

This value was 43.45% in group 1 before PRP combined with rEMS and 43.50% after the

procedures. The mean change was 0.05% on average during the 13-month follow-up ($p = 0.90$). In group 2, the m-FPDI was 46.13% at the first measurement and 43.45% after PRP injections. The change was -2.68% on average during the mean 13-month follow-up ($p = 0.01$). In group 3, the m-FPDI was 54.30% at the initial examination and 45.38% at the last examination. The change was -8.78% on average during the mean 13-month follow-up ($p = 0.01$) (Tables 1, 2, 3, 4; Figs. 6, 7, 8, 9, 10).

Mean Best Corrected Visual Acuity (m-BCVA)

Group 1 could identify 91.6 letters before PRP combined with rEMS applications and 92.3

Left / OS

Fig. 3 Horizontal EZWs of a patient with retinitis pigmentosa receiving only aPRP (Table 2, patient no. 1). **a** Before treatment, 2.23 mm. **b** The 13th month of follow-up post-treatment, 2.51 mm

letters after the procedure. During the mean 13-month follow-up, the change was found to be an average of 0.7 letters ($p = 0.08$). Group 2 had an m-BCVA of 88.2 letters at baseline and 87.6 letters after PRP injections. The change was -0.6 letters on average ($p = 0.07$) during the mean 13-month follow-up. Group 3 had an m-BCVA score of 89.8 letters at the initial examination and 88.4 letters at the end. The change was found to be an average of -1.4 letters during the mean 13-month follow-up ($p = 0.02$).

When groups 1, 2, and 3 were compared by the Sidak test according to the HEZW, VEZW, and FPDI changes, the combined application of rEMS and subtenon aPRP significantly increases the three assessment parameters (Table 4).

DISCUSSION

There are currently over 260 different genetic mutations known to cause retinitis pigmentosa. Genetic inheritance can be autosomal dominant (AD), autosomal recessive (AR), X-linked, mitochondrial, mosaicism, or sporadic patterns [1]. Thus, the prognosis is usually quite heterogeneous. Acquired factors such as nutrition, smoking, anemia, pregnancy, as well as long-term exposure to ultraviolet and blue light also affect the course of the disease [2–4]. Autosomal dominant inheritance shows the slowest progression with an average annual loss of 5% photoreceptors [20, 21]. X-linked inheritance shows the fastest progression with an average annual loss of 15% of photoreceptors [21, 22].
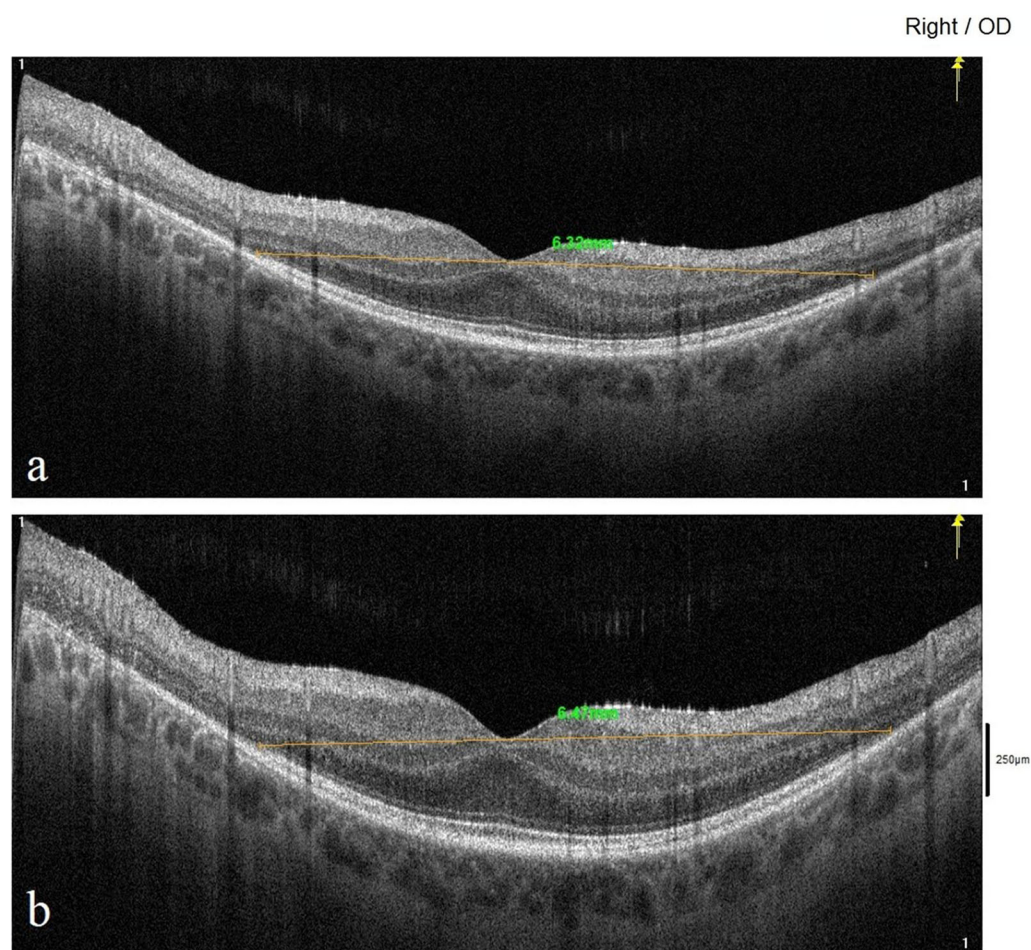
Right / OD

Fig. 4 Vertical EZWs of a patient with retinitis pigmentosa receiving only aPRP (Table 2, patient no. 1). **a** Before treatment, 6.32 mm. **b** The 13th month of follow-up post-treatment, 6.47 mm

Knowledge about which genetic mutation affects the progression is increasing owing to widespread genetic testing. The annual progression rate of retinitis pigmentosa was reported to be 5% in *RHO* gene mutation that was inherited as AD, and 15% in *RPGR* gene mutation inherited as X-linked [20–22]. The photoreceptors have cilia tubule functions that provide the transport of opsin and rhodopsin and can be impaired by X-linked mutations— they can be distinguished by the presence of widespread lipofuscin deposits in the fundus examination. The ciliopathy gene mutations have threefold faster progression than non-ciliopathy mutations [23]. Retinitis pigmentosa progresses with an average of 10% annual photoreceptor loss when AD, AR, X-linked, and mitochondrial inheritance patterns are collectively evaluated [6, 24, 25]. In our study, the annual photoreceptor loss rate was found to be 9.3% on average in the RP group without interventional procedures (group 3, natural course) similar to the literature.

The visual function begins with the photochemical conversion of light energy, which comes from the objects and focuses on the retina with conversion to electrical signals. Photochemical conversion occurs in the sensorial unit and microenvironment consisting of a choriocapillaris–retina pigment epithelium–photoreceptor trio. The retina pigment epithelium is the unit center where the synthesized peptide growth factors (GFs) regulate photochemical reactions. These include the
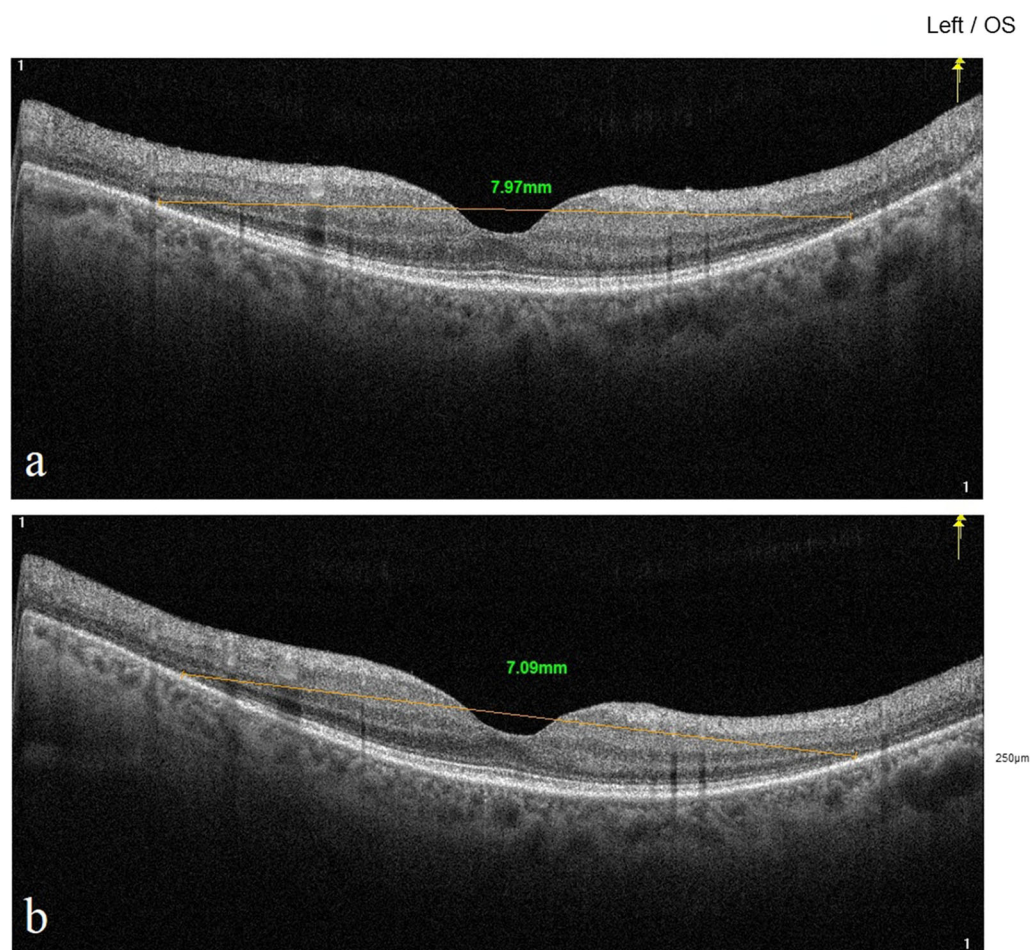
Left / OS

Fig. 5 Vertical EZWs of a patient with retinitis pigmentosa, natural course (Table 3, patient no. 1). **a** Before treatment, 7.97 mm. **b** The 13th month of follow-up post-treatment, 7.09 mm

oxidative phosphorylation and energy cycle of glucose in the blood; transport of vitamin A, minerals, anions, cations, and necessary coenzymes; the synthesis of opsin–rhodopsin and necessary peptides in the visual cycle; and the removal of metabolic waste that occurs in RPE [26–29].

The growth factors, peptides, and fragments required for these functions are encoded by over 260 genes in RPE. Mutations in any of these genes leads to progressive vision loss and progressive degeneration of the sensorial unit [1]. In particular, mutations that affect the conversion of glucose to adenosine triphosphate (ATP) lead to a condition in photoreceptor cells called sleep mode or dormant phase [30, 31]. Cells in this state have more solid plasma—they are live

but metabolically inactive [32]. The photoreceptors in the dormant phase can be metabolically reactive if neurotrophins and GFs can be delivered the microenvironment of the sensorial unit [33]. Neurotrophins and GFs are key molecules in the cellular energy cycle [34]. Prolonged dormant phase or conditions impairing sensorial unit homeostasis eventually lead to apoptosis and cell loss [33]. RPE forms the outer blood–retinal barrier with its tight connections. Defects in the external blood retinal barrier due to apoptosis disrupt the immune-protected state in the retina and lead to low-density inflammation in the sensory unit. Neuroinflammation accelerates the apoptosis process and sensorial unit loss [5].
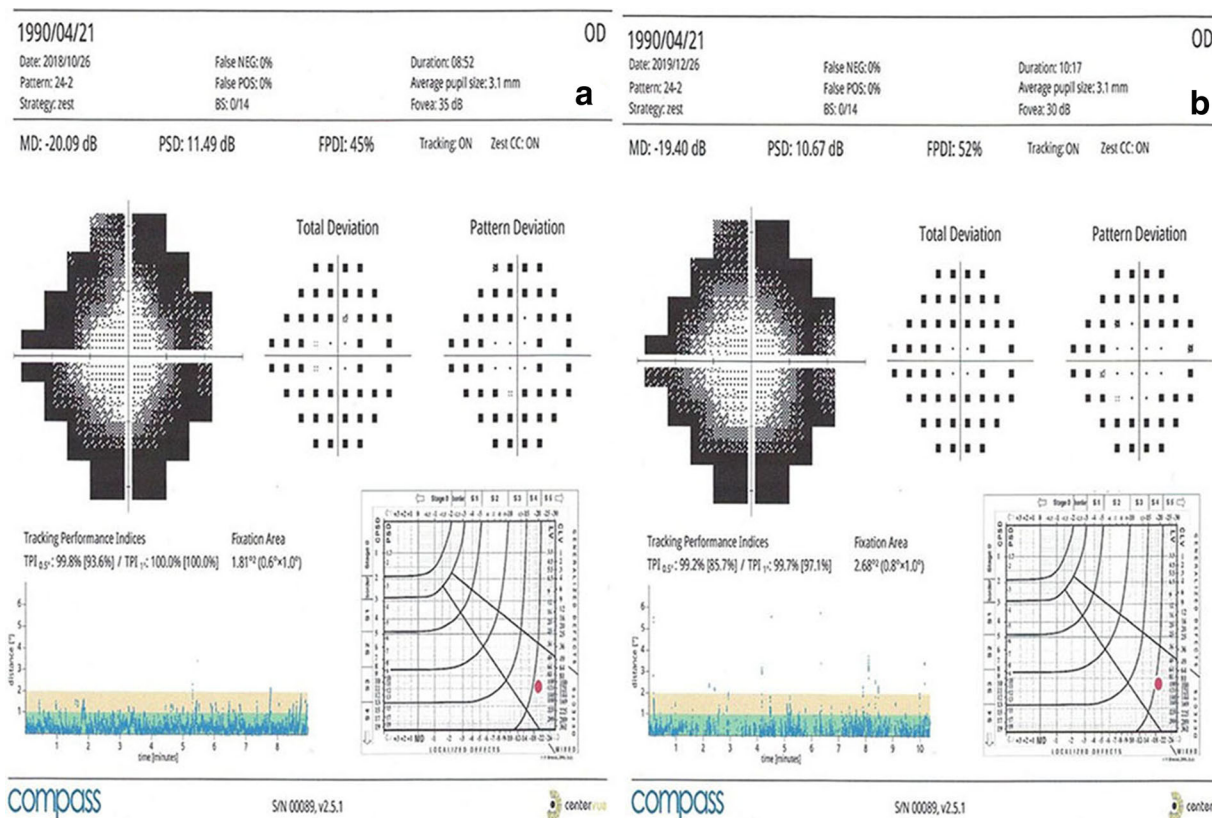
Fig. 6 Visual field FPDI changes of the retinitis pigmentosa patient receiving aPRP + rEMS (Table 1, patient no. 1). **a** Before treatment, 45%. **b** The 13th month of follow-up post-treatment, 52%

Platelet-rich plasma is a good source of growth factors. Platelets have more than 30 GFs and cytokines in α-granules such as neurotrophic growth factor (NGF), neural factor (NF), BDNF, basic fibroblast growth factor (bFGF), IGF, transforming growth factor (TGFβ), vascular endothelial growth factor (VEGF), platelet-derived growth factor (PDGF), etc. These peptides regulate the energy cycle at the cellular level, local capillary blood flow, neurogenesis, and cellular metabolism [8–10]. Anti-inflammatory effects of PRP are also associated with soluble cytokines [35].

Our previous clinical and prospective study showed that subtenon injection of aPRP significantly increased the visual functions [10, 11]. Clinical and preclinical studies showed that the half-life of GFs in tissue derived from PRP is 4–6 months [36–38]. Our clinical observations are similar. Here, we investigated the effects of three loading doses with a 2-week interval and two boosters with 6-month interval of subtenon aPRP injections on photoreceptor loss (measured by EZW on SD-OCT) during the 1-year follow-up. The photoreceptor loss rates during the follow-up period were 9.3% in the natural course group (group 3) and 3% in the aPRP-only group (group 2). These results suggest that subtenon aPRP injection can decrease the photoreceptor loss rate by approximately threefold.

The growth factors applied into the subtenon region reach the suprachoroidal area through the scleral pores. GFs in the choroidal matrix reach the subretinal area through Trk receptors. Tyrosine kinase receptors are commonly found around the limbus, extraocular muscle insertions, and the optic nerve [19]. Molecules smaller than 75 kDa can pass through the sclera via passive transport to the suprachoroidal space [17]. BDNF and IGF are key growth factors in PRP and are larger than 75 kDa [9].
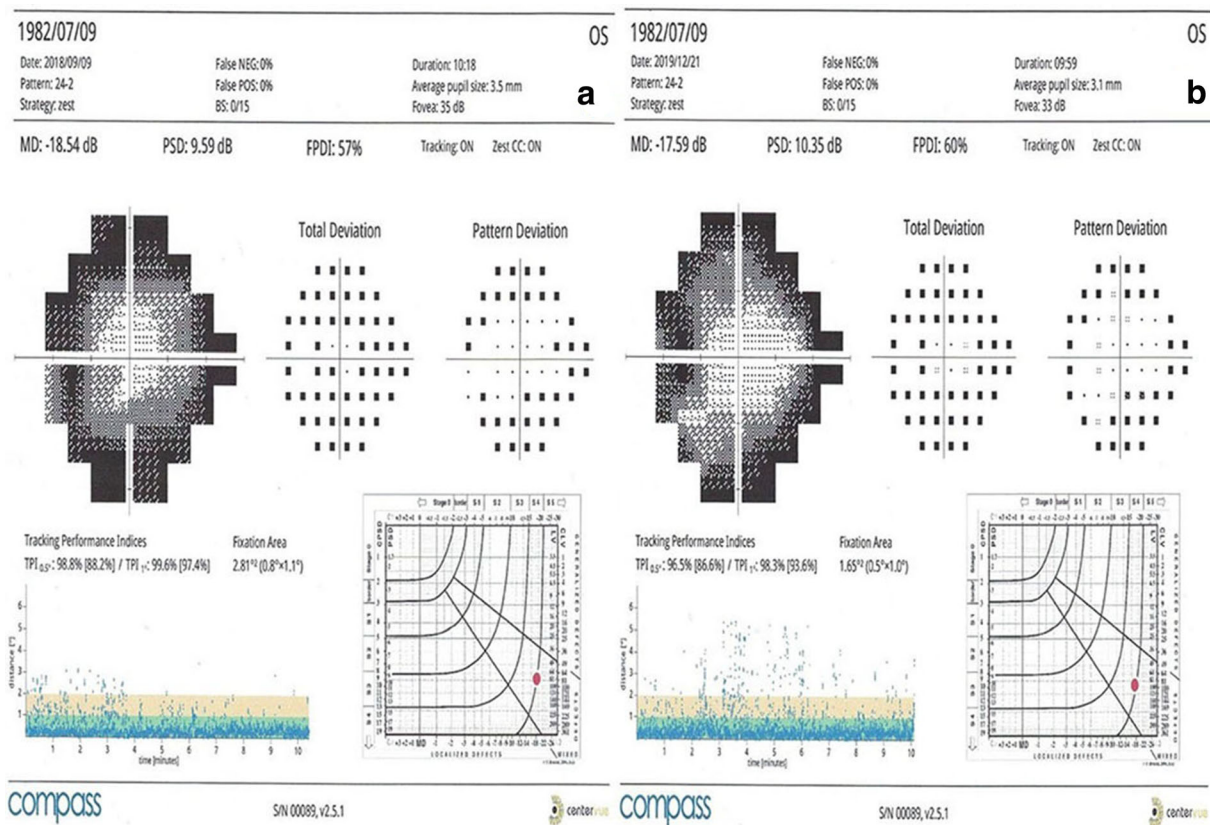
Fig. 7 Visual field FPDI changes of a patient with retinitis pigmentosa receiving aPRP + rEMS (Table 1, patient no. 2). **a** Before treatment, 57%. **b** The 13th month of follow-up post-treatment, 60%

Repetitive electromagnetic stimulation increases the affinity and synthesis of Trk growth factor receptors on neural tissues [11–14]. rEMS also provides electromagnetic iontophoresis effects by changing the electrical charges of the scleral pores and the peptides. Electrical or electromagnetic iontophoresis accelerates the passage of the large molecules such as BDNF and IGF through the sclera [15–17]. rEMS creates hyperpolarization–depolarization waves in neurons, which increases neurotransmission and capillary blood flow [18]. In group 1, rEMS was applied along with aPRP, and we found the change in mean EZW rate to be 0.7% at the end of 1 year versus baseline. This result suggests that rEMS increases the effects of aPRP. The combined use of rEMS and aPRP has synergistic effects to prevent photoreceptor loss and reactivate the photoreceptor cells in sleep (dormant) mode. The electromagnetic field used here is far below the safety limits set by the World Health Organization [39].

In our study, ellipsoid zone widths and FPDI ratios in visual field showed similar changes. This proves that the visual field is related to the
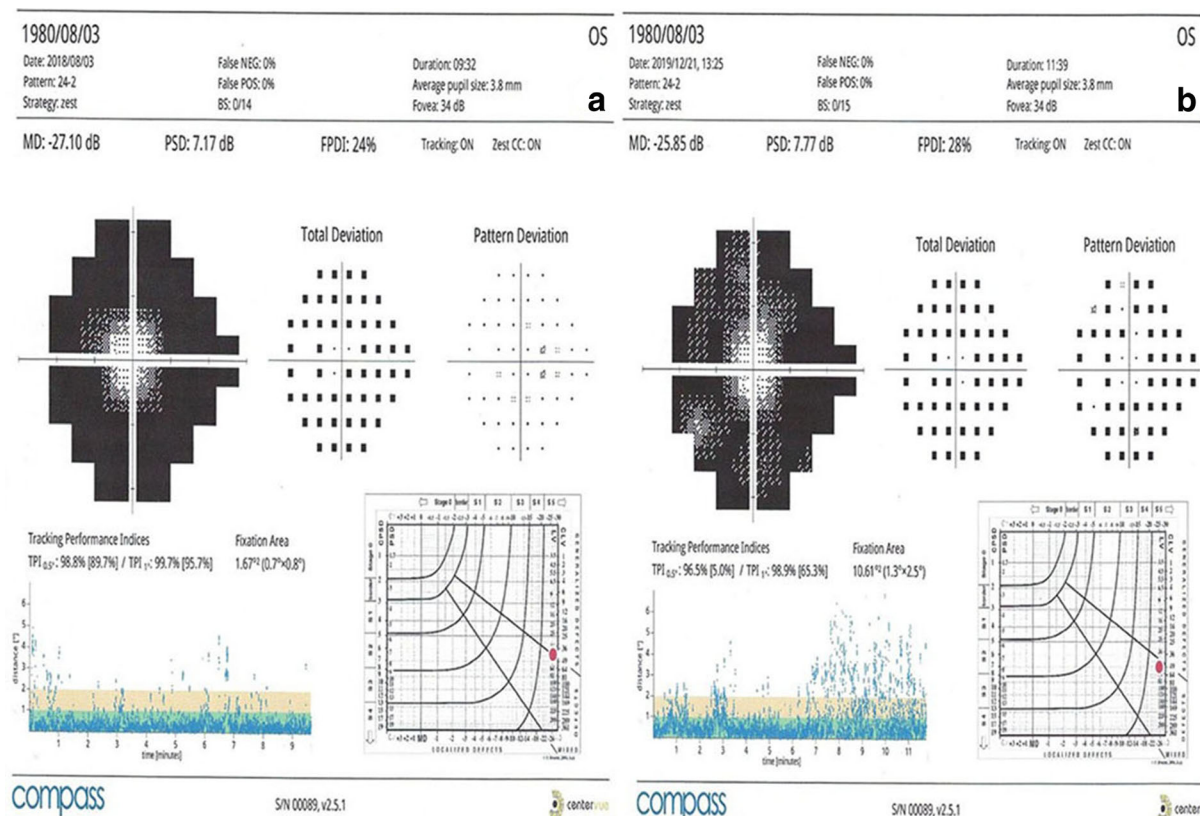
Fig. 8 Visual field FPDI changes of a patient with retinitis pigmentosa receiving only aPRP (Table 2, patient no. 1). **a** Before treatment, 24%. **b** The 13th month of follow-up post-treatment, 28%

number of photoreceptors. The visual field is a subjective test and can be influenced by many parameters such as refractive error, media opacity, illumination intensity, the patient's current attention, learning curve, etc. [40]. The visual field test gives indirect data about the number and functions of photoreceptors. EZW is an objective parameter in tracking the number of photoreceptors, it is not affected by subjective situations. We believe that EZW can be used for diagnosis and follow-up as a substitute for visual field and electroretinography in most cases. In our opinion, EZW should be the gold standard diagnostic follow-up criterion for RP.

In contrast to the visual field, the central visual acuity is affected too late in RP. Apoptosis occurring in photoreceptors in the periphery leads to Müller cell hypertrophy and ectopic synaptogenesis in the central 19-degree area. As a result of the paracrine effects of Müller cells, the cone cells are not affected by apoptosis for a long time. Consequently, BCVA can remain stable for a long time [41]. In our study, BCVA in all three groups did not change during an average of 13 months follow-up.

Local and systemic adverse events related to rEMS and/or aPRP were not detected during the 1-year follow-up. Patients did not describe any
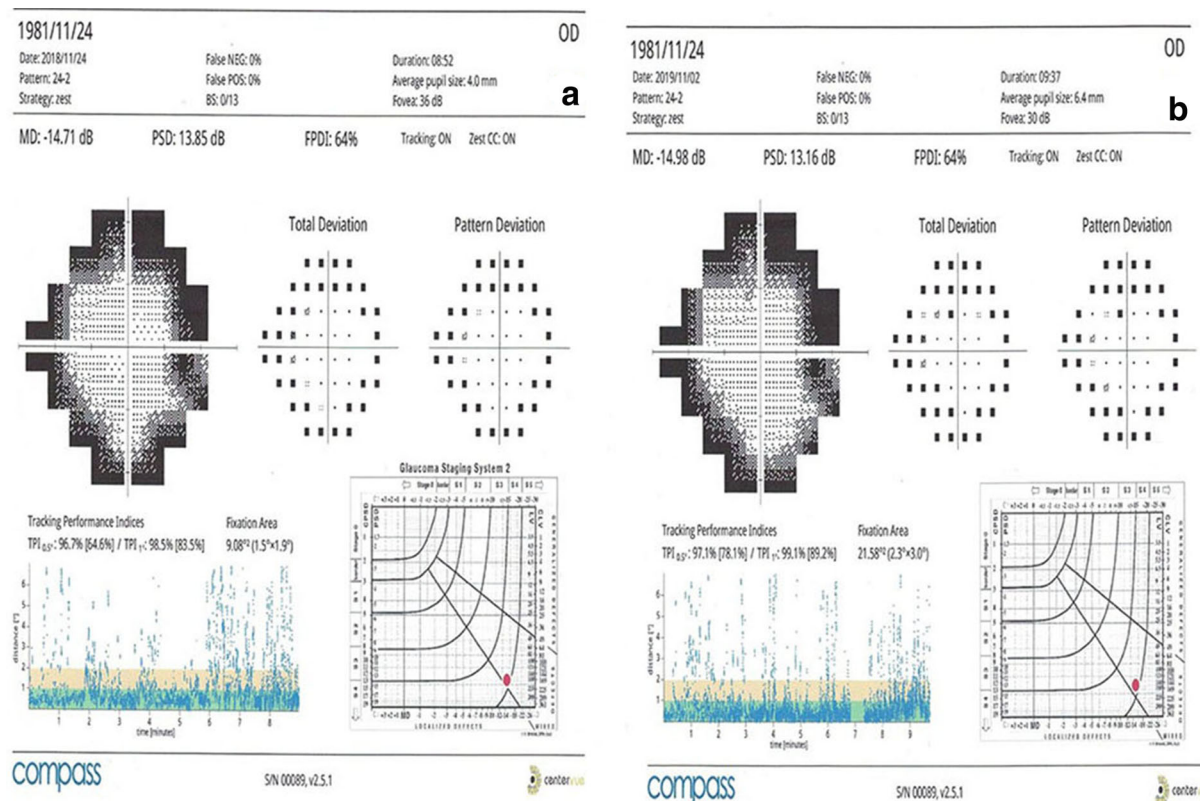
Fig. 9 Visual field FPDI changes of a patient with retinitis pigmentosa patient receiving only aPRP (Table 2, patient no. 2). **a** Before treatment, 64%. **b** The 13th month of follow-up post-treatment, 64%

uncomfortable condition except for temporary light sensitivity (which may last several days as a result of aPRP injection) and headache (which may last several hours as a result of rEMS application).

This retrospective clinical study has some limitations. The annual progression rate of retinitis pigmentosa varies depending on the type of genetic mutation. However, this issue was not analyzed here because the genetic mutation analysis of each patient could not be performed. Inflammatory findings were observed in some genetic mutation types of RP or in some stages of the disease. There were no measurements such as a laser flare meter regarding how aPRP or combined procedures affect the inflammatory response. The progression rate of each genetic type and the effects of interventional procedures on inflammation are additional research topics.
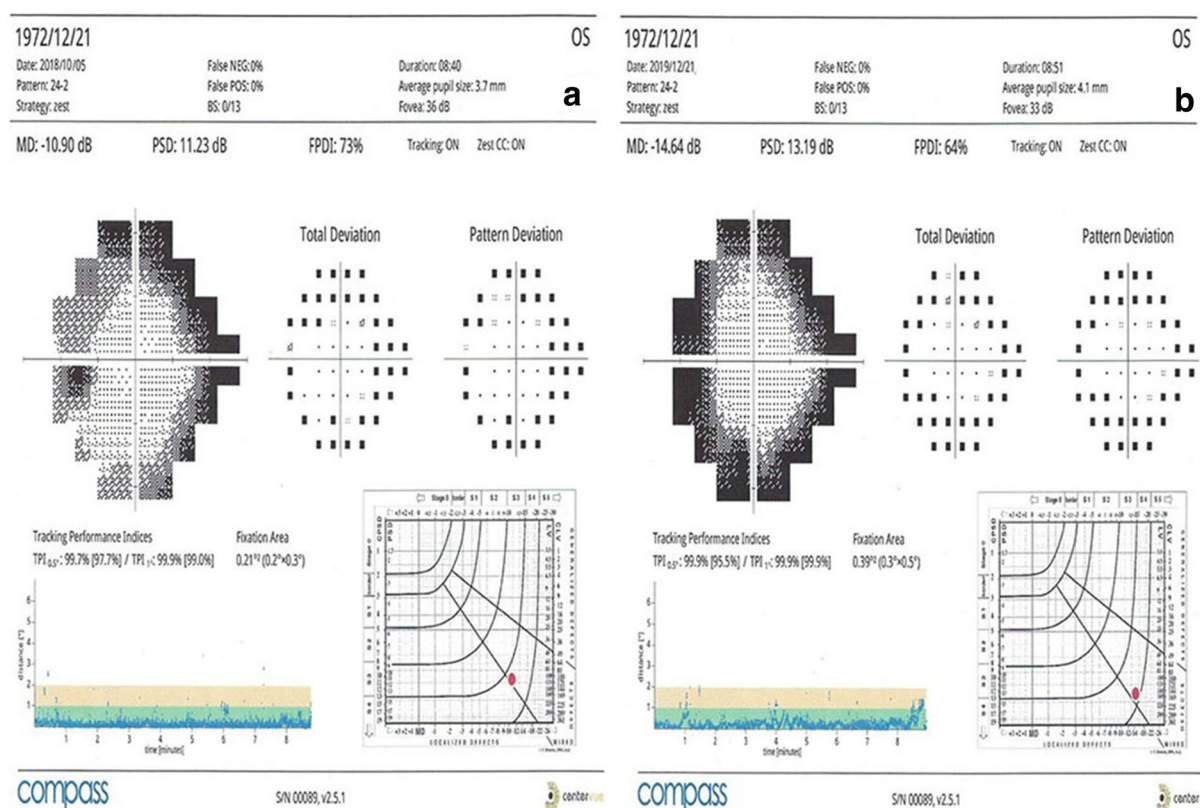
Fig. 10 Visual field FPDI changes of a patient with retinitis pigmentosa, natural course (Table 3, patient no. 1). **a** Before treatment, 73%. **b** The 13th month of follow-up post-treatment, 64%

CONCLUSION

Retinitis pigmentosa is a neurodegenerative genetic disorder with progressive photoreceptor loss. In recent years, growth factor injections, stem cell applications, or gene therapy options have come into clinical use to slow or stop disease progression. Platelet-rich plasma is a good source of growth factors, but its half-life is 4–6 months. aPRP might more effectively slow down photoreceptor loss when repeated as booster injections and combined with retinal electromagnetic stimulation.

ACKNOWLEDGEMENTS

Arslan and Emin Özmert have no conflicts of interest to disclose.

Compliance with Ethics Guidelines. Ethics committee approval for the transcranial electromagnetic stimulation study was obtained from the Ankara University Faculty of Medicine Clinical Research Ethics Committee (17-1177-18). This committe had already approved the GFs work (19-1293-18). The study was performed in accordance with the tenets of the 2013 Declaration of Helsinki. Written informed consent was obtained from the patients prior to enrollment.

Data Availability. The datasets generated during and/or analyzed during the study are available from the corresponding author on reasonable request.

REFERENCES

1. Ali MU, Rahman MSU, Cao J, Yuan PX. Genetic characterization and disease mechanism of retinitis pigmentosa; current scenario. 3 Biotech. 2017;7(4): 251–2.

2. Wang AL, Knight DK, Vu TT, Mehta MC. Retinitis pigmentosa: review of current treatment. Int Ophthalmol Clin. 2019;59:263–80. https://doi.org/10.1097/IIO.0000000000000256.

3. Zhang Q. Retinitis pigmentosa. Asia-Pac J Ophthalmol. 2016;5:265–71. https://doi.org/10.1097/apo.0000000000000227.

4. Hartong DT, Berson EL, Dryja TP. Retinitis pigmentosa. Lancet. 2006;368:1795–809. https://doi.org/10.1016/s0140-6736(06)69740-7.

5. Yoshida N, Ikeda Y, Notomi S, et al. Clinical evidence of sustained chronic inflammatory reaction in retinitis pigmentosa. Ophthalmology. 2013;120: 100–5. https://doi.org/10.1016/j.ophtha.2012.07.006.

6. Poornachandra B, Khurana AK, Sridharan P, et al. Quantifying microstructural changes in retinitis pigmentosa using spectral domain—optical coherence tomography. Eye Vis (Lond). 2019;15(6):13. https://doi.org/10.1186/s40662-019-0139-0.

7. Lima LH, Sallum JM, Spaide RF. Outer retina analysis by optical coherence tomography in cone-rod dystrophy patients. Retina. 2013;33:1877–80. https://doi.org/10.1097/IAE.0b013e31829234e6.

8. Anitua E, Muruzabal F, Tayebba A, et al. Autologous serum and plasma rich in growth factors in ophthalmology: preclinical and clinical studies. Acta Ophthalmol. 2015;93(8):e605–e614614.

9. Amable PR, Carias RB, Teixeira MV, et al. Platelet-rich plasma preparation for regenerative medicine: optimization and quantification of cytokines and growth factors. Stem Cell Res Ther. 2013;4(3):67.

10. Arslan U, Özmert E, Demirel S, Örnek F, Şermet F. Effects of subtenon-injected autologous platelet-rich plasma on visual functions in eyes with retinitis pigmentosa: preliminary clinical results. Graefes Arch Clin Exp Ophthalmol. 2018;256(5): 893–908. https://doi.org/10.1007/s00417-018-3953-5.

11. Özmert E, Arslan U. Management of deep retinal capillary ischemia by electromagnetic stimulation and platelet-rich plasma: preliminary clinical results. Adv Ther. 2019. https://doi.org/10.1007/s12325-019-01040-2.

12. Maziarz A, Kocan B, Bester M, et al. How electromagnetic fields can influence adult stem cells: positive and negative impacts. Stem Cell Res Ther. 2016;7:54. https://doi.org/10.1186/s13287-016-0312-5.

13. Parate D, Kadir ND, Celik C, et al. Pulsed electromagnetic fields potentiate the paracrine function of mesenchymal stem cells. Stem Cell Res Ther. 2020;11:46. https://doi.org/10.1186/s13287-020-1566-5.

14. Patruno A, Ferrone A, Costantini E, et al. Extremely low-frequency electromagnetic fields accelerates wound healing modulating MMP-9 and inflammatory cytokines. Cell Prolif. 2018;51(2):e12432. https://doi.org/10.1111/cpr.12432.

15. Demetriades AM, Deering T, Liu H, et al. Transscleral delivery of antiangiogenic proteins. J Ocul Pharmacol Ther. 2008;24(1):70–9. https://doi.org/10.1089/jop.2007.0061.

16. Meng T, Kulkarni V, Simmers R, Brar V, Xu Q. Therapeutic implications of nanomedicine for ocular drug delivery. Drug Discov Today. 2019. https://doi.org/10.1016/j.drudis.2019.05.00.

17. Li SK, Hao J. Transscleral passive and iontophoretic transport: theory and analysis. Expert Opin Drug Deliv. 2017;15(3):283–99. https://doi.org/10.1080/17425247.2018.1406918.

18. Luo J, Zheng H, Zhang L, et al. High-frequency repetitive transcranial magnetic stimulation (rTMS)

improves functional recovery by enhancing neurogenesis and activating BDNF/TrkB signaling in ischemic rats. Int J Mol Sci. 2017;18(2):455. https://doi.org/10.3390/ijms18020455.

19. Mysona BA, Zhao J, Bollinger KE. Role of BDNF/TrkB pathway in the visual system: therapeutic implications for glaucoma. Expert Rev Ophthalmol. 2017;12(1):69–81.

20. Takahashi VKL, Takiuti JT, Carvalho-Jr JRL, et al. Fundus autofluorescence and ellipsoid zone (EZ) line width can be an outcome measurement in RHO-associated autosomal dominant retinitis pigmentosa. Graefes Arch Clin Exp Ophthalmol. 2019;257:725–31. https://doi.org/10.1007/s00417-018-04234-6.

21. Cai CX, Locke KG, Ramachandran R, Birch DG, Hood DC. A comparison of progressive loss of the ellipsoid zone (EZ) band in autosomal dominant and x-linked retinitis pigmentosa. Invest Ophthalmol Vis Sci. 2014;23(55):7417–22. https://doi.org/10.1167/iovs.14-15013.

22. Sandberg MA, Rosner B, Weigel-DiFranco C, Dryja TP, Berson EL. Disease course of patients with X-linked retinitis pigmentosa due to RPGR gene mutations. Invest Ophthalmol Vis Sci. 2007;48:1298–304.

23. Takahashi VKL, Xu CL, Takiuti JT, et al. Comparison of structural progression between ciliopathy and non-ciliopathy associated with autosomal recessive retinitis pigmentosa. Orphanet J Rare Dis. 2019;14:187. https://doi.org/10.1186/s13023-019-1163-9.

24. Friberg TR. Natural course of retinitis pigmentosa over a three-year interval. Am J Ophthalmol. 1985;100(4):621–2.

25. Birch DG, Anderson JL, Fish GE. Yearly rates of rod and cone functional loss in retinitis pigmentosa and cone-rod dystrophy. Ophthalmology. 1999;106:258–68.

26. Fuhrmann S, Zou CJ, Levine EM. Retinal pigment epithelium development, plasticity, and tissue homeostasis (Invited review for Experimental Eye Research). Exp Eye Res. 2014;123:141–50. https://doi.org/10.1016/j.exer.2013.09.003.

27. Strauss O. The retinal pigment epithelium in visual function. Physiol Rev. 2005;85:845–81. https://doi.org/10.1152/physrev.00021.2004.

28. Cacares PS, Boulan ER. Retinal pigment epithelium polarity in health and blinding diseases. Curr Opin Cell Biol. 2020;62:37–45.

29. Dalvi S, Galloway CA, Singh R. Pluripotent stem cells to model degenerative retinal diseases: the RPE perspective. In: Bharti K, editor. Pluripotent stem cells in eye disease therapy, advances in experimental medicine and biology. Cham: Springer Nature Switzerland; 2019. p. 1186. https://doi.org/10.1007/978-3-030-28471-8.

30. Collins MK, Perkins GR, Rodriguez-Tarduchy G, Nieto MA, López-Rivas A. Growth factors as survival factors: regulation of apoptosis. Bioessays. 1994;16(2):133–8.

31. Julian JL, Bauer DE, Kong M, et al. Growth factor regulation of autophagy and cell survival in the absence of apoptosis. Cell. 2005;120(2):237–48.

32. Munder MC, Midtvedt D, Franzmann T, et al. A pH-driven transition of the cytoplasm from a fluid- to a solid-like state promotes entry into dormancy. eLife. 2016;5:e09347.

33. Koenekoop RK. Why some photoreceptors die, while others remain dormant: lessons from RPE65 and LRAT associated retinal dystrophies. Ophthalmic Genet. 2011;32:126–8.

34. Wang W, Lee SJ, Scott PA, et al. Two-step reactivation of dormant cones in retinitis pigmentosa. Cell Rep. 2016;15:372–85.

35. Papait A, Cancedda R, Mastrogiacomo M, Poggi A. Allogeneic platelet-rich plasma affects monocyte differentiation to dendritic cells causing an anti-inflammatory microenvironment, putatively fostering wound healing. Tissue Eng Regen Med. 2018;12(1):30–433. https://doi.org/10.1002/term.2361.

36. Reed GL, Fitzgerald ML, Polgár J. Molecular mechanisms of platelet exocytosis: insights into the B secrete life of thrombocytes. Blood. 2000;96(10):3334–42.

37. Anitua E, Muruzabal F, AlcaldeI M-L, Orive G. Plasma rich in growth factors (PRGFs-Endoret) stimulates corneal wound healing and reduces haze formation after PRK surgery. Exp Eye Res. 2013;115:153–61.

38. Limoli PG, Limoli C, Vingolo EM, Scalinci SZ, Nebbioso M. Cell surgery and growth factors in dry age-related macular degeneration: visual prognosis and morphological study. Oncotarget. 2016;7(30):46913–23.

39. Chandra T, Chavhan GB, Sze RW, et al. Practical considerations for establishing and maintaining a magnetic resonance imaging safety program in a pediatric practice. Pediatr Radiol. 2019;49(4):458–68. https://doi.org/10.1007/s00247-019-04359-8.

40. Wu Z, Medeiros FA. Recent developments in visual field testing for glaucoma. Curr Opin Ophthalmol. 2018;29(2):141–6. https://doi.org/10.1097/ICU.0000000000000461.

41. Michalakis S, Schäferhoff K, Spiwoks-Becker I, et al. Characterization of neurite outgrowth and ectopic synaptogenesis in response to photoreceptor dysfunction. Cell Mol Life Sci. 2013;70(10):1831–47.

Regenerative Medicine

Treatment of resistant chronic central serous chorioretinopathy via platelet-rich plasma with electromagnetic stimulation

Umut Arslan*,[1] [ID] & Emin Özmert[2]

[1]Ankara University Technopolis, Ankara, Turkey
[2]Ankara University Faculty of Medicine Department of Ophthalmology, Ankara, Turkey
*Author for correspondence: Tel.: +90 312 284 4313; drumutarslan@hotmail.com

Background: To evaluate whether subtenon injection of platelet-rich plasma (PRP) with retinal electromagnetic stimulation (rEMS) is effective in therapy-resistant chronic central serous chorioretinopathy (CSCR). **Design:** Prospective, sequential. **Materials & methods:** The study included 22 eyes with resistant chronic CSCR. Cases receiving micropulse laser or additional photodynamic therapy, subtenon PRP, and subtenon PRP + rEMS were classified as times 1, 2 and 3, respectively. **Results:** At time 3, the mean best-corrected visual acuity was 85.7 and 97.0 letters before and after the procedures, respectively (p = 0.01). Submacular thickness improved by 17, 27 and 51% at times 1, 2 and 3 respectively. **Conclusion:** For treating resistant CSCR, subtenon PRP + rEMS should be considered as an effective and safe option.

Trial Registration: ClinicalTrials.gov ID: NCT04224831

Central serous chorioretinopathy (CSCR) is a mostly unilateral retinal disorder that predominantly affects middle-aged men. Serous neuroretinal detachment occurs due to fluid accumulation in the submacular area via leakage through the damaged retinal pigment epithelium (RPE) layer [1,2]. The main risk factors for CSCR are emotional stress (type A personality), systemic arterial hypertension, corticosteroid use, sympathomimetic drug use, pregnancy, Cushing's syndrome, the presence of large choroid vessels under the RPE layer and an increase in choroidal thickness (pachychoroid) [3]. CSCR may be classified as acute or chronic. The acute form regresses spontaneously without causing damage; the chronic form progresses and some subretinal fluid can persist. Vision prognosis is worse if serous retinal detachment continues for more than 3–6 months because of the progressive photoreceptor loss [2,4]. In chronic CSCR, widespread RPE changes and diffuse multifocal hyperfluorescent areas are seen in fluorescein angiography (FA) and indocyanine green angiography (ICGA) [1,2]. In etiopathogenesis, RPE cells, choroidea or both are thought to be dysfunctional. Various treatments – including acetazolamide, mineralocorticoid receptor antagonists, intravitreal anti-VEGF injections, subthreshold micropulse laser (MPL) applications and photodynamic therapy (PDT) – are used depending on the stage of the disease [5,6]. However, some cases may be resistant or unresponsive to treatment due to the complex etiopathogenesis. New treatment options and approaches are needed to reduce serious complications. In addition to choroidal congestion, deep retinal capillary ischemia and widespread RPE dysfunction contribute to the pathogenesis of therapy-resistant chronic CSCR [4,7]. Deep retinal capillary ischemia and RPE dysfunction can be treated with restorative-regenerative growth factors [8].

Platelets are enucleated cells that produce several growth factors (GFs), including epithelial, fibroblast, transforming, nerve, platelet-derived and insulin-like. GFs and their receptors, expressed in epithelial and endothelial cells, play a key role in tissue healing. EGF stimulates the proliferation and migration of epithelial cells. NGF is a neurotrophin that stimulates the growth and maintenance of intraretinal glial cells, Müller cells, and neurons [9,10]. Platelet-rich plasma (PRP) contains many GFs and autologous PRP (aPRP) is used in the treatment of retinitis

Future Medicine

pigmentosa and deep retinal capillary ischemia; such treatment has produced promising functional and structural improvements [8,11].

Repetitive high-frequency electromagnetic stimulation/iontophoresis (rEMS/IP) is a physical treatment method that promotes wound healing and epithelialzation by increasing the synthesis and affinity of the tyrosine kinase (Trk) receptor and local blood flow [13]. Moreover, it improves epithelial integrity and neural function by altering the balance of GFs and Trk receptor activity in the damaged microenvironment [13–16]. However, the iontophoresis may increase the passage of active molecules at the tissue level [17–20]. Positive results can be obtained by combining rEMS/IP and aPRP in deep retinal capillary ischemia resulting from various etiologies and without a known treatment [8].

In this prospective clinical study, different treatment methods were compared as sequential phases. The goal was to demonstrate the effectiveness of rEMS/IP and to use subtenon aPRP as a new treatment approach in eyes with chronic CSCR, where current treatment methods are insufficient.

Materials & methods

Approval for the study was obtained from the Ankara University Medical School Clinical Research Ethics Committee (17-1177-18) and Republic of Turkey Ministry of Health Drug and Medical Device Department (2018-136). This research was carried out in accordance with the principles of the Helsinki Declaration. Written consent forms were obtained from the patients before starting the study.

This prospective, open-label, sequentially controlled clinical study in a single group was conducted between December 2018 and September 2019 at Ankara University Faculty of Medicine, Department of Ophthalmology. The study group consisted of 22 unilateral eyes of 22 patients with chronic CSCR who were resistant or unresponsive to current treatment methods.

Diagnostic criteria for chronic CSCR in patients with typical complaints & clinical history

1. The presence of chronic subretinal fluid and elongated outer segments of the photoreceptors on B-scan spectral domain optical coherence tomography (OCT) (Heidelberg-RA2, SW-FAF 488 nm, Germany);
2. Widespread atrophic changes in the RPE layer and/or the presence of serous pigment epithelial detachment (PED);
3. Presence of thick choroid or wide choroid vessels (pachychoroid) on enhanced depth imaging spectral domain OCT;
4. A typical view of the boundaries between chronic subretinal fluid and hyperfluorescent fluorophores in the fundus autofluorescence examination;
5. FA and ICGA examinations were performed simultaneously to detect choroidal neovascularization (CNV) or polypoidal choroidal vasculopathy in suspect eyes with flat irregular PED and chronic subretinal fluid.

Subjects

Inclusion criteria

Eyes with chronic CSCR containing one or more of the following findings constituted the study group (22 unilateral eyes of 22 patients):

1. Symptoms lasting longer than 6 months with relapses.
2. The eyes do not respond or are resistant to all known current treatment methods, including half-fluence PDT and sub-threshold MPL or drugs (acetazolamide, mineralocorticoid receptor antagonists).
3. Presence of widespread RPE changes, atrophic foci and chronic serous retinal detachment areas in the macula and/or outside the macula.

Exclusion criteria

1. Presence of CNV secondary to chronic CSCR;
2. Presence of cataract or dense vitreous opacities (capillary density measurement cannot be done correctly in these cases);
3. Patients taking oral corticosteroids or mineralocorticoid receptor antagonists;
4. The eyes respond well to MPL or PDT.

Time frame

Time 1

MPL was first applied to patients with symptoms lasting for more than 6 months, with chronic signs. Cases with good response to MPL were excluded from the study. We waited at least 3 months for the response to MPL. PDT was performed on MPL-resistant cases. Cases that responded well to PDT were excluded from the study. At least 3 months passed before the response to PDT.

Time 2

Only subtenon aPRP injection was applied to MPL- or PDT-resistant cases. PRP injection was performed three times at 2-week intervals. Patients who responded well after three PRP injections in 1 month were excluded from the study.

Time 3

rEMS/IP combined with subtenon aPRP injection was applied to aPRP-resistant cases. At least 1 month was allowed to elapse after the last aPRP injection. In this group, rEMS/IP was applied daily for 30 min on 10 consecutive days. Subtenon PRP injections were applied on the 1st, 5th and 10th days of the 10-day therapy (a total of three injections). Responses to treatment were evaluated in the first month after the procedures.

We then evaluated new treatment methods applied to the study group at three times according to the 'sequential processes' method [21,22]. The cases were analyzed in three consecutive stages:

Stage 1

This consisted of 22 eyes of 22 patients with chronic symptoms lasting more than 6 months. MPL or, if required, PDT was applied to this group. Necessary consultations for the underlying cause were requested (Table 1).

Stage 2

This was a consecutive group of 22 eyes of 22 patients who did not respond to classical treatments. Subtenon fresh aPRP injections were applied to this group for three sessions at 2-week intervals (Table 2).

Stage 3

This was a consecutive group of 22 eyes of 22 patients who did not respond to aPRP injections. This group received rEMS/IP application for 10 consecutive days and subtenon aPRP injections on the 1st, 5th, and 10th days (Table 3).

The formation of the time 1, 2 and 3 groups after the inclusion and exclusion criteria were applied is seen in the flow diagram (Figure 1).

Two new treatment methods were applied and evaluated over approximately 10 months to a single study group in consecutive stages. Treatment efficacy was compared within and between time groups. Complete ophthalmologic examination was performed on all patients. Best-corrected visual acuity (BCVA) was measured using Early Treatment Diabetic Retinopathy Study cards (Topcon CC 100 XP, Japan). Changes after treatments were evaluated simultaneously via multimodal imaging using the optic coherence tomography angiography (OCTA) device (Optovue Inc., CA, USA). Projection artifacts were removed by activating the 'artifact removal' function of the OCTA device. Thus deep capillary density could be measured accurately.

Quantitative follow-up parameters

1. Submacular thickness (SMT, μm): the space between the ellipsoid zone and Bruch's membrane, manually measured where the volume of the submacular fluid is the highest.
2. Central macular thickness (CMT, μm): the macular thickness between the internal limiting membrane and Bruch's membrane, automatically measured using an OCTA device.
3. Deep retinal capillary density (DRCD, %): automatically calculated using the 'AngioAnalytic' software of the OCTA device and displayed as a sequential density map. The 'Link-B Scans' function of the device was activated to compare vessel densities in exactly the same sections during follow-up.

The primary outcome measure of the study is the difference in BCVA as an indicator of functional changes. Secondary outcome measures are the differences in SMT, CMT and DRCD, which represent structural changes.

					SMT (μm)		CMT (μm)		DRCD (%)		BCVA[†]	
No	**Age (years)/sex**	**Application**	**Medical status**	**Eye (n = 22)**	**Before**	**After**	**Before**	**After**	**Before**	**After**	**Before**	**After**
1	47 M	MPL + PDT	Hypertension Type A	R	312	220	426	334	57.7	40.7	35	35
2	45 M	MPL + PDT	Hypertension Type A	L	380	321	482	419	54.4	33.6	92	80
3	28 M	MPL	Type A personality	L	479	350	570	456	55.0	54.4	94	94
4	59 M	MPL + PDT	Obstructive lung Steroid use	R	270	202	373	305	50.8	45.0	74	70
5	48 M	MPL	Type A personality	L	292	236	384	338	46.6	45.9	80	80
6	44 M	MPL	Hypertension Type A	L	478	376	582	480	50.1	47.9	80	90
7	45 F	MPL	Rheumatoid arthritis Steroid use	L	332	242	421	335	49.6	49.2	74	74
8	51 F	MPL	Brucella arthritis Steroid use	R	257	186	389	311	44.3	43.5	15	20
9	41 M	MPL + PDT	Hypertension Type A personality	R	344	291	466	433	59.8	50.4	91	80
10	46 M	MPL	Type A personality	L	351	322	407	386	55.9	55.9	95	95
11	43 M	MPL	Ulcerative colitis Steroid use	L	404	381	552	537	53.5	52.0	70	80
12	34 M	MPL	Type A personality	L	310	247	421	361	59.8	58.9	92	92
13	35 M	MPL	Bronchial asthma Steroid use	L	151	150	327	325	49.2	47.9	92	92
14	60 F	MPL + PDT	Obstructive lung Steroid use	R	265	232	416	386	45.2	40.7	80	70
15	49 M	MPL + PDT	Hypertension Type A	R	247	132	356	244	50.2	46.2	74	70
16	37 M	MPL	Chronic urticaria Steroid use	R	401	317	497	397	56.9	54.1	80	80
17	52 F	MPL	Fibromyalgia Steroid use	R	408	311	509	432	58.7	55.1	80	80
18	42 M	MPL	Type A personality	R	220	197	396	357	51.5	51.1	80	80
19	36 M	MPL	Hypertension	L	593	490	716	601	46.5	46.3	92	92
20	49 M	MPL	Chronic urticaria Steroid use	R	242	226	341	321	50.1	50.9	98	100
21	39 M	MPL	Hypertension Hypothyroid	L	307	312	409	416	48.8	48.0	94	100
22	46 M	MPL	Hypertension	R	298	291	401	390	54.1	54.2	100	100

Table 1. Time 1: demographic and medical data and treatment response parameters for patients with chronic central serous chorioretinopathy who underwent photodynamic therapy after micropulse laser or micropulse laser.

[†] Measured using the Early Treatment Diabetic Retinopathy Study letters.

BCVA: Best-corrected visual acuity; CMT: Central macular thickness; DRCD: Deep retinal capillary density; MPL: Micropulse laser; PDT: Photodynamic therapy; SMT: Submacular thickness.

PRP preparation & application

20 ml of blood was taken from the antecubital vein of the patients and placed into two sterile sodium citrate PRP tubes (T-LAB Kit, T-Biotech, Turkey). The PRP tubes were centrifuged in a refrigerated (4.0°C) centrifuge (1200 NF, Nüve Technology Turkey) at 2500 rpm for 8 min. The lower one-third of the upper plasma was drawn into a 2.5-ml sterile syringe. This plasma is rich in GFs. For each application, 1.5 ml of fresh aPRP suspension was injected into the subtenon space under topical anesthesia. Injections were performed under sterile conditions with a 26G needle tip from the upper temporal region, which was preferred due to its large absorption area and easy access.

Table 2. Time 2: consecutive central serous chorioretinopathy cases that were resistant to classical treatment modalities and given only subtenon autologous platelet-rich plasma injections.

No	Age (years)/sex	Application	Eye (n = 22)	SMT (μm)		CMT (μm)		DRCD (%)		BCVA[†]	
				Before	After	Before	After	Before	After	Before	After
1	47 M	PRP	R	220	198	334	298	40.7	56.1	35	50
2	45 M	PRP	L	321	202	419	301	33.6	34.7	80	90
3	28 M	PRP	L	350	242	456	347	54.4	58.2	94	100
4	59 M	PRP	R	202	114	305	216	45.0	51.4	70	74
5	48 M	PRP	L	236	141	338	241	45.9	50.1	80	85
6	44 M	PRP	L	376	291	480	391	47.9	51.3	90	100
7	45 F	PRP	L	242	164	335	252	49.2	51.6	74	80
8	51 F	PRP	R	186	134	311	239	43.5	50.2	20	30
9	41 M	PRP	R	291	239	433	381	50.4	60.0	80	85
10	46 M	PRP	L	322	238	386	293	55.9	57.9	95	100
11	43 M	PRP	L	381	299	537	441	52.0	54.1	80	85
12	34 M	PRP	L	247	151	361	272	58.9	60.0	92	100
13	35 M	PRP	L	150	136	325	301	47.9	50.0	92	95
14	60 F	PRP	R	232	135	386	281	40.7	43.3	70	80
15	49 M	PRP	R	132	110	244	221	46.2	49.7	70	74
16	37 M	PRP	R	317	237	397	322	54.1	58.9	80	90
17	52 F	PRP	R	311	182	432	288	55.1	58.5	80	85
18	42 M	PRP	R	197	171	357	322	51.1	52.6	80	90
19	36 M	PRP	L	490	296	601	424	46.3	50.9	92	92
20	49 M	PRP	R	226	198	321	292	50.9	51.4	100	100
21	39 M	PRP	L	312	216	416	317	48.0	51.6	100	100
22	46 M	PRP	R	291	246	390	344	54.2	56.0	100	100

[†] Measured using the Early Treatment Diabetic Retinopathy Study letters.

BCVA: Best-corrected visual acuity; CMT: Central macular thickness; DRCD: Deep retinal capillary density; PRP: Platelet-rich plasma; SMT: Submacular thickness.

rEMS/IP

rEMS/IP was applied in the form of a helmet with a medical device containing coils designed to stimulate the retina, optic nerve and visual pathways (Magnovision MG10, Bioretina Biyoteknoloji, Turkey). rEMS/IP was applied just before PRP with an electromagnetic field intensity of 2000 mG at 42 Hz for 30 min. These parameters were determined to be effective and safe in clinical and preclinical studies and are recommended by the manufacturer.

Statistical analysis

Mean changes in BCVA, SMT, CMT and DRCD values were calculated as standard deviation. Here, a paired Wilcoxon test analysis was performed to examine the pre- and post-treatment measurements of the group. The Kruskal–Wallis test was performed to examine differences between pre- and post-treatment measurements according to different groups. In order to identify different groups, a double comparison was made using the Mann–Whitney U test. The study was carried out using the SPSS 22.00 package (IBM Corp, NY, USA). The critical decision-making value α was set at 0.05.

Results

The study group consisted of 22 unilateral eyes of 22 patients who did not respond or were resistant to various treatments (16 eyes MPL, 6 eyes MPL + PDT). The aPRP and rEMS/IP methods were applied at time 3 and compared with consecutive stages. Eighteen patients were male and four were female; their mean age was 44.4 years (range: 28–60). Eight patients had systemic diastolic hypertension and nine had a history of cortisone use for chronic diseases. Type A personality was seen in 10 of 22 patients. All cases had chronic CSCR sequelae findings in the fellow eye, such as an RPE irregularity or pachydrusen.

Table 3. Time 3; consecutive central serous chorioretinopathy cases that did not respond after subtenon autologous platelet-rich plasma injection and applied autologous platelet-rich plasma in combination with retinal electromagnetic stimulation/iontophoresis.

No	Age (years)/sex	Application	Eye (n = 22)	SMT (μm)		CMT (μm)		DRCD (%)		BCVA†	
				Before	After	Before	After	Before	After	Before	After
1	47 M	rEMS/IP + PRP	R	198	96	298	218	56.1	56.7	50	70
2	45 M	rEMS/IP + PRP	L	202	124	301	243	34.7	56.7	90	110
3	28 M	rEMS/IP + PRP	L	242	86	347	224	58.2	63.2	100	110
4	59 M	rEMS/IP + PRP	R	114	77	216	146	51.4	57.0	74	89
5	48 M	rEMS/IP + PRP	L	141	88	241	202	50.1	55.0	85	91
6	44 M	rEMS/IP + PRP	L	291	89	391	219	51.3	56.9	100	110
7	45 F	rEMS/IP + PRP	L	164	79	252	180	51.6	55.6	80	83
8	51 F	rEMS/IP + PRP	R	134	94	239	206	50.2	61.5	30	45
9	41 M	rEMS/IP + PRP	R	239	87	381	233	60.0	60.4	85	100
10	46 M	rEMS/IP + PRP	L	238	82	293	226	57.9	59.9	100	110
11	43 M	rEMS/IP + PRP	L	299	96	441	257	54.1	58.0	85	85
12	34 M	rEMS/IP + PRP	L	151	81	272	217	60.0	60.2	100	110
13	35 M	rEMS/IP + PRP	L	136	90	301	225	50.0	57.7	95	97
14	60 F	rEMS/IP + PRP	R	135	86	281	193	43.3	50.7	80	89
15	49 M	rEMS/IP + PRP	R	110	82	221	186	49.7	54.2	74	83
16	37 M	rEMS/IP + PRP	R	237	102	322	238	58.9	61.0	90	110
17	52 F	rEMS/IP + PRP	R	182	97	288	222	58.5	62.5	85	91
18	42 M	rEMS/IP + PRP	R	171	88	322	227	52.6	57.1	90	110
19	36 M	rEMS/IP + PRP	L	296	71	424	224	50.9	54.9	92	110
20	49 M	rEMS/IP + PRP	R	198	90	292	201	51.4	54.9	100	110
21	39 M	rEMS/IP + PRP	L	216	84	317	216	51.6	57.0	100	110
22	46 M	rEMS/IP + PRP	R	246	87	344	201	56.0	58.2	100	110

†Measured using the Early Treatment Diabetic Retinopathy Study letters.
BCVA: Best-corrected visual acuity; CMT: Central macular thickness; DRCD: Deep retinal capillary density; PRP: Platelet-rich plasma; rEMS/IP: Retinal repetitive electromagnetic stimulation/iontophoresis; SMT: Submacular thickness.

BCVA

At time 1, mean BCVA was 80.1 and 79.7 letters before and after the classical treatment procedures were applied, respectively (p = 0.81). At time 2, mean BCVA was 79.7 and 85.7 letters before and after the aPRP application, respectively (p = 0.72). At time 3, mean BCVA was 85.7 and 97.0 letters before and after the application of aPRP combined with rEMS/IP, respectively (p = 0.01; Δp 3 >1,2) (Tables 1–5). In fellow eyes, mean BCVA was 97 and 97 letters at times 1 and 3, respectively.

SMT

At time 1, mean SMT was 333.7 and 274.2 μm before and after the classical treatment procedures, respectively (p = 0.01). At time 2, mean SMT was 274.2 and 198.1 μm before and after the aPRP applications, respectively (p = 0.01). At time 3, mean SMT was 198.1 and 88.9 μm before and after applying aPRP combined with rEMS/IP, respectively (p = 0.01). A comparison of SMT percentage change showed a 17% improvement at time 1, 27% at time 2, and 51% at time 3 (Δp 3 >2,1). In 19/22 eyes (86.4%), the submacular fluid disappeared completely at time 3 (Figures 2–6, Tables 1–5). In fellow eyes, mean SMT was 90.1 and 90.2 μm at times 1 and 3, respectively.

CMT

At time 1, mean CMTs were 447.3 and 389.7 μm before and after the classical treatment procedures, respectively (p = 0.01). At time 2, mean CMTs were 389.7 and 310.6 μm before and after the aPRP application, respectively (p = 0.01). At time 3, mean CMTs were 310.6 and 213.8 μm before and after applying aPRP combined with rEMS/IP, respectively (p = 0.01). When the CMT percentage changes were compared, a 13% improvement at time
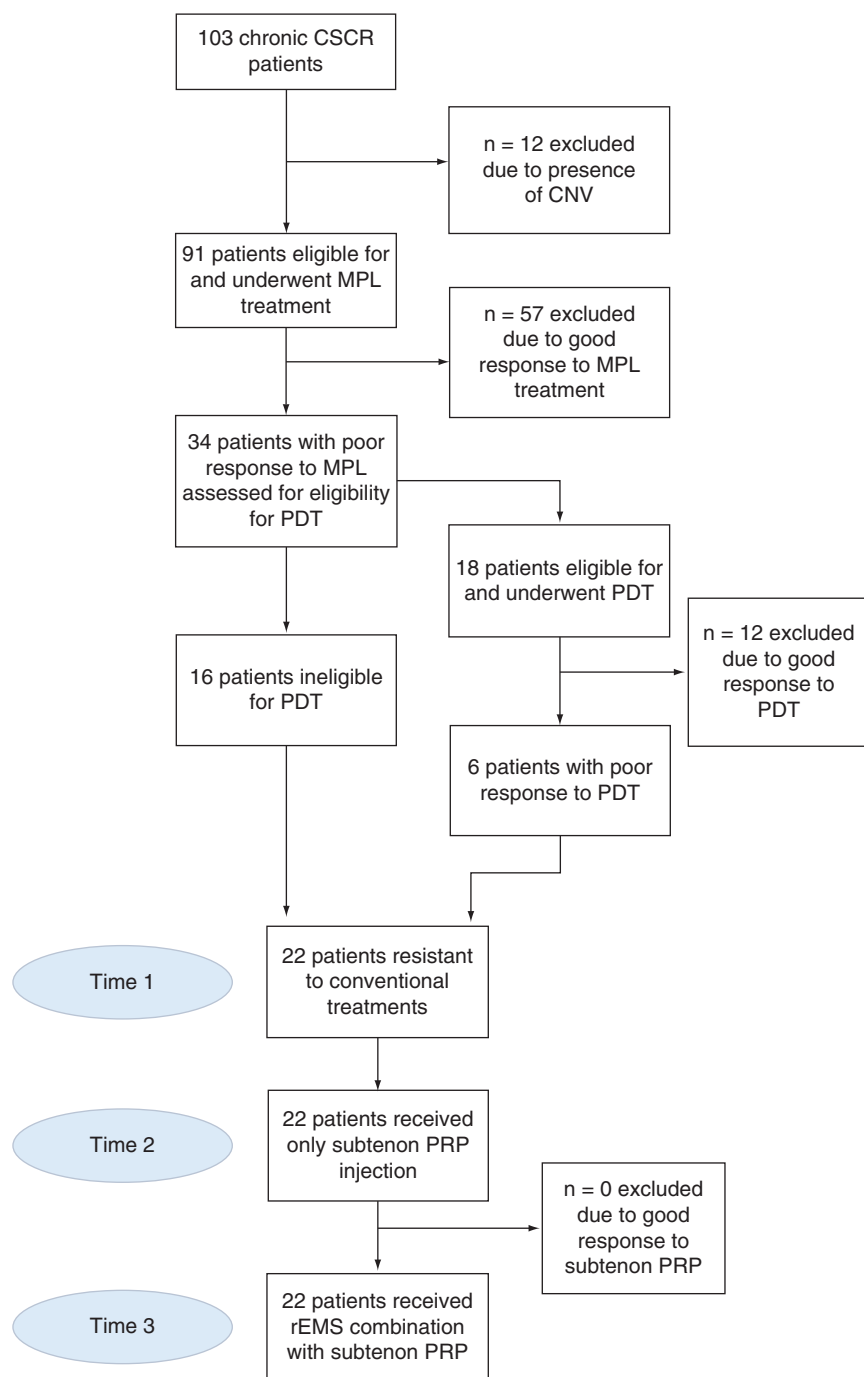
Figure 1. Flow diagram illustrating the formation of the time groups after inclusion and exclusion criteria were applied.
CSCR: Central serous chorioretinopathy; CNV: Choroidal neovascularization; MPL: Micropulse laser; PDT: Photodynamic therapy; PRP: Platelet-rich plasma; rEMS: Retinal repetitive electromagnetic stimulation.

1, 20% at time 2 and 30% at time 3 (Δp 3 >2,1) was observed (Figures 2–6, Tables 1–5). In fellow eyes, mean CMTs were 221.0 and 223.2 µm at times 1 and 3, respectively.

DRCD

At time 1, mean DRCDs were 52.2 and 48.7% before and after the classical treatment procedures, respectively (p = 0.03). At time 2, mean DRCDs were 48.7 and 52.7% before and after the aPRP applications, respectively (p =

Table 4. Comparison of follow-up parameters within and between groups.

Times	Time 1 Classical treatments		Time 2 Only aPRP		Time 3 aPRP + rEMS/IP		p-value
Follow-up parameters	Before	After	Before	After	Before	After	
SMT (μm)	333.7	274.2	274.2	198.1	198.1	88.9	**3 >2,1**
	p = 0.01		p = 0.01		p = 0.01		
CMT (μm)	447.3	389,7	389.7	310.6	310.6	213.8	**3 >2,1**
	p = 0.01		p = 0.01		p = 0.01		
DRCD (%)	52.2	48.7	48.7	52.7	52.7	57.7	**3,2 >1**
	p = 0.03		p = 0.01		p = 0.01		
BCVA†	80.1	79.7	79.7	85.7	85.7	97.0	**3 >1,2**
	p = 0.81		p = 0.72		p = 0.01		

Kruskal–Wallis test was used for triple comparison; Mann–Whitney *U* test was used for binary comparison. p-value comparison: All parameters were significantly higher in time 3.
† Measured using the Early Treatment Diabetic Retinopathy Study letters.
aPRP: Autologous platelet-rich plasma; BCVA: Best-corrected visual acuity; CMT: Central macular thickness; DRCD: Deep retinal capillary density; rEMS/IP: Retinal repetitive electromagnetic stimulation/iontophoresis; SMT: Submacular thickness.

Table 5. Comparison of percentage and delta changes between groups.

SMT difference (%)			p-value	Comparison
Time 1 (n = 22)	Time 2 (n = 22)	Time 3 (n = 22)		
X ± s.d	X ± s.d	X ± s.d	0.01	**3 >2,1**
17±11	27±11	**51±15**		
CMT difference (%)				
X ± s.d	X ± s.d	X ± s.d	0.01	**3 >2,1**
13±8	20±8	**30±9**		
DRCD difference (%)				
X ± s.d	X ± s.d	X ± s.d	0.01	**3,2 >1**
−3.5 ± 2.6	**+4.0 ± 2.4**	**+5.1 ± 2.4**		
BCVA difference†				
X ± s.d	X ± s.s.	X ± s.s.	0.01	**3 >1,2**
0.4 ± 1.1	6 ± 1.3	**11.3 ± 1.2**		

Kruskal–Wallis test was used for triple comparison; Mann–Whitney U test was used for binary comparison.
p < 0.05 statistically significant, expressed in bold and italics.
†Measured using the Early Treatment Diabetic Retinopathy Study letters.
BCVA: Best-corrected visual acuity; CMT: Central macular thickness; DRCD: Deep retinal capillary density; s.d: Standart deviation; SMT: Submacular thickness (%)

0.01). At time 3, mean DRCDs were 52.7 and 57.7% before and after applying aPRP combined with rEMS/IP, respectively (p = 0.01). The DRCD percentage changed by –3.5% at time 1, +4% at time 2 and +5% at time 3 (Δp 3,2 >1) (Figures 2–5, Tables 1–5). In fellow eyes, mean DRCDs were 55.2 and 56.4% at times 1 and 3, respectively.

No serious ocular or systemic adverse events were encountered during the follow-up in any group related to rEMS/IP or aPRP applications.

Discussion

Acute and chronic CSCR differ in clinical presentation and prognosis. In acute CSCR a sudden deterioration in central vision occurs as a result of rapid accumulation of fluid in the submacular area. Impairments in color vision and dark adaptation, central or paracentral scotoma and metamorphopsia or micropsia are also observed [2,5]. The acute form usually heals spontaneously and without sequelae, but if the chronic form is not treated, progressive vision loss develops. The outer segments of the photoreceptor may appear elongated on B-scan spectral domain OCT. Flat irregular PEDs may be surrounded by subretinal fluid containing fibrin/fluorophore [4,7,12]. Diffuse RPE irregularities, intraretinal fluid accumulation, cystic retinal changes, retinal atrophy, subretinal fibrinous accumulation, fibrosis and secondary CNV are late complications and can cause permanent visual loss [1–3,6–8]. The pathophysiology of CSCR is not fully understood. RPE dysfunction and loss of integrity may be due to the
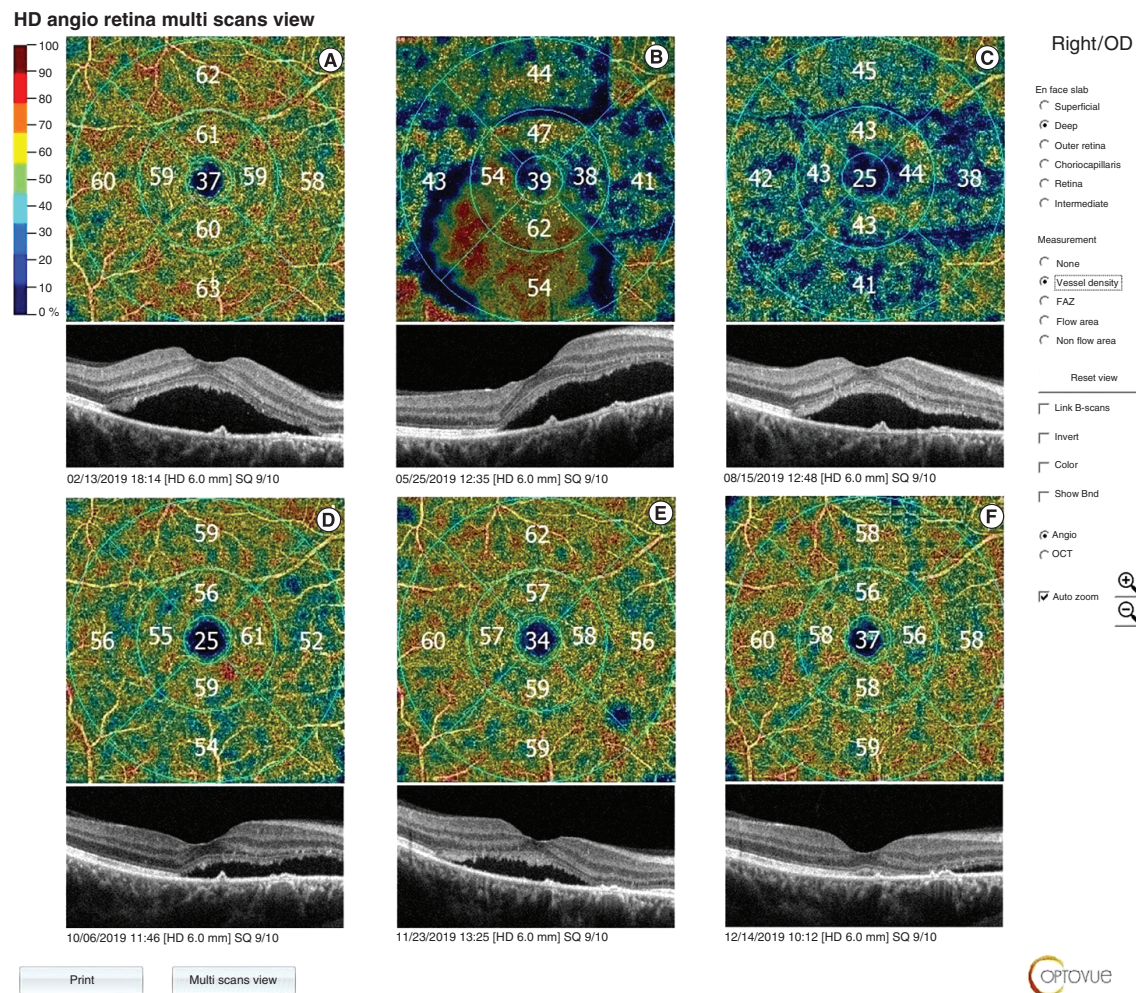
Figure 2.   Submacular thickness and deep retinal capillary density changes according to time groups (patient 1). (A–C) First MPL then PDT were applied at time 1 (SMT: 312 μm before, 220 μm after application; DRCD: 57.7% before and 40.7% after application). **(D)** Only aPRP was applied at time 2 (SMT: 220 μm before, 198 μm after application; DRCD: 40.7% before and 56.1% after application). **(E)** rEMS/IP combined with aPRP were applied at time 3 (SMT: 198 μm before application; DRCD: 56.1% before application). **(F)** After combined application (SMT: 96 μm after application; DRCD: 56.7% after application), see also Tables 1–3.
aPRP: Autologous platelet-rich plasma; DRCD: Deep retinal capillary density; MPL: Micropulse laser; OD: Right eye; PDT: Photodynamic therapy; rEMS/IP: Retinal repetitive electromagnetic stimulation; SMT: Submacular thickness.

increased blood cortisol level and increased choroidal hydrostatic pressure caused by a thick choroid (pachychoroid) or high systemic arterial diastolic pressure. Thick choroidea and wide vessels can be visualized by swept-source OCT and by enhanced depth imaging spectral domain OCT [4,7,12]. These findings support the hypothesis that the choroidea vasculature is congested and extremely permeable in CSCR, as seen with ICGA [1–3,6–8]. OCTA has become the gold standard in the diagnosis and follow-up of retinal disease. FA and ICG are invasive procedures, whereas OCTA provides detailed anatomical and vascular structure information of the retinal and choroidal layers with a single noninvasive scan. FA and ICGA are used in the differential diagnosis of latent CNV or polypoidal vasculopathy when suspicious irregular PED is detected in OCTA.

High blood cortisol levels disrupt Trk receptor activity and balance between various GFs. The integrity of the zonula occludens between RPE cells is then disrupted, and ion channels and fluid movements are affected by the RPE layer. As a result, RPE/photoreceptor damage and dysfunction are observed and visual functions are affected by accumulating fluid under the sensory retina [1–3,6–8]. Because of complex etiopathogenesis, treatments that target only choroidal thickness and leakage – including acetazolamide, intravitreal anti-VEGF injection or PDT – may not be sufficient to correct the underlying pathology [5,6]. In addition to choroidal pathology, widespread RPE
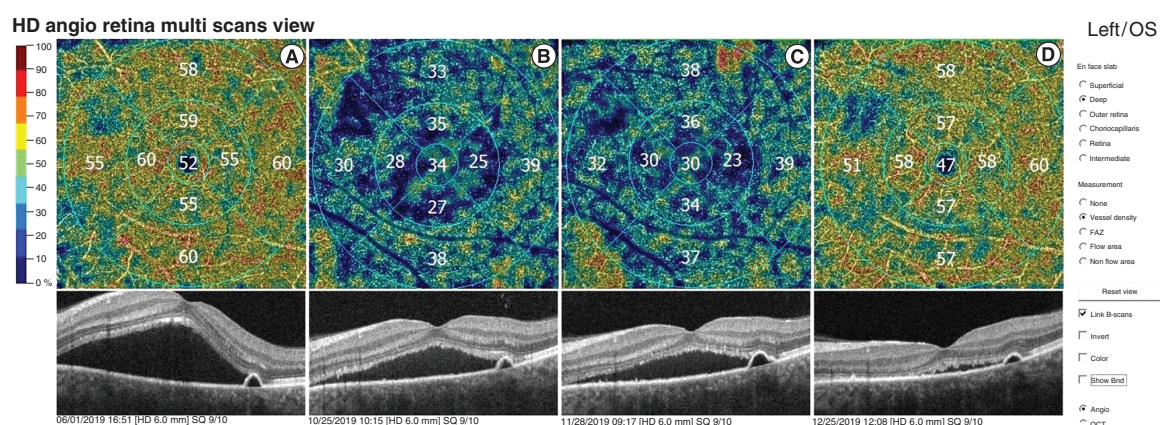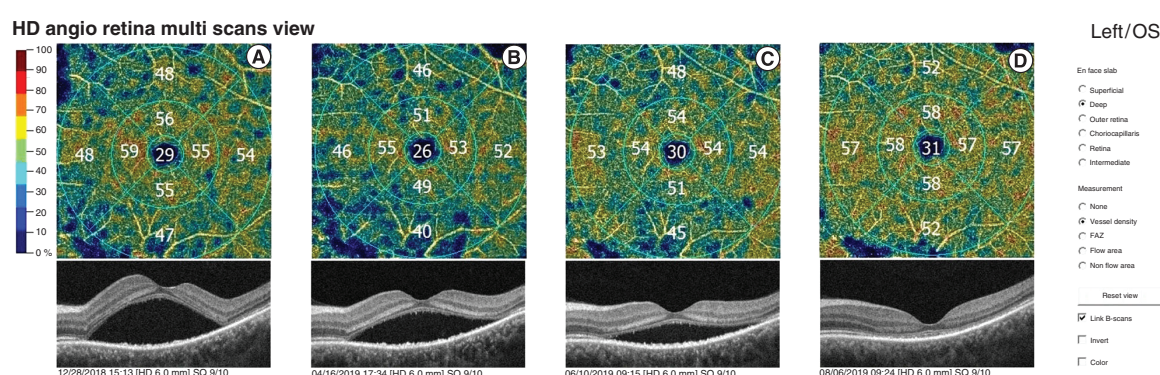
Figure 3.   Submacular thickness and deep retinal capillary density changes according to time groups (patient 2). (A) First MPL then PDT were applied at time 1 (SMT: 380 μm before, 321 μm after application; DRCD: 54.4% before, 33.6% after application). **(B)** Only aPRP was applied at time 2 (SMT: 321 μm before, 202 μm after application, DRCD: 33.6% before, 34.7% after application). **(C)** rEMS/IP combined with aPRP were applied at time 3 (SMT: 202 μm before application; DRCD: 34.7% before application). **(D)** After combined application (SMT: 124 μm after application; DRCD: 56.7% after application), see also Tables 1–3.
aPRP: Autologous platelet-rich plasma; DRCD: Deep retinal capillary density; MPL: Micropulse laser; OS: Left eye; PDT: Photodynamic therapy; rEMS/IP: Retinal repetitive electromagnetic stimulation/iontophoresis; SMT: Submacular thickness.

Figure 4.   Submacular thickness and deep retinal capillary density changes according to time groups (patient 6). (A) MPL was applied at time 1 (SMT: 478 μm before, 376 μm after application; DRCD: 50.1% before, 47.9% after application). **(B)** Only aPRP was applied at time 2 (SMT: 376 μm before, 291 μm after application; DRCD: 47.9% before, 51.3% after application). **(C)** rEMS/IP combined with aPRP were applied at time 3 (SMT: 291 μm before application; DRCD: 51.3% before application). **(D)** After combined application (SMT: 89 μm after application; DRCD: 56.9% after application), see also Tables 1–3.
aPRP: Autologous platelet-rich plasma; DRCD: Deep retinal capillary density; MPL: Micropulse laser; OS: Left eye; PDT: Photodynamic therapy; rEMS/IP: Retinal repetitive electromagnetic stimulation/iontophoresis; SMT: Submacular thickness.

dysfunction (often accompanied by deep retinal capillary ischemia) can contribute to the development of CSCR. Thus it may be reasonable to support the microenvironment of the outer retinal complex (choriocapillaris–Bruch's membrane–RPE) via restorative GFs. Various treatment methods are currently applied depending on the stage of the disease, the extent of the lesion and the presence of CNV [5,6]. However, some cases may be resistant or unresponsive to current treatments. PDT is generally effective but can only be applied in local RPE defects; it cannot be applied in cases with multifocal diffuse retinal pigment epitheliopathy due to possible complications, including choroidal ischemia, retinal artery occlusion, retinal pigment epithelial atrophy and central scotoma [4–6]. The disease may recur in 15–50% of cases. Bilateral involvement may occur in approximately one-third of cases. Secondary CNV development can be seen in 2–9% of patients with chronic CSCR and seriously threatens vision [1–3,6–8]. In etiopathogenesis, RPE cells, choroidea, or both are thought to dysfunction together. Due to
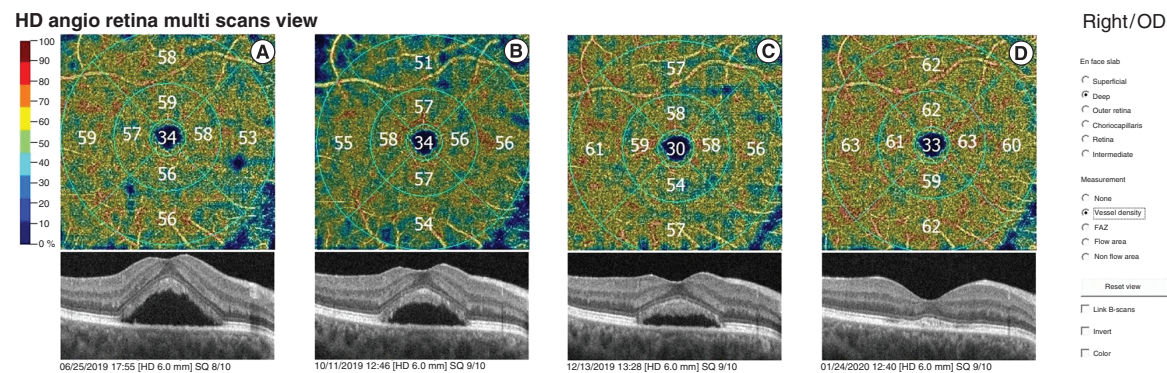
Figure 5.   Submacular thickness and deep retinal capillary density changes according to time groups (patient 16). (A) MPL was applied at time 1 (SMT: 401 μm before, 317 μm after application; DRCD: 56.9% before, 54.1% after application). **(B)** Only aPRP was applied at time 2 (SMT: 317 μm before, 237 μm after application; DRCD: 54.1% before, 58.9% after application). **(C)** rEMS/IP combined with aPRP were applied at time 3 (SMT: 237 μm before application; DRCD: 58.9% before application). **(D)** After combined application (SMT: 102 μm after application; DRCD: 61% after application), see also Tables 1–3.
aPRP: Autologous platelet-rich plasma; DRCD: Deep retinal capillary density; MPL: Micropulse laser; OD: Right eye; PDT: Photodynamic therapy; rEMS/IP: Retinal repetitive electromagnetic stimulation/iontophoresis; SMT: Submacular thickness (μm)
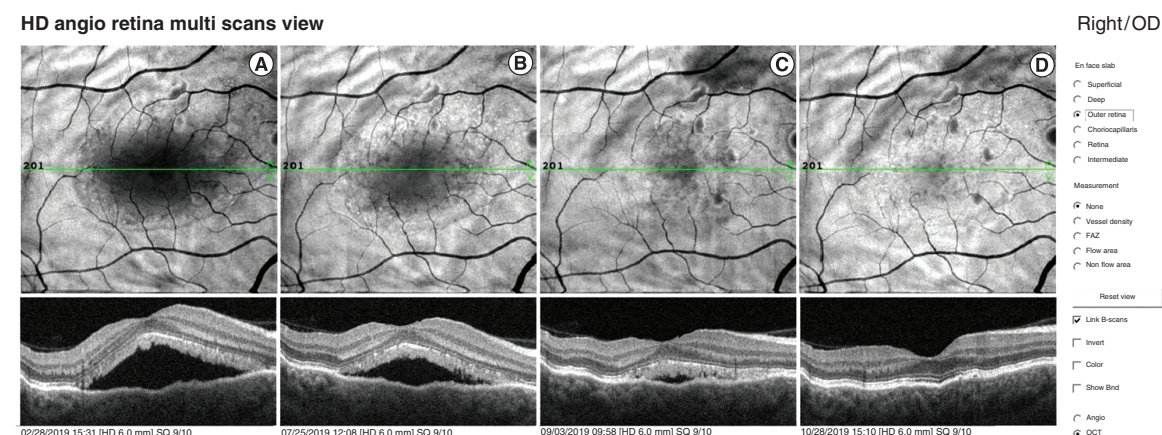

Figure 6.   Submacular thickness and central macular thickness changes according to time groups (patient 17). (A) MPL was applied at time 1 (SMT: 408 μm before, 311 μm after application; CMT: 509 μm before, 432 μm after application). **(B)** Only aPRP was applied at time 2 (SMT: 311 μm before, 182 μm after application; CMT: 432 μm before, 288 μm after application). **(C)** rEMS/IP combined with aPRP were applied at time 3 (SMT: 182 μm before application; CMT: 288 μm before application). **(D)** After combined application (SMT 97 μm after application; CMT 222 μm after application), see also Tables 1–3.
aPRP: Autologous platelet-rich plasma; CMT: Central macular thickness; MPL: Micropulse laser; OD: Right eye; rEMS/IP: Retinal repetitive electromagnetic stimulation/iontophoresis; SMT: Submacular thickness.

the complex etiopathogenesis, new treatment options and approaches are needed to reduce serious complications. Thus we investigated the effectiveness of GFs as an alternative and new treatment modality for the treatment of chronic CSCR that cannot be managed by current treatment modalities.

Fresh autologous PRP was used at time 2 as a source of GFs. Submacular fluid decreased significantly and deep retinal capillary blood flow increased significantly at time 2. However, no significant increase in visual acuity was observed. EGF and PDGF play a key role in wound healing and epithelialization. EGF is responsible for epithelial proliferation and integration and PDGF for increasing capillary blood flow [9,16]. NGF is a neurotrophin that stimulates the growth and maintenance of intraretinal glial cells, Müller cells and neurons; it also plays a key role in ensuring the integrity and function of epithelial cells and nerve fibers [9,10].

Scleral pores allow passive diffusion for molecules smaller than 75 kDa. The electrical charges of larger molecules must be changed for them to pass through. For this purpose, electrical or electromagnetic iontophoresis is needed [17–19]. NGF and IGF, both larger than 75 kDa, are responsible for the oxidative phosphorylation required for neural functions [9–11]. We think that when subtenon aPRP is used alone, a significant number of GFs cannot pass from the scleral pores to the choroidal matrix. In our previous study, we showed that the use of rEMS with aPRP is more effective than aPRP alone in the treatment of eyes affected by deep retinal capillary ischemia [8]. Another study proved that aPRP and rEMS are effective in slowing disease progression in patients with retinitis pigmentosa [23].

The prolonged presence of submacular fluid can reduce the ability of RPE to benefit from choroidal circulation. We think that the development of deep retinal capillary ischemia may be the cause of resistance to treatment. GFs in PRP can reduce this ischemia. When we applied subtenon aPRP in combination with rEMS/IP at time 3, the submacular fluid decreased significantly and deep retinal capillary blood flow increased. BCVA significantly increased only at time 3. The GFs in the choroidal matrix can pass to the subretinal space through the Trk receptors [20]. Moreover, rEMS/IP can increase the transition of GFs from scleral pores to the choroidal matrix. Growth factor affinity of Trk receptors can be increased by rEMS [13–20]. At time 3, we can explain the significant increase in visual acuity and all parameters by the iontophoresis effect of rEMS. Coils in the Magnovision helmet form an electromagnetic field without touching the scalp or face. Importantly, the intensity of the electromagnetic field at the tissue level is far below the safety limit defined by WHO [24,25]. PRP, as a growth factor source, can be obtained from the patient at a low cost. The electromagnetic iontophoresis device also seems to be affordable in terms of purchase, periodic maintenance and repair costs. With this method, we found the highest increase in DRCD. The reduction of deep capillary ischemia may have strengthened connections between RPE cells and decreased submacular fluid by increasing the pump function of RPE.

This study has some limitations. The aPRP injections combined with rEMS/IP appear to repair the RPE defect, strengthen the external blood retinal barrier and correct dysfunction due to retinal ischemia. However, long-term follow-up is needed. Determining the relationship between underlying systemic conditions and relapses is a separate research topic. Existing OCTA instruments have some artifact problems. It is important to identify and remove these artifacts to evaluate DRCD accurately in consecutive measurements. Some chronic CSCR cases may recover spontaneously. Causes of disease are not homogeneous. For this reason, it is not possible to create a control group. Another limitation is that we examined the changes according to time periods instead of using an independent control group.

Conclusion

Resistant chronic CSCR is an important socioeconomic and psychological problem in the productive aged population. In the treatment of resistant CSCR, subtenon PRP combined with rEMS should be considered as an effective and safe treatment option. This combined approach can regulate dysfunctional or damaged external retinal microenvironment using the restorative and circulation-enhancing effect of various GFs.

Executive summary

- Central serous chorioretinopathy is a retinal disease that predominantly affects middle-aged men.
- Various treatment methods (e.g., acetazolamide, mineralocorticoid receptor antagonists, intravitreal anti-VEGF injections, sub-threshold micropulse laser applications and photodynamic therapy) are used.
- Some cases may be resistant or unresponsive to current treatments.
- Due to the complex etiopathogenesis, new treatment options and approaches are needed to reduce serious complications.
- We investigated whether subtenon platelet-rich plasma injection combined with retinal electromagnetic stimulation is effective in chronic central serous chorioretinopathy cases resistant to classical therapies.
- A combination of autologous platelet-rich plasma and noninvasive electromagnetic stimulation/iontophoresis is a safe, effective and novel therapeutic approach.
- This combined approach can regulate a dysfunctional or damaged external retinal microenvironment using the restorative and circulatory enhancing effect of various growth factors.

Ethical conduct of research

Approval for the study was obtained from the Ankara University Medical School Clinical Research Ethics Committee (17-1177-18) and Republic of Turkey Ministry of Health Drug and Medical Device Department (2018-136). This research was carried out in accordance with the principles of the Helsinki Declaration. Written consent forms were obtained from the patients before starting the study.

Data sharing statement

The authors certify that this manuscript reports original clinical trial data (ClinicalTrials.gov identifier: NCT04224831). Individual, personal patient data will not be made available however clinical data, the study protocol and statistical analyses will be made available 1 year after publication. Requests should be made to the corresponding author.

References

1   Nicholson B, Noble J, Forooghian F, Meyerle C. Central serous chorioretinopathy: update on pathophysiology and treatment. *Sur. Ophthalmol.* 58(2), 103–126 (2003).

2   Daruich A, Matet A, Behar-Cohen F. Central serous chorioretinopathy. *Dev. Ophthal.* 58, 27–38 (2017).

3   Scarinci F, Ghiciuc CM, Patacchioli FR, Palmery M, Parravano M. Investigating the hypothesis of stress system dysregulation as a risk factor for central serous chorioretinopathy: a literature mini-review. *Curr. Eye Res.* 44(6), 583–589 (2019).

4   Cennamo G, Montorio D, Comune C *et al.* Study of vessel density by optical coherence tomography angiography in patients with central serous chorioretinopathy after low-fluence photodynamic therapy. *Photodiagn. Photodyn. Ther.* 30, 101742 (2020).

5   Manayath GJ, Ranjan R, Karandikar SS *et al.* Central serous chorioretinopathy: current update on management. *Oman J. Ophthalmol.* 11(3), 200–206 (2018).

6   Özmert E, Demirel S, Yanık Ö, Batıoğlu F. Low-fluence photodynamic therapy versus subthreshold micropulse yellow wavelength laser in the treatment of chronic central serous chorioretinopathy. *J. Ophthalmol.* 2016, 1–8 (2016).

7   Battista M, Borrelli E, Parravano M *et al.* OCTA characterisation of microvascular retinal alterations in patients with central serous chorioretinopathy. *Br. J. Ophthalmol.* 104(10), 1453–1457 (2020).

8   Özmert E, Arslan U. Management of deep retinal capillary ischemia by electromagnetic stimulation and platelet-rich plasma: preliminary clinical results. *Adv. Ther.* 36(9), 2273–2286 (2019).

9   Anitua E, Muruzabal F, Tayebba A *et al.* Autologous serum and plasma rich in growth factors in ophthalmology: preclinical and clinical studies. *Acta Ophthalmol.* 93(8), e605–e614 (2015).

10   Amable PR, Carias RB, Teixeira MV *et al.* Platelet-rich plasma preparation for regenerative medicine: optimization and quantification of cytokines and growth factors. *Stem Cell Res. Ther.* 4(3), 67 (2013).

11   Arslan U, Özmert E, Demirel S, Örnek F, Şermet F. Effects of subtenon-injected autologous platelet-rich plasma on visual functions in eyes with retinitis pigmentosa: preliminary clinical results. *Graefe's Arch. Clin. Exp. Ophthalmol.* 256(5), 893–908 (2018).

12   Novais EA, Lane M, Waheed NK *et al.* Central serous chorioretinopathy. In: *Optical Coherence Tomography Angiography of the Eye.* Huang D, Lumbroso B, Jia Y, Waheed NK (Eds). Slack Incorporated, USA. 163–169 (2018).

13   Patruno A, Ferrone A, Costantini E *et al.* Extremely low-frequency electromagnetic fields accelerates wound healing modulating MMP-9 and inflammatory cytokines. *Cell Prolif.* 51(2), e12432 (2018).

14   Maziarz A, Kocan B, Bester M *et al.* How electromagnetic fields can influence adult stem cells: positive and negative impacts. *Stem Cell Res. Ther.* 7, 54 (2016).

15   Parate D, Kadir ND, Celik C *et al.* Pulsed electromagnetic fields potentiate the paracrine function of mesenchymal stem cells. *Stem Cell Res. Ther.* 11, 46 (2020).

16   Yamakawa S, Hayashida K. Advances in surgical applications of growth factors for wound healing. *Burn Trauma.* 7, 10 (2019).

17   Demetriades AM, Deering T, Liu H *et al.* Transscleral delivery of antiangiogenic proteins. *J. Ocul. Pharmacol. Ther.* 24(1), 70–79 (2008).

18   Meng T, Kulkarni V, Simmers R, Brar V, Xu Q. Therapeutic implications of nanomedicine for ocular drug delivery. *Drug Discov. Today* 24(8), 1524–1538 (2019).

19   Li SK, Hao J. Transscleral passive and iontophoretic transport: theory and analysis. *Expert Opin. Drug Deliv.* 15(3), 283–299 (2017).

20 Mysona BA, Zhao J, Bollinger KE. Role of BDNF/TrkB pathway in the visual system: therapeutic implications for glaucoma. *Expert Rev. Ophthalmol.* 12(1), 69–81 (2017).

21 Cheng Y, Shen Y. An efficient sequential design of clinical trials. *J. Stat. Plan. Inference.* 143(2), 283–295 (2013).

22 Arani RB, Chen JJ. A power study of a sequential method of p-value adjustment for correlated continuous endpoints. *J. Biopharm. Stat.* 8(4), 585–598 (1998).

23 Arslan U, Özmert E. Management of retinitis pigmentosa via platelet-rich plasma or combination with electromagnetic stimulation: retrospective analysis of 1-year results. *Adv. Ther.* 37(5), 2390–2412 (2020).

24 Chandra T, Chavhan GB, Sze RW *et al.* Practical considerations for establishing and maintaining a magnetic resonance imaging safety program in a pediatric practice. *Pediatr. Radiol.* 49(4), 458–468 (2019).

25 Sandoval DJ, Chambers GD, Adolphi NL Biological effects of magnetic resonance imaging. In: *Radiation Biology of Medical Imaging*. Kelsey CA, Heintz PH, Sandoval DJ *et al.*. (Eds). Wiley,Haboken. 281–295 (2018).

RESEARCH

Management of toxic optic neuropathy via a combination of Wharton's jelly-derived mesenchymal stem cells with electromagnetic stimulation

Emin Özmert[1] and Umut Arslan[2]*

Abstract

Purpose: To investigate the effect of the combination of Wharton's jelly derived mesenchymal stem cells (WJ-MSC) and high frequency repetitive electromagnetic stimulation (rEMS) in the therapy of toxic optic neuropathies with severe symptoms after the available current therapy modalities which were unsucessful.

Material and methods: This prospective, open-label clinical phase-3 study was conducted at Ankara University Faculty of Medicine, Department of Ophthalmology between April 2019 and April 2021. Thirty-six eyes of 18 patients with toxic optic neuropathy (TON) were included in the study. Within 1–3 months after the emergency interventions, patients with various degrees of sequela visual disturbances were studied in this clinical trial. The cases were divided into three groups according to similar demographic characteristics. Group 1: Consists of 12 eyes of 12 patients treated with the WJ-MSC and rEMS combination in one eye. Group 2: Consists of 12 eyes of 12 patients treated with only rEMS in one eye. Group 3: Consists of 12 eyes of six patients treated with only WJ-MSC in both eyes. The course was evaluated by comparing the quantitive functional and structural assessment parameters measured before and at the fourth month of applications in each group.

Results: The mean best corrected visual acuity (BCVA) delta change percentages of the groups can be ranked as: Group 1 (47%) > Group 3 (32%) > Group 2 (21%). The mean fundus perimetry deviation index (FPDI) delta change percentages of the groups can be ranked as: Group 1 (95%) > Group 2 (33%) > Group 3 (27%). The mean ganglion cell complex (GCC) thickness delta change (decrease in thickness) percentages can be ranked as: Group 1 (− 21%) > Group 3 (− 15%) > Group 2 (− 13%). The visual evoked potential (VEP) P100 latency delta change percentages of the groups can be ranked as: Group 1 (− 18%) > Group 3 (− 10%) > Group 2 (− 8%). The P100 amplitude delta change percentages of the groups can be ranked as: Group 1 (105%) > Group 3 (83%) > Group 2 (24%).

Conclusion: Toxic optic neuropathies are emergent pathologies that can result in acute and permanent blindness. After poisoning with toxic substances, progressive apoptosis continues in optic nerve axons and ganglion cells. After the proper first systemic intervention in intensive care clinic, the WJ-MSC and rEMS combination seems very effective in the short-term period in cases with TON. To prevent permanent blindness, a combination of WJ-MSC and rEMS application as soon as possible may increase the chance of success in currently untreatable cases.

*Correspondence: drumutarslan@hotmail.com; bioretina.net@gmail.com
[2] Ankara University Technopolis, Bioretina Eye Clinic, Neorama Ofis 55-56
Yaşam Cad. No 13/A, Beştepe /Yenimahalle, Ankara, Turkey
Full list of author information is available at the end of the article

Introduction

The visual function begins with converting light energy into biochemical, electrical signals in the outer layers of the retina. Electrical signals are transmitted from the photoreceptors (first neuron) to the bipolar cells (second neuron) and then to the ganglion cells (third neuron). The axons of the ganglion cells (retinal nerve fibers) form the optic nerve. The number of optic nerve axons from the post-laminar region to the lateral geniculate nucleus is approximately 1,200,000. The optic nerve transmits electrical signals to the visual center located in the brain's occipital cortex through various synapses, including the lateral geniculate nucleus (fourth neuron) [1–3]. Optic nerve fibers are more sensitive to various toxins than the retina because they are outside the protecting feature of the blood-retinal barrier. Methanol, various solvents and heavy metals, carbon dioxide, antiarrhythmic and antiepileptic drugs, some antibiotics, and vasoactive drugs can cause toxic optic neuropathy (TON). There is different pathophysiology for each toxic substance resulting in optic nerve damage. Metabolites of some toxins disrupt adenosine three phosphate (ATP) synthesis by blocking mitochondrial function and oxidative phosphorylation. Metabolites of some other toxins cause demyelination as a result of protein denaturation. Neuroinflammation occurs when denatured proteins block axoplasmic flow. Neuroinflammation also develops secondary to the cessation of axoplasmic flow after hypoxia. Hypoxic neurons stop their metabolism and switch to OFF mode. If hypoxia and neuroinflammation persist, apoptosis and permanent vision loss develop [4, 5].

Wharton's jelly-derived mesenchymal stem cells (WJ-MSC) can increase mitochondrial ATP synthesis via various growth factors (GF) and suppress neuroinflammation with an immunomodulatory effect [6–10]. High frequency repetitive electromagnetic stimulation (rEMS) can rearrange ion channel balances and axoplasmic flow. The effects of rEMS are also known to increase blood flow and synaptic transmission in neural tissues, decrease toxic glutamine levels and increasing the passage of large therapeutic molecules into the cell [11–14].

The aim of this prospective clinical study is to investigate the effect of the combined use of WJ-MSC and rEMS in the management of TON after the interventions in emergency or intensive care units. This combination therapy is the first study in the literature to treat TON with severe symptoms, in which available current therapy modalities were unsucessful.

Materials and methods

Ethics committee approval for the umbilical cord Wharton's jelly-derived mesenchymal stem cell (WJ-MSC) study was obtained from the Ankara University Faculty of Medicine Clinical Research Ethics Committee (19-1293-18). It was also approved by the Review Board of the Cell, Organ, and Tissue Transplantation Department within the Turkish Ministry of Health (56733164/203 E.1925). Ethics committee approval for the transcranial electromagnetic stimulation study was obtained from the Ankara University Faculty of Medicine Clinical Research Ethics Committee (17-1177-18) and the Review Board of the Drug and Medical Device Department within the Turkish Ministry of Health (2018-136). The study was performed following the tenets of the 2013 Declaration of Helsinki. Written informed consent was obtained from the patients before enrollment.

This prospective, open-label clinical phase-3 study was conducted at Ankara University Faculty of Medicine, Department of Ophthalmology between April 2019 and April 2021. Thirty-six eyes of 18 patients with toxic optic neuropathy (TON) were included in the study. The primary toxic optic neuropathy (TON) diagnosis of the affected patients was made in an emergency or intensive care clinic. Within 1–3 months after the emergency interventions, patients with various degrees of sequela visual disturbances were studied in this clinical trial. All patients enrolled underwent a complete routine ophthalmic examination, including the best-corrected visual acuity (BCVA) measurement with the early treatment of diabetic retinopathy study (ETDRS) chart (Topcon CC 100 XP, Japan). The patients were further evaluated with optical coherence tomography angiography (OCTA) from RTVue XR (Avanti, Optovue, Fremont, CA, USA), which provides a co-registered en-face and cross-sectional multimodal imaging platform to analyze and measure the changes in the ganglion cell layer (GCL). Functional evaluation of optic nerve was made by Compass 24/2 visual field (VF) test (Compass, CenterVue, Padova, Italy) and the 120-pattern visual evoked potential (pVEP) test (Mon 2018F, Metrovision, Perenchies, France). Before the different treatment modalities with WJ-MSC and rEMS and at the fourth month after the

treatments, quantitative assessment parameters were compared.

Subjects

Thirty-six eyes of 18 patients with toxic optic neuropathy (TON) due to four different kinds of toxic substances (mainly methanol, CO_2, sildenafil, amiodaron) were included in the clinical study. Different ophthalmic therapy modalities (only WJ-MSC, only rEMS or both) were applied to the cases between 1 to 3 months after discharge from hospital, so as to eliminate the possible therapeutic effect of the medical treatment done for intoxication, and before the development of irreversible optic nerve damage, which might occur after 3 months.

The inclusion criteria were: The patients who could be assessed by quantitative parameters of aforementioned tests at baseline (just before the treatment) and at fourth month after the treatment; patients with best-corrected visual acuity (BCVA) better than 35 letters, for performing appropriate visual field testing; any degree of visual field loss; and patients over 18 years old.

The exclusion criteria were: Cases poisoned with toxic substances for more than 3 months; patients with BCVA less than 35 letters, in whom visual field test can not be done properly; non-cooperated patients because of neurological sequelae; previous history of diabetes mellitus and cardiovascular diseases; and smokers.

Study groups

Thirty-six eyes of 18 patients exposed to four types of toxic substances composed the study cohort. The eyes could be divided into three groups according to the applied treatment modalities with similar demographic characteristics.

In 12 patients with TON, due to ethical considerations, the worse eye received one subtenon injection of WJ-MSC. Ten days after the injection, rEMS was applied on both eyes of these patients for 30 min via a custom-designed helmet. rEMS applications were repeated ten times with a 1-week interval during the trial. So the 12 eyes of the patients received both WJ-MSC and rEMS constitute Group 1, and other 12 eyes of the same patients received only rEMS constitute Group 2. Another different 6 patients' both eyes (total 12 eyes) with TON received only one subtenon injection of WJ-MSC without rEMS application, which form Group 3.

The course was evaluated by comparing the BCVA, FDPI, GCC thickness, pVEP-p100 latency, and amplitude parameters measured before and at the fourth month of applications in each group (Tables 1, 2, 3).

Group 1

Consists of 12 eyes of 12 patients treated with the WJ-MSC and rEMS combination in one eye. WJ-MSC was applied first to the patients after necessary preparations. rEMS application was started 10 days after the WJ-MSC application. The rEMS was applied with a custom-designed helmet for 30 min after the subtenon WJ-MSC application. WJ-MSC was applied only one time. rEMS applications were repeated ten times with a 1-week interval. The course was evaluated by comparing the BCVA, FDPI, GCC thickness, pVEP-p100 latency, and amplitude

Table 1 Group1: Demonstration of demographic characteristics, structural and functional changes of group1 to which WJ-MSC and rEMS combination was applied

Patient no	Eye	Toxin	BCVA		Visual field FPDI		GCC thickness		VEP P100 lat.VEP P100 lat		VEP P100 ampl	
			Before	After	Before	After	Before	After	Before	After	Before	After
1	L	Methanol	80	98	49	69	101	82	132	105	3.1	5.8
2	R	Methanol	35	92	15	72	92	64	148	112	2.1	4.7
3	L	Amiodarn	89	110	34	98	103	88	136	101	3.4	7.2
4	L	Methanol	35	80	47	65	88	61	154	114	1.1	4.2
5	R	Sildenafil	50	83	38	61	94	60	144	114	1.8	3.4
6	L	Methanol	50	98	37	59	91	70	139	106	2.9	6.3
7	L	C0$_2$	39	65	11	28	71	52	140	118	3.6	7.1
8	R	Methanol	35	45	7	14	62	50	149	131	2.7	3.9
9	R	Methanol	40	50	5	11	64	51	157	136	1.4	2.6
10	R	Methanol	54	54	8	10	62	58	147	128	1.6	2.9
11	L	Methanol	35	40	4	11	58	56	145	130	1.0	2.6
12	R	Methanol	35	35	1	2	55	50	153	132	1.2	2.3

WJ-MSC Wharton's jelly derived mesenchymal stem cell, *rEMS* repetitive electromagnetic stimulation, *BCVA* best corrected visual acuity (ETDRS letters), *FPDI* fundus perimetry deviation index (%), *GCC thickness* Ganglion cell complex (μm), *VEP* visual evoked potential, *P100 lat* latency (ms), *P100 ampl* amplitude (mV)

Table 2 Group2: Demonstration of demographic characteristics, structural and functional changes of group2 to which only rEMS was applied

Patient no	Eye	Toxin	BCVA		Visual Field FPDI		GCC Thickness		VEP P100 lat		VEP P100 ampl	
			Before	After	Before	After	Before	After	Before	After	Before	After
1	R	Methanol	80	89	61	71	103	91	129	114	3.2	4.7
2	L	Methanol	35	80	13	42	88	78	144	126	2.2	3.4
3	R	Amiodaron	90	100	49	72	112	108	131	110	3.5	4.1
4	R	Methanol	35	50	46	53	74	58	156	128	1.0	2.1
5	L	Sildenafil	60	74	42	56	89	64	141	119	2.0	2.9
6	R	Methanol	50	74	40	52	88	74	137	120	3.0	4.1
7	L	CO_2	40	50	13	17	74	59	138	124	3.7	4.3
8	L	Methanol	35	35	12	12	57	52	144	141	2.9	2.9
9	L	Methanol	45	45	7	8	65	53	154	155	1.7	1.6
10	L	Methanol	59	59	8	8	62	59	146	145	1.6	1.4
11	R	Methanol	36	36	3	2	58	57	153	150	1.7	1.7
12	L	Methanol	39	39	2	2	56	54	152	151	1.3	1.3

rEMS repetitive electromagnetic stimulation, *BCVA* best corrected visual acuity (ETDRS letters), *FPDI* fundus perimetry deviation index (%), *GCC thickness* Ganglion cell complex (μm), *VEP* visual evoked potential, *P100 lat* latency (ms), *P100 ampl* amplitude (mV)

Table 3 Group3: Demonstration of demographic characteristics, structural and functional changes of group3 to which only WJ-MSC was applied

Patient no	Eye	Toxin	BCVA		Visual field FPDI		GCC thickness		VEP P100 lat		VEP P100 ampl	
			Before	After	Before	After	Before	After	Before	After	Before	After
1	R	Methanol	65	85	61	78	89	76	141	121	2.9	4.8
2	L	Methanol	60	80	56	68	82	73	145	123	2.7	3.8
3	R	Sildenafil	35	60	28	36	68	59	151	129	1.4	2.6
4	L	Sildenafil	40	70	32	37	72	63	146	119	1.8	2.9
5	R	Methanol	35	40	7	12	68	56	159	153	1.5	3.1
6	L	Methanol	35	45	10	15	71	58	152	152	1.6	6.5
7	R	Methanol	35	35	14	18	66	57	153	151	1.2	2.7
8	L	Methanol	45	60	21	27	69	59	149	141	1.7	3.2
9	R	Methanol	50	65	31	39	81	70	144	131	2.1	3.6
10	L	Methanol	54	70	33	41	86	75	140	121	2.6	3.9
11	R	Methanol	65	80	41	52	98	81	138	119	3.1	4.9
12	L	Methanol	60	74	39	49	94	80	140	121	2.9	4.6

WJ-MSC Wharton's jelly derived mesenchymal stem cell, *BCVA* best corrected visual acuity (ETDRS letters), *FPDI* fundus perimetry deviation index (%), *GCC thickness* Ganglion cell complex (μm), *VEP* Visual evoked potential, *P100 lat* latency (ms), *P100 ampl* amplitude (mV)

parameters measured before and fourth month of applications (Table 1).

Group 2

Consists of 12 eyes of 12 patients treated with only rEMS in one eye. rEMS was applied with a custom-designed helmet for 30 min. rEMS applications were repeated ten times with 1-week intervals. The course was evaluated by comparing the BCVA, FDPI, GCC thickness, pVEP-p100 latency, and amplitude parameters measured before and fourth month of applications (Table 2).

Group 3

Consists of 12 eyes of six patients treated with only WJ-MSC in two eyes. Only WJ-MSC was applied to the patients after necessary preparations. WJ-MSC was applied only one time for both eyes. The course was evaluated by comparing the BCVA, FDPI, GCC thickness, pVEP-p100 latency, and amplitude parameters

measured before and in the fourth month of applications (Table 3).

Umbilical cord Wharton's jelly-derived mesenchymal stem cells preparation

The mesenchymal stem cells used in this study were isolated from Wharton's jelly of the umbilical cord collected allogenicly from a single donor with the mother's consent. The umbilical cord sample was treated following several steps. Briefly, cord tissue was washed twice with phosphate-buffered saline (Lonza, Switzerland), and the Wharton's jelly part was minced using forceps and a scalpel. Minced pieces were cultivated in a cell culture dish (Greiner Bio-One, Germany) with Dulbecco's modified Eagle's medium F12 (DMEM)-low glucose with no L-glutamine (Biological Industries, Israel) and 10% human AB serum (Capricorn, Germany), 1% 10.000 U/mL penicillin, and 10.000 μg/mL streptomycin (Gibco, USA). All cell preparations and cultivation procedures were conducted in a current Good Manufacturing Practice (cGMP) accredited laboratory (Onkim Stem Cell Technologies, Turkey). The culture-expanded cells were cryopreserved at P3 using standard cryopreservation protocols until used in the following experiment. CryoSure-DEX40 (WAK-Chemie Medical, Germany) containing 55% Dimethyl Sulfoxide and 5% Dextran 40 was used as cryopreservant. The cells were characterized at the time of cryopreservation using flow cytometric analysis to determine the expression of the positive cluster of differentiation (CD) surface markers, CD90, CD105, CD73, CD44, CD29, and negative for CD34, CD45, and CD11b (Fig. 1a, b). Using real-time polymerase chain reaction (qPCR), the expressions of several genes, such as tumor necrosis alpha (*TNF alpha*) and vimentin (*VIM*), were analyzed. Additionally, quality control analyses, such as mycoplasma and endotoxin analyses (using the PCR and LAL test combined with sterility analysis, respectively) were also completed. Cells were solubilized from cryopreservation before being prepared for injection. The average cell viability for each treatment was over 90.0%, and each patient received $2–6 \times 10^6$ cells in a 1.5 ml saline solution (Fig. 1a, b).

Injection of umbilical cord WJ-MSCs

The WJ-MSCs suspension from the culture was delivered to the operating room by cold chain and used within 24 h. A total of 1.5 ml of the WJ-MSC suspension was immediately injected into the subtenon space of each eye. The procedure was conducted under topical anesthesia with proparacaine hydrochloride drops (Alcaine, Alcon, USA) and sterile conditions. A 5/0 atraumatic traction suture was applied to the limbus for easy access

and manipulation to the application area. A small cut was made through the conjunctiva and tenon capsule up to the sclera in the superior-temporal quadrant, 13 mm away from the limbus, to insert a 20 G subtenon curved cannula (BD, Visitec, UK). Subsequently, a 7/0 vicryl suture was passed through the conjunctiva and tenon and tied down with a loop creation. A curved subtenon cannula attached to the 2.5 cc syringe filled with 1.5 ml fluid containing stem cells was inserted through the cut and forwarded into the extraocular muscle conus until reaching the sclera. Fluid (1.5 ml) was then injected. While the cannula was drawn back, a loop was tightened to prevent leakage. Postoperatively, loteprednol and tobramycin combination eye drops were given four times per day for 1 week, and oral amoxicillin-clavulanate (1 g) was given twice a day for 5 days.

Retinal repetitive electromagnetic stimulation (rEMS)

Specifically designed helmet producing repetitive high-frequency electromagnetic stimulation (rEMS) Magnovision™, Bioretina Biotechnology, Ankara, Turkey) stimulated the retinas and visual pathways in both eyes with an electromagnetic field strength of 2000 miligauss, frequency of 42 Hz, and duration of 30 min. These values were previously determined to be effective for other clinical and preclinical studies (Fig. 2).

Timeframe

The patients were evaluated at several study timepoints:

- **T0**: Baseline evaluation; to evaluate the structural and functional conditions of the eyes due to toxicity just before the treatment modalities
- **T1**: First-month assessment; for clinical/ophthalmoscopic evaluation and possible complications. Quantitative parameters were not studied.
- **T2**: Fourth-month assessment; structural and functional evaluation to assess the value of treatment modalities. An ophthalmic examination was made to detect possible complications.

Primary outcome measure

ETDRS visual acuity: The visual acuity scores obtained from the T0 and T2 examinations were analyzed and compared using statistical tests to determine effectiveness.

Secondary outcome measures: The following scores obtained from the T0 and T2 examinations were analyzed and compared using statistical tests to determine effectiveness.

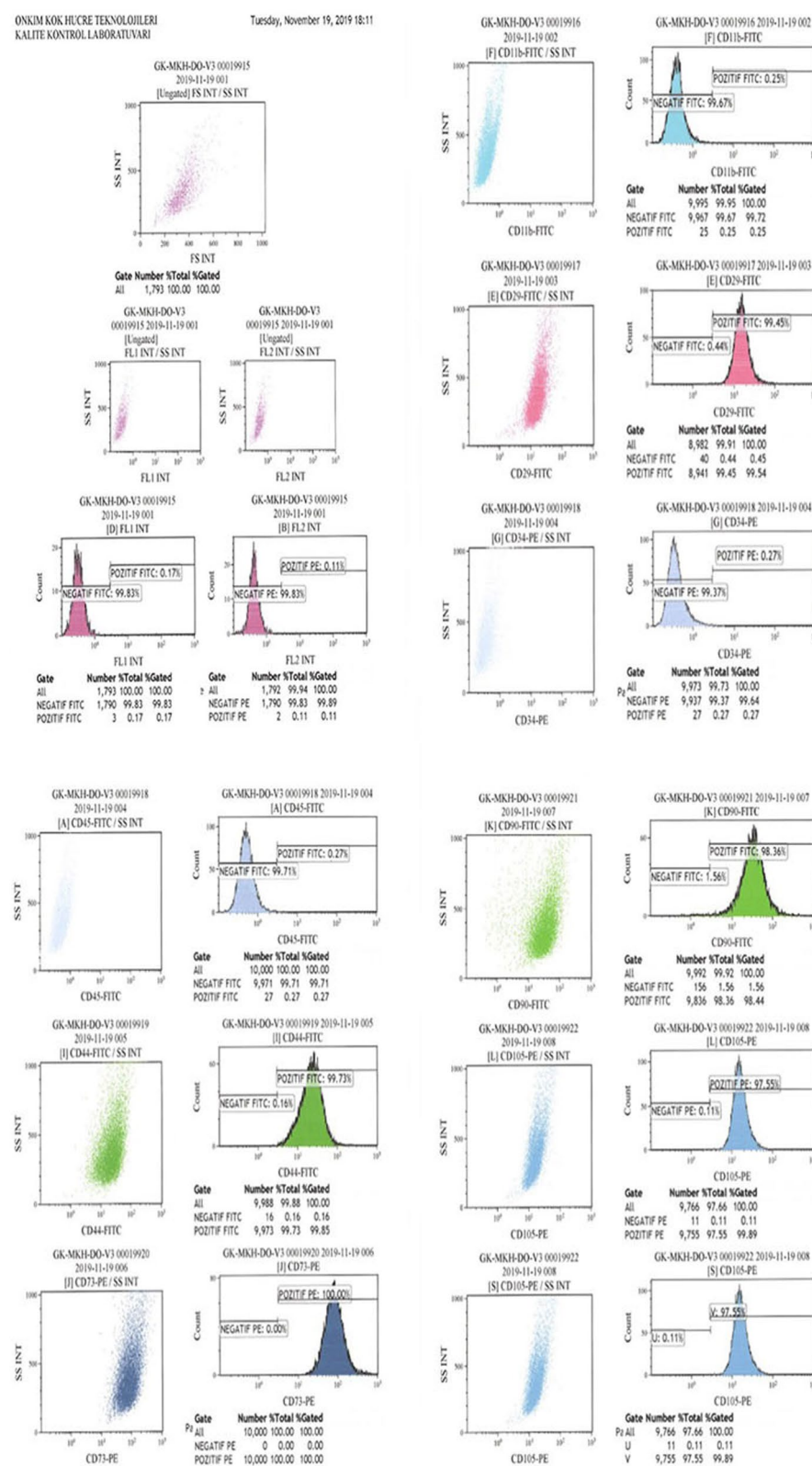*Visual field sensitivity*: Fundus perimetry deviation index (FPDI, %).

Fig. 1 **a** The phenotypic characterization of Wharton jelly derived mesenchymal stem cells before cryopreservation. **b** The phenotypic characterization of Wharton jelly derived mesenchymal stem cells after cryopreservation
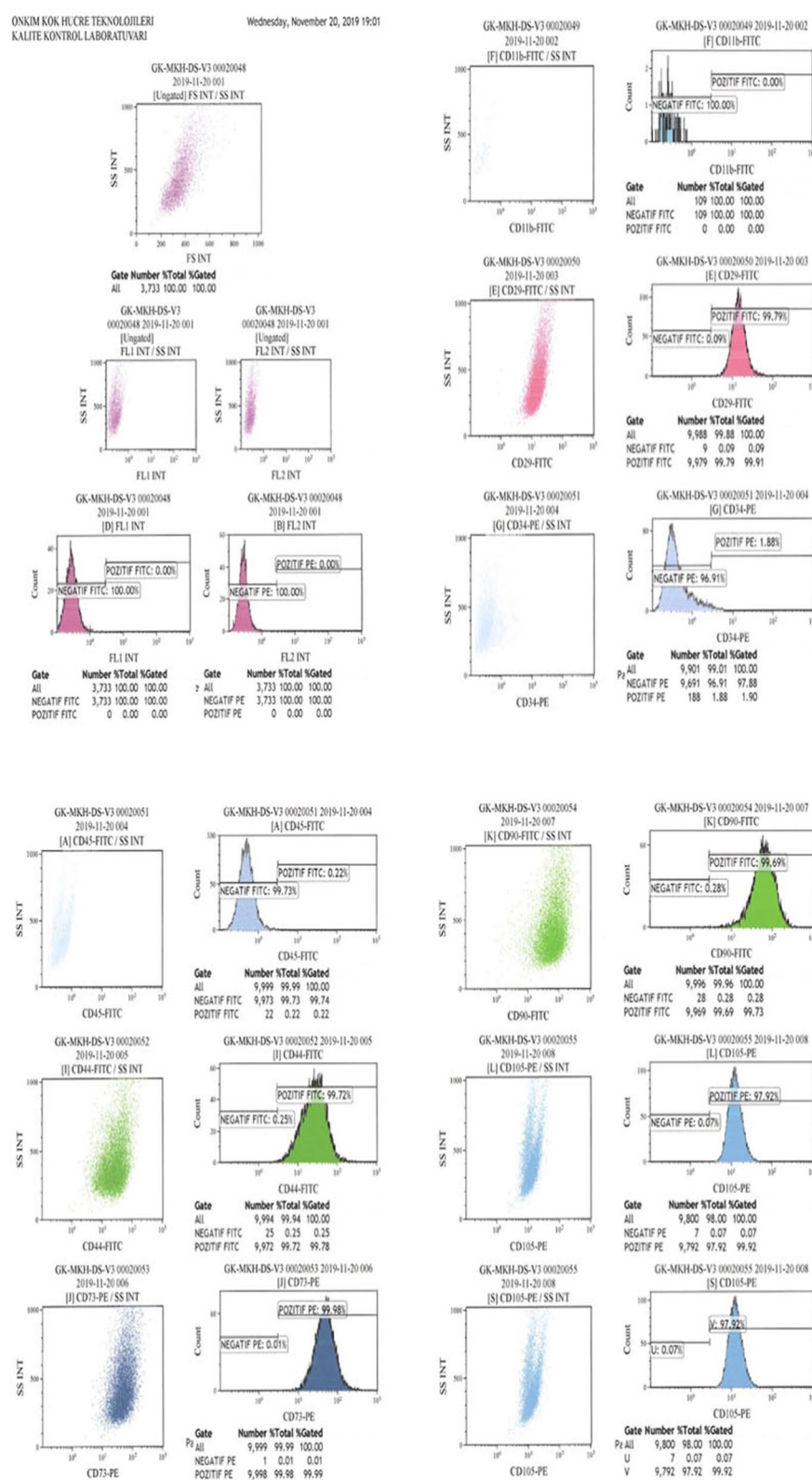
Fig. 1 continued

Fig. 2 Retinal electromagnetic stimulator (rEMS) device. Application of the helmet to stimulate the retina-optic nerve and visual pathways [35–37]

FPDI was examined in the 24/2 visual field of the computerized perimetry records. The FPDI offers data explaining how many of the 100 flashing points and what percentage of the visual field could be correctly seen by the patient. For VF analysis, practice rounds were carried out three times before applications to avoid mistakes during the test.

Ganglion cell complex thickness (GCC thickness, µm): GCC is the thickness from the internal limiting membrane to the inner plexiform layer in the 3×3 mm of foveal area. The measurement is done automatically by the OCTA device. GCC is the total thickness of the ganglion cells and retinal nerve fibers (OCTA from RTVue XR, Avanti, Optovue, Fremont, CA, USA).

Pattern visual evoked potential (pVEP): pVEP is an objective test that measures the electrical activity of the optical pathway in response to a light stimulus. The 120 patterns reveal responses from all retinal quadrants. The measurements were taken according to the ISCEV standards for both eyes. We used the 120-pattern VEP protocol, which combines p100 implicit time and amplitude, to create a numerical result.

Definition of safety outcome

Orbital inflammation, diplopia, ocular allergic reactions, intraocular hemorrhages, retinal vessel occlusions, retinal detachment, and acute glaucoma were serious adverse ocular events. B-scan orbital ultrasonography was also used to detect and confirm complications at T1 and T2 time points. Systemic allergic reactions and anaphylaxis were considered to be systemic side effects.

Statistical methods

Descriptive statistics are presented with frequency, percentage, mean, and standard deviation values. The Kruskal Wallis test was used to analyze the differences in BCVA, FPDI, GCC thickness, pVEP P100 amplitude, and implicit time scores according to the T0 and T2 times. The Mann–Whitney U test was used for measurement differences between groups. The Sidak test was used to compare delta changes between groups. In the study, p-values < 0.05 were considered statistically significant ($\alpha = 0.05$). Analyses were done with the SPSS 25.0 package program.

Results

The mean age and type of toxicity: The mean age was 39.9 years (range, 22–58 years) in Group 1 (10 male, two female); 39.9 years (range, 22–58 years) in Group 2 (10 male, two female); and 38.3 years (range, 26–59 years) in Group 3 (12 male). There was no statistical difference between the groups in terms of age ($p = 0.63$). In Group 1, methanol was the main cause of intoxication in nine cases, amiodarone in one case, sildenafil in one case, and CO_2 in one case. Group 2 consisted of the fellow eyes of the patients in Group 1, which is why the reasons for intoxication were the same. Group 3 consisted of 12 eyes of six patients, and methanol was the main cause of intoxication in ten cases and sildenafil in two cases (Tables 1, 2, 3). Overall, methanol toxicity was the main reason seen in 77.7% of cases.

The mean best-corrected visual acuity (m-BCVA): Group 1 could identify a mean of 48.1 letters before with WJ-MSC + rEMS applications and mean 70.8 letters after the procedures at fourth month ($p = 0.01$). Group 2 had an m-BCVA of 50.3 letters at baseline and 60.9 letters after rEMS applications at the fourth month ($p = 0.03$). Group 3 had an m-BCVA score of 48.3 letters before WJ-MSC applications and 63.7 letters after the applications in the fourth month ($p = 0.02$). The BCVA delta change

Table 4 Statistical comparison of measurements according to groups

Measurements	Group			pG1	pG2	pG3
	Group1	Group2	Group3			
	$X \pm$ s.s	$X \pm$ s.s	$X \pm$ s.s			
BCVA before	48.08 ± 18.44	50.33 ± 18.58	48.25 ± 12.26	0.01*	0.03*	0.02*
BCVA after	70.83 ± 25.84	60.92 ± 21.93	63.67 ± 16.33			
Visual field FPDI before	21.33 ± 18.14	24.67 ± 21.12	31.08 ± 16.81	0.01*	0.02*	0.04*
Visual field FPDI after	41.67 ± 32.29	32.92 ± 27.31	39.33 ± 20.31			
GCC thickness	78.42 ± 17.99	77.17 ± 18.77	78.67 ± 11.16	0.01*	0.04*	0.02*
GCC thickness	61.83 ± 12.47	67.25 ± 17.41	67.25 ± 9.54			
VEP P100 lat. before	145.33 ± 7.56	143.75 ± 8.95	146.5 ± 6.4	0.01*	0.03*	0.02*
VEP P100 lat. after	118.92 ± 12.03	131.92 ± 15.67	131.75 ± 13.73			
VEP P100 ampl before	2.16 ± 0.94	2.32 ± 0.91	2.13 ± 0.68	0.01*	0.04*	0.01*
VEP P100 ampl after	4.42 ± 1.79	2.88 ± 1.24	3.88 ± 1.14			

**Mann Whitney *U* test, *p < 0.05: statistically significant

BCVA best corrected visual acuity, (ETDRS letters), *FPDI* fundus perimetry deviation index (%), *GCC thickness* Ganglion cell complex (µm), *VEP* Visual evoked potential, *P100 lat* latency (ms), *P100 ampl* amplitude (mV)

Table 5 Statistical comparison of delta changes (Δ) according to groups

Measurements	Group			*p* comparision
	Group1	Group2	Group3	
	Δ	Δ	Δ	
BCVA	47% [G1]	21% [G2]	32% [G3]	0.01* G1 > G3 > G2
Visual field FPDI	95% [G1]	33% [G2]	27% [G3]	0.01* G1 > G2 > G3
GCC thickness	− 21% [G1]	− 13% [G2]	− 15% [G3]	0.01* G1 > G3 > G2
VEP P100 lat	− 18% [G1]	− 8% [G2]	− 10% [G3]	0.01* G1 > G3 > G2
VEP P100 ampl	105% [G1]	24% [G2]	83% [G3]	0.01* G1 > G3 > G2

Δ rate of change was calculated as the last–first measurement / first measurement. **(Sidak comparision test, *p < 0.05: statistically significant)
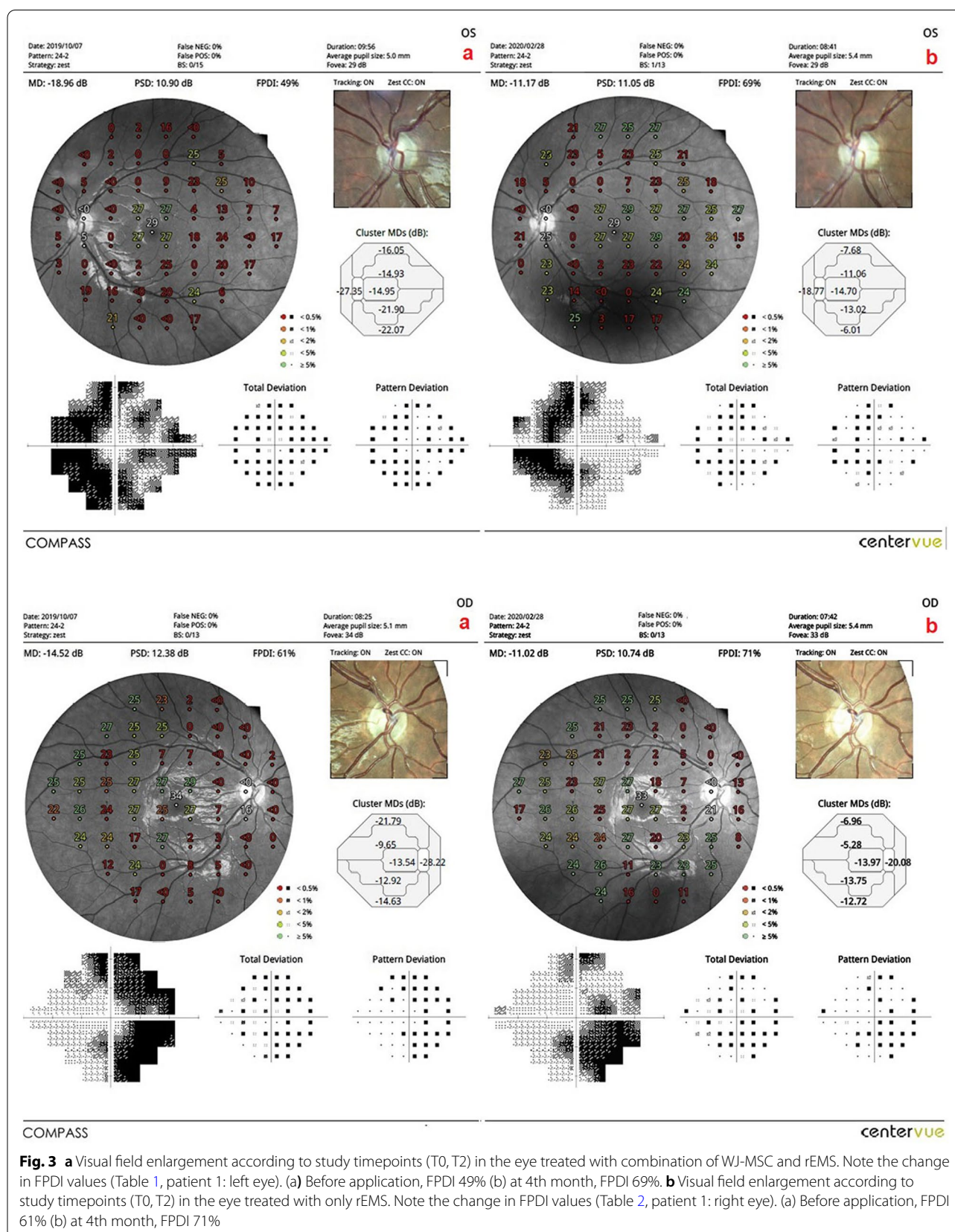
BCVA best corrected visual acuity (ETDRS letters), *FPDI* fundus perimetry deviation index (%), *GCC thickness* Ganglion cell complex (µm), *VEP* visual evoked potential, *P100 lat* latency (ms), *P100 ampl* amplitude (mV)
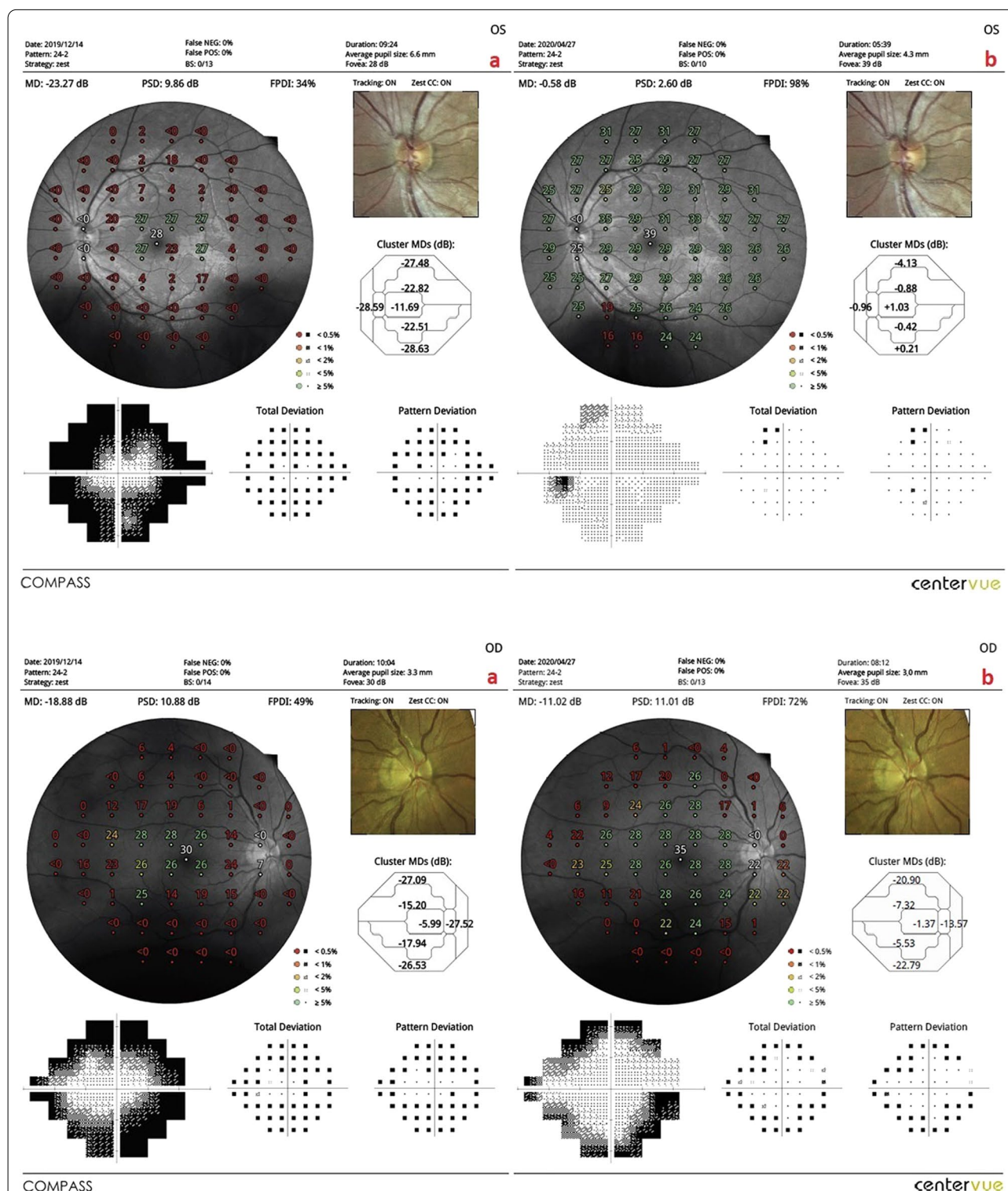
percentages of the groups can be ranked as: Group 1 (47%) > Group 3 (32%) > Group 2 (21%) (Tables 1, 2, 3 4, 5).
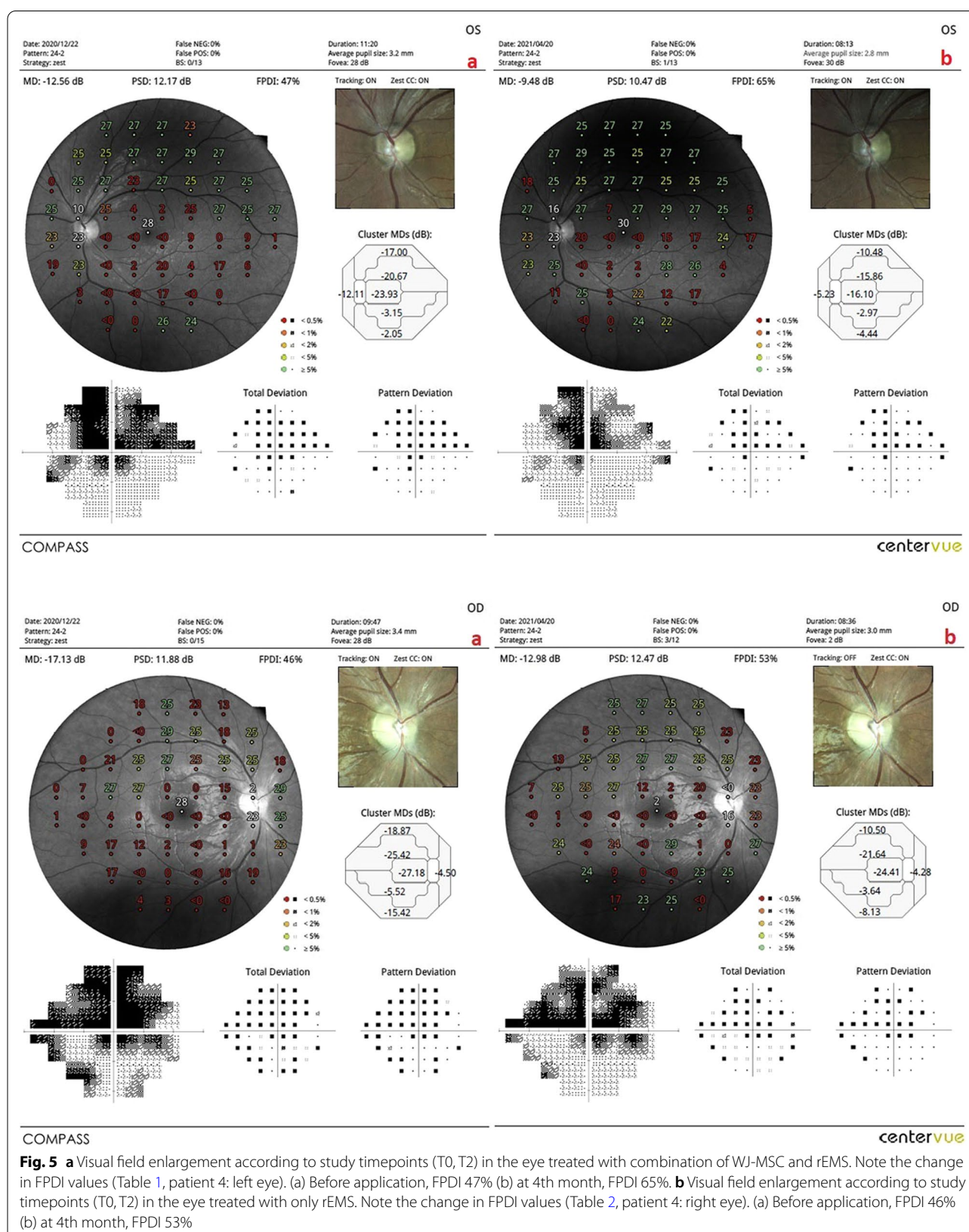
The mean of the fundus perimetry deviation index (m-FDPI): This value was 21.3% in Group 1 before the combined WJ-MSC and rEMS applications and 41.7% after the procedures at the fourth month ($p = 0.01$). In Group 2, the m-FDPI was 24.7% at the first measurement and 32.9% after only rEMS applications at the fourth month ($p = 0.02$). In Group 3, the m-FDPI was 31.1% before WJ-MSC applications and 39.3% at the last examination in the fourth month ($p = 0.04$). The m-FDPI delta change percentages of the groups can be ranked as: Group 1 (95%) > Group 2 (33%) > Group 3 (27%) (Tables 1, 2, 3, 4, 5; Figs. 3, 4, 5, 6).
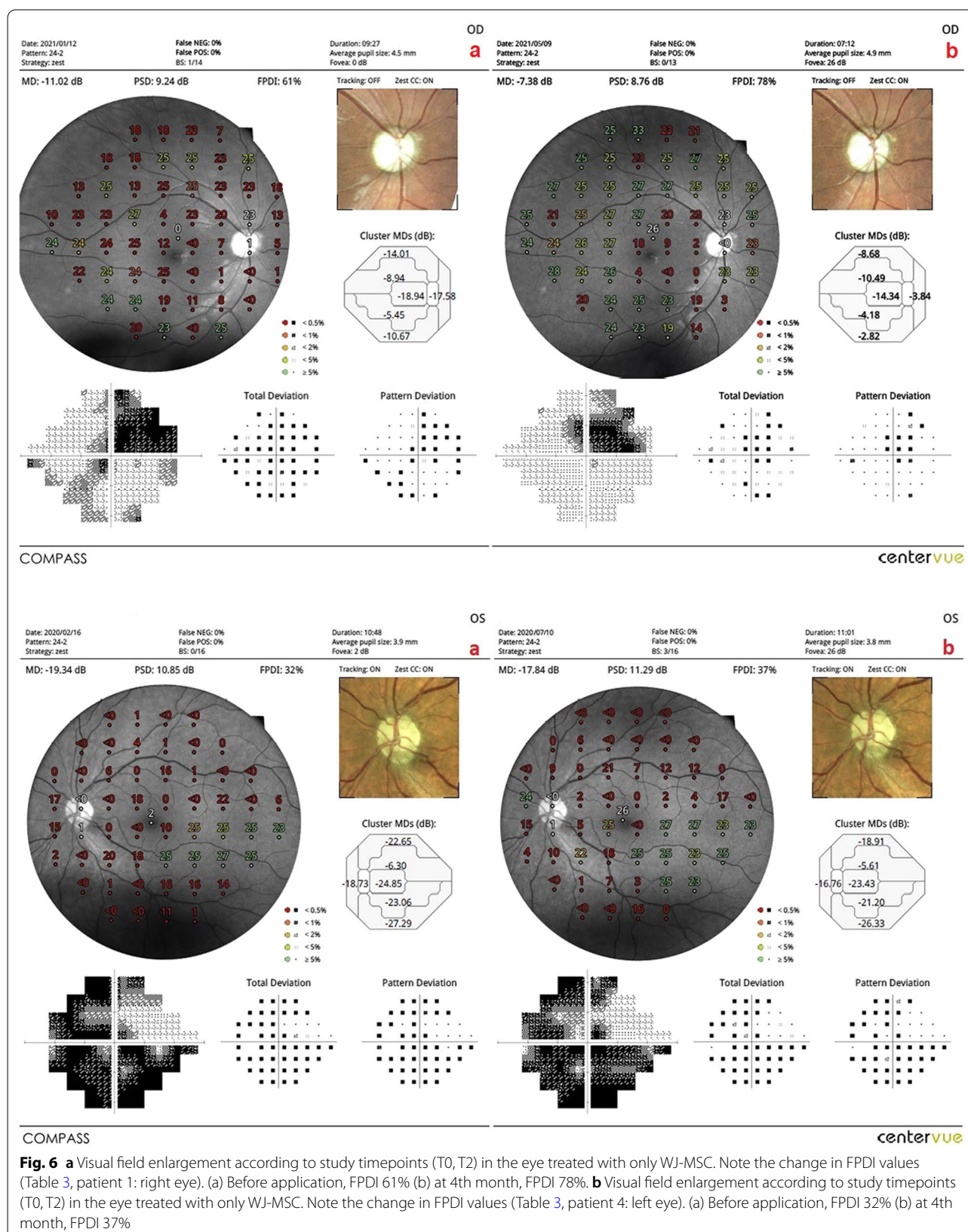
The mean ganglion cell complex (m-GCC) thickness in Group 1 was 78.4 µm before combined management and 61.8 µm after the procedures ($p = 0.01$). In Group 2, the m-GCC thickness was 77.2 µm at the first and 67.3 µm after the rEMS applications ($p = 0.04$). In Group 3, the m-GCC thickness was 78.7 µm before WJ-MSC applications and 67.3 µm after the applications ($p = 0.02$). The m-GCC thickness delta change (decrease in thickness) percentages can be ranked as: Group 1 (− 21%) > Group 3 (− 15%) > Group 2 (− 13%) (Tables 1, 2, 3, 4, 5; Figs. 7 and 8).
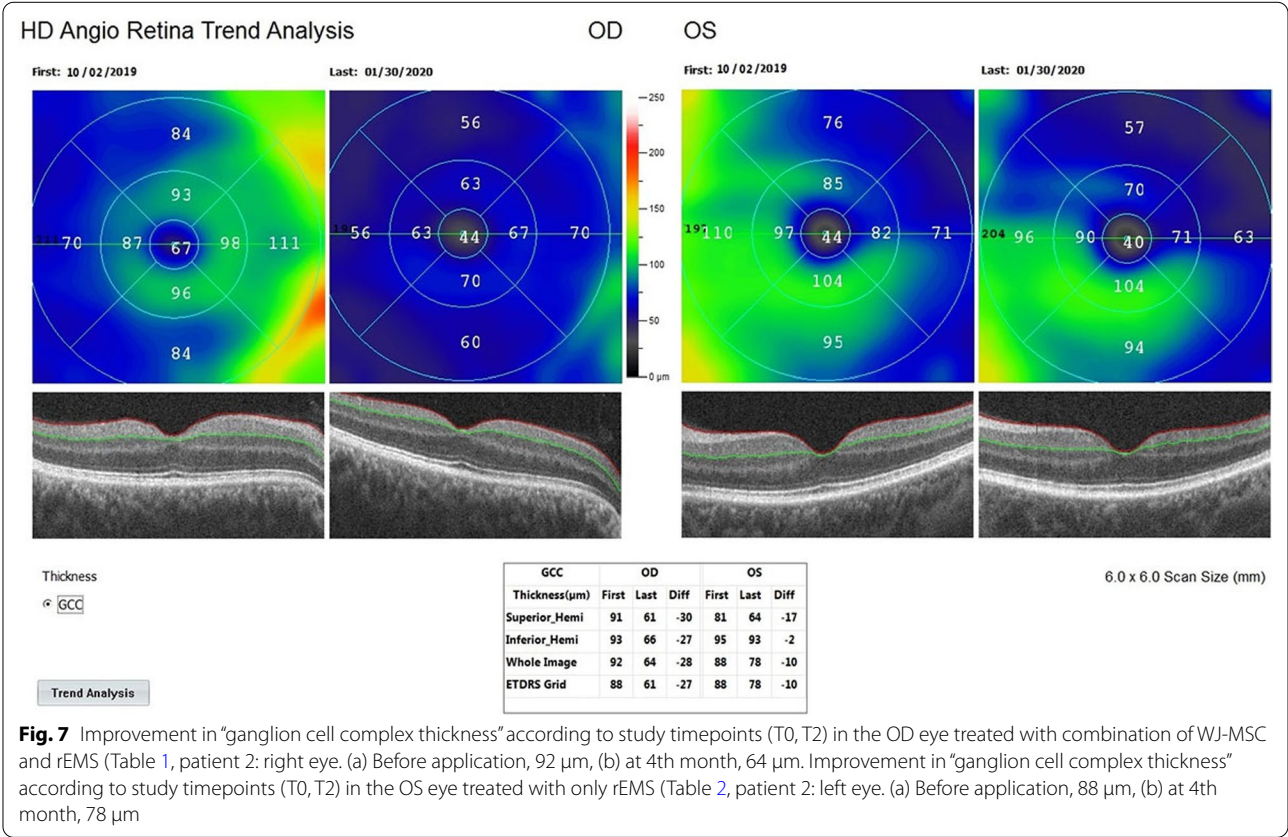
The mean pattern visual evoked potentials P100 (m-P100) amplitudes and latency: The mean P100 latency was 145.3 m in Group 1 before the combined application and 118.9 ms after the procedures ($p = 0.01$). In Group 2, the P100 latency was 143.8 ms at the first measurement and 131.9 ms after rEMS applications ($p = 0.03$). In Group 3, the mean P100 latency was 146.5 ms before WJ-MSC applications and 131.8 ms at the last examination ($p = 0.02$). The P100 latency delta change percentages of the groups can be ranked as: Group 1 (− 18%) > Group 3 (− 10%) > Group 2 (− 8%). The mean P100 amplitude was 2.2 mV in Group 1 before the combined application and 4.4 mV after the procedures ($p = 0.01$). In Group 2, the P100 amplitude was 2.3 mV at the first and 2.9 mV after rEMS applications (p$p = 0.04$). In Group 3, the mean P100 amplitude was 2.1 mV before WJ-MSC applications and 3.9 mV at the last examination ($p = 0.01$). The P100 amplitude delta change percentages of the groups can be ranked as: Group 1 (105%) > Group 3 (83%) > Group 2 (24%) (Tables 1, 2, 3, 4, 5; Figs. 9, 10, 11).

Fig. 3 **a** Visual field enlargement according to study timepoints (T0, T2) in the eye treated with combination of WJ-MSC and rEMS. Note the change in FPDI values (Table 1, patient 1: left eye). (a) Before application, FPDI 49% (b) at 4th month, FPDI 69%. **b** Visual field enlargement according to study timepoints (T0, T2) in the eye treated with only rEMS. Note the change in FPDI values (Table 2, patient 1: right eye). (a) Before application, FPDI 61% (b) at 4th month, FPDI 71%

Fig. 4 **a** Visual field enlargement according to study timepoints (T0, T2) in the eye treated with combination of WJ-MSC and rEMS. Note the change in FPDI values (Table 1, patient 3: left eye). (a) Before application, FPDI 34% (b) at 4th month, FPDI 98%. **b** Visual field enlargement according to study timepoints (T0, T2) in the eye treated with only rEMS. Note the change in FPDI values (Table 2, patient 3: right eye). (a) Before application, FPDI 49% (b) at 4th month, FPDI 72%

Fig. 5 **a** Visual field enlargement according to study timepoints (T0, T2) in the eye treated with combination of WJ-MSC and rEMS. Note the change in FPDI values (Table 1, patient 4: left eye). (a) Before application, FPDI 47% (b) at 4th month, FPDI 65%. **b** Visual field enlargement according to study timepoints (T0, T2) in the eye treated with only rEMS. Note the change in FPDI values (Table 2, patient 4: right eye). (a) Before application, FPDI 46% (b) at 4th month, FPDI 53%

Fig. 6 **a** Visual field enlargement according to study timepoints (T0, T2) in the eye treated with only WJ-MSC. Note the change in FPDI values (Table 3, patient 1: right eye). (a) Before application, FPDI 61% (b) at 4th month, FPDI 78%. **b** Visual field enlargement according to study timepoints (T0, T2) in the eye treated with only WJ-MSC. Note the change in FPDI values (Table 3, patient 4: left eye). (a) Before application, FPDI 32% (b) at 4th month, FPDI 37%

Fig. 7 Improvement in "ganglion cell complex thickness" according to study timepoints (T0, T2) in the OD eye treated with combination of WJ-MSC and rEMS (Table 1, patient 2: right eye). (a) Before application, 92 μm, (b) at 4th month, 64 μm. Improvement in "ganglion cell complex thickness" according to study timepoints (T0, T2) in the OS eye treated with only rEMS (Table 2, patient 2: left eye. (a) Before application, 88 μm, (b) at 4th month, 78 μm

When Groups 1, 2, and 3 were compared using the Sidak test according to the delta change percentages, the combined application of WJ-MSC and rEMS significantly increases all assessment parameters (Table 5).

No serious ocular or systemic adverse events were encountered in any group related to WJ-MSC and rEMS applications in the fourth month. The patients are still being followed for the assessment of long-term results.

Discussion

The axons of the ganglion cells, which form the retinal nerve fiber layer, are unmyelinated until the lamina cribrosa. Retinal nerve fibers are composed of the optic nerve head in the prelaminar region. Microtubules form the skeleton of the axons, and retinal nerve fibers are surrounded by oligodendrocytes and become myelinated in the post-laminar region. Organelles, mitochondria, protein synthesis, intracellular digestion, and all vital activities take place in ganglion cells. Bidirectional axoplasmic flow occurs for the vital and functional activities of axons. From the ganglion cells to the lateral geniculate nucleus, structural and functional proteins, neurotransmitters in vesicles, mitochondria, and ions flow towards the synaptic end. Neurotransmitters, organelles, and ions need to be regenerated, and cellular wastes need to be
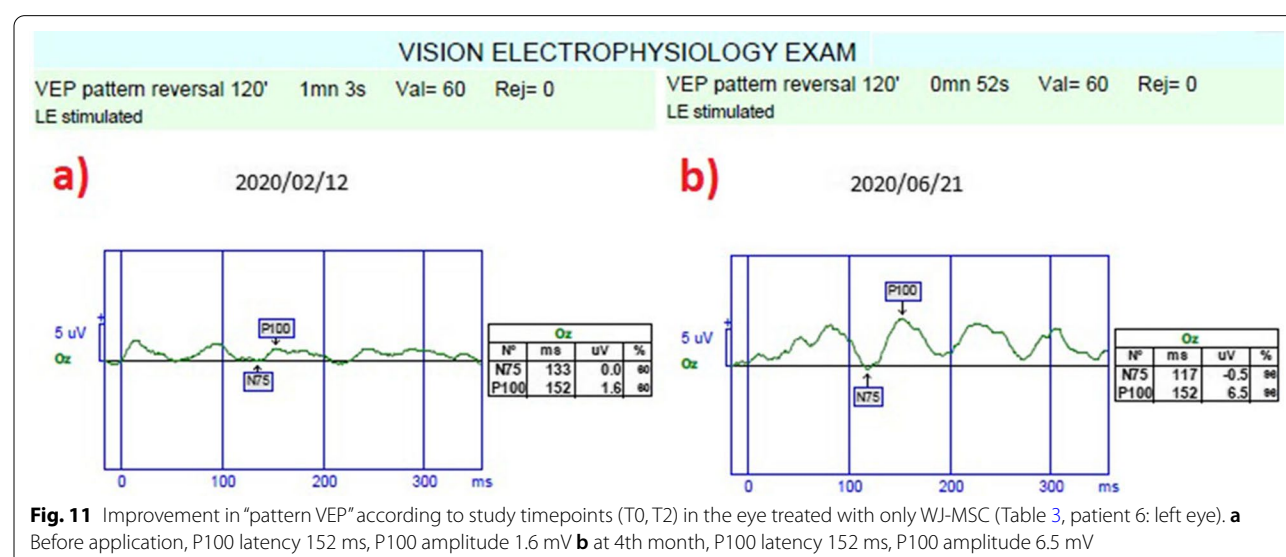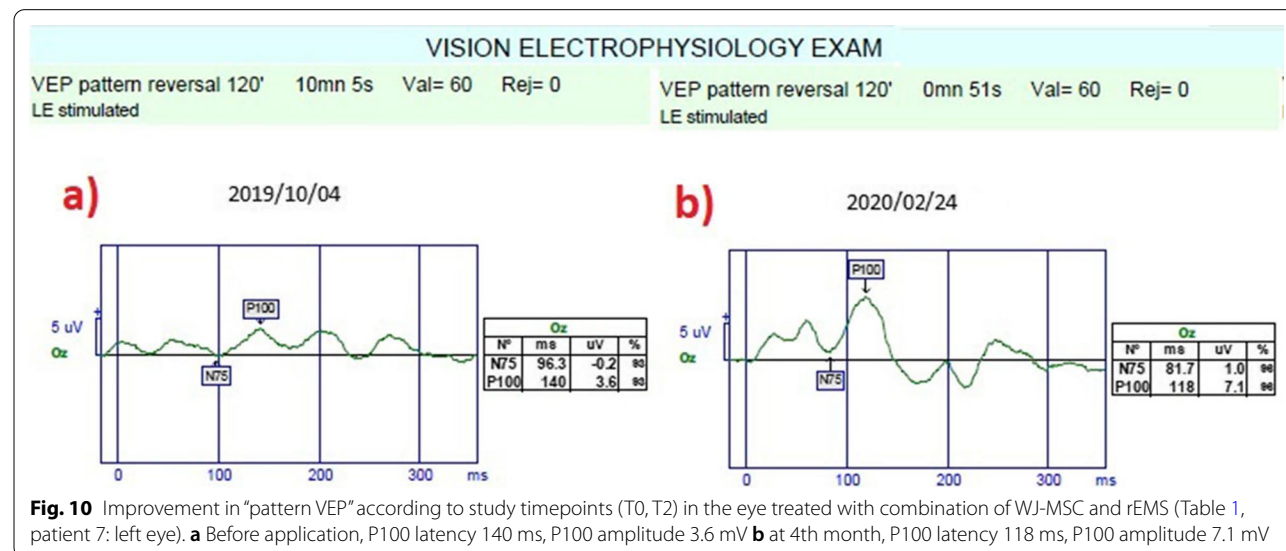
digested to flow from the synaptic end to the ganglion cells [15–18]. Oligodendrocytes secrete exosomes containing neurotrophic growth factors for healthy functioning of myelinization and axoplasmic flow [17]. The intracranial portion of the optic nerve is more sensitive to toxins than the retinal portion, as various toxins target the myelin sheath and axoplasmic proteins. In fact, this portion lacks the protective role of the blood-retinal barrier. Long-term stasis of the axoplasmic flow and imbalance of ion channels triggers the neuroinflammation and apoptosis mechanisms [15, 19].

Methanol is the most accessible industrial alcohol and disinfectant and the most common public health problem for optic nerve toxins in clinical practice, mostly due to fake alcohol production and drinks. When methanol is metabolized in the liver by the alcohol dehydrogenase enzyme, it is converted into formic acid and formaldehyde. Formic acid destroys oligodenrocytes and myelin sheath (demyelination) by causing metabolic acidosis. Formaldehyde disrupts adenosintriphosphate (ATP) synthesis by blocking the mitochondrial function and oxidative phosphorylation in the axons. Both metabolites block axoplasmic flows and destabilize the Na–K-ATPase and Ca/Calmodulin ion channels. Denatured proteins accumulate in axons and cause swelling in the ganglion

Fig. 8 Improvement in "ganglion cell complex thickness" according to study timepoints (T0, T2) in the OD eye treated with combination of WJ-MSC and rEMS (Table 1, patient 5: right eye). (a) Before application, 94 μm, (b) at 4th month, 60 μm. Improvement in "ganglion cell complex thickness" according to study timepoints (T0, T2) in the OS eye treated with only rEMS (Table 2, patient 5: left eye). (a) Before application, 89 μm, (b) at 4th month, 64 μm

Fig. 9 Improvement in "pattern VEP" according to study timepoints (T0, T2) in the eye treated with combination of WJ-MSC and rEMS (Table 1, patient 6: left eye). **a** Before application, P100 latency 139 ms, P100 amplitude 2.9 mV **b** at 4th month, P100 latency 106 ms, P100 amplitude 6.3 mV

cell complex (GCC). These swelling changes were also displayed in our study: by one of the features of OCTA. The accumulation of denatured proteins within axons leads to neuroinflammation. Neuroinflammation, disruption of ion channel balances, and blockage of ATP

synthesis in mitochondria cause calcium ions to initiate apoptosis mechanisms in axons [4, 5, 20]. Methanol was the most common toxic substance (77.7%) encountered in our cohort study. Sildenafil is a vasoactive agent used in the treatment of erectile dysfunction. Its frequent use

Fig. 10 Improvement in "pattern VEP" according to study timepoints (T0, T2) in the eye treated with combination of WJ-MSC and rEMS (Table 1, patient 7: left eye). **a** Before application, P100 latency 140 ms, P100 amplitude 3.6 mV **b** at 4th month, P100 latency 118 ms, P100 amplitude 7.1 mV

Fig. 11 Improvement in "pattern VEP" according to study timepoints (T0, T2) in the eye treated with only WJ-MSC (Table 3, patient 6: left eye). **a** Before application, P100 latency 152 ms, P100 amplitude 1.6 mV **b** at 4th month, P100 latency 152 ms, P100 amplitude 6.5 mV

might lead to decreased optic nerve head blood flow and hypoxia. It is stated that non-arteritic ischemic optic neuropathy (NAION) occurring in male patients of a certain age may be associated with phofodiesterase inhibitors taken before [4, 21]. Carbon dioxide poisoning similarly leads to neural hypoxia. Hypoxia causes blockage of mitochondrial ATP synthesis and axoplasmic flow. It triggers axoplasmic swelling, neuroinflammation, and apoptosis [4]. Amiodarone is a potassium ion channel blocker drug used in the treatment of cardiac arrhythmias. Long-term use may cause disruption of ion channel balance in the optic nerve and blockage of axoplasmic

flow. Changes in intra-axonal ion balances can lead to asymmetric neuroinflammation and apoptosis [4, 5].

Wharton's jelly-derived mesenchymal stem cells (WJ-MSC) have a high paracrine effect and secrete exosomes into the chorioretinal microenvironment. Exosomes contain neurotrophic growth factors, various cytokines, and micro-RNA fragments. Neurotrophic growth factors accelerate ATP synthesis in mitochondria. The interleukin family and some other cytokines found in exosomes accelerate the digestion of denatured proteins and defective mitochondria found in the axoplasm. Autophagy and mitophagy help restore axoplasmic flow. Similar to the

exosomes of oligodendrocytes, micro-RNA fragments contribute to remyelination. Some cytokines in exosomes prevent glial phagocytosis by immunomodulation and suppress neuroinflammation. All these factors cause inhibition of apoptosis mechanisms and increase the survival rate of axons and ganglion cells [6–10, 22, 23]. The subtenon space is a relatively avascular region and is a suitable culture medium for WJ-MSCs [22–24]. Retinal progenitor stem cells are administered subretinally or intravitreally due to their neuronal transformation properties. WJ-MSCs are used in clinical practice for secretory exosomes, not neuronal transformation [25–27]. Molecules smaller than 75 kD can pass through the scleral pores by passive diffusion. The passage of molecules larger than 75 kD through the sclera is possible with electrical/electromagnetic iontophoresis. Exosomes secreted by WJ-MSCs can pass from the sclera to the choroidal matrix passively or by electromagnetic iontophoresis. Growth factors in the exosome pass from the choroidal matrix to the subretinal space via tyrosine kinase receptors [28–37]. In our study, it was aimed that exosomes, not cells, reach the retina. For this reason, the subtenon region was preferred for WJ-MSCs.

Na/K-ATPase and Ca/Calmodulin ion channels in axons perform neurotransmission by providing neuronal polarization-depolarization and repolarization. Ion channels and intracellular and extracellular ion balances are disturbed in toxic optic neuropathies. Ion imbalances cause cells to switch to dormant phase or "off mode". At this stage, neurons and axons are alive but unable to perform neurotransmission [19]. Repetitive electromagnetic stimulation provides rearrangement of ion channels and ion balances. rEMS accelerates neurotransmission and synaptic transmission with alternating current in neural tissues. rEMS increases the passage of large therapeutic molecules into neural cells by electromagnetic iontophoresis. rEMS accelerates blood flow and metabolism in neural tissues, increasing the intracellular elimination of glutamate and other metabolites. The ability of the axons to perform the polarization-depolarization-repolarization cycle allows the axons in "off mode" to be reactivated, that is, to switch to "on mode" [11–14, 34–37]. For these reasons, we investigated the effects of WJ-MSC and rEMS on toxic optic neuropathies as they are compatible with pathophysiology and mechanism of action.

BCVA improved significantly in all three groups. We observed that the combination of WJ-MSC and rEMS synergistically provides a more significant BCVA increase. We also observed the same synergistic effect on FPDI. GCC thickness decreased more in stem cell-treated groups 1 and 3 than non-stem cell-treated Group 2 (only rEMS applied). GCC thickness indicates the combined thickness of ganglion cells and retinal nerve fiber layer. GCC thickness may increase due to blockade of axoplasmic flow. This thickness may decrease with an improvement of axoplasmic flow or apoptosis of ganglion cells. We observed no significant improvement in visual acuity and visual field when GCC thickness was less than 60 μm, indicating atrophy. We believe that a GCC < 60 μm may be a sign of severe apoptosis and poor prognosis, according to our clinical observation. The decrease in GCC thickness in the stem cell groups was associated with significant improvement in BCVA and FPDI. In these groups, the higher rate of GCC over 60 μm can be explained by the improvement of the axoplasmic flow and less apoptosis rate. If there is no improvement in visual functions with the decrease in GCC thickness, we can think that this decrease is related to apoptosis. Another opinion; It may be that neurons surviving after a severe apoptosis increase the transition to ON mode with regenerative-restorative applications [38]. When pVEP p100 amplitudes were compared for all groups, we observed a similar increase in WJ-MSC when applied in Group 1 and Group 3. We found that this increase was less in the rEMS group alone. We believe that this situation is related to the increase in the number of reactive axons. All anatomical and functional data show that the combination of WJ-MSC and rEMS is synergistically more effective than individual applications of WJ-MSC or rEMS. We believe that the increase in intracellular transport of growth factors greater than 75 kD by electromagnetic iontophoresis also causes the combined treatment to be more effective [30–37].

The quantity of methanol consumed, hemodialysis application in the first 2 days, the use of bicarbonate to neutralize acidosis, the early use of ethanol as a competitive inhibitor of the enzyme alcohol-dehydrogenase, and of steroids with anti-edema and anti-inflammatory action, the serum level of vitamin B12 and the individual characteristics of the alcohol dehydrogenase enzyme in the liver influence the rate of toxicity and the relative extent of permanent damage to the optic nerve. The first emergency intervention was performed for all patients in specialized intensive care clinics participating in this study. The success rate was 77.8% in patients who received WJ-MSC and rEMS combination therapy in methanol intoxication. We think that 22.2% of unresponsive cases can be accounted for by the individual variables mentioned above. It is reported that progressive vision loss develops in the first 3 months when no treatment other than emergency intervention is applied in methanol intoxication. It is known that apoptosis continues rapidly and permanent axon and ganglion cell loss develop in the first 3 months. In toxic optic neuropathies, axons and ganglion cells are in the dormant/off mode before apoptosis. Incompatible axonal

microenvironmental imbalance with vital conditions triggers apoptosis [4, 5, 20]. We believe that the increase in visual functions results from the neurotrophic growth factors, cytokines, and microRNA in WJ-MSC exosomes through a rearrangement of the microenvironmental balance. When the visual results were compared according to the groups, we observed that rEMS synergistically increased the efficacy of WJ-MSC. This can be explained by the fact that rEMS restores ion channels and ion balance, making axons suitable for impulse transmission [39–41].

Amiodarone is a cardiac antiarrhythmic that inhibits K channels. Long-term use of amiodarone can result in asymmetric toxic optic neuropathy. A patient who applied to our clinic complaining of a sudden decrease in vision in the left eye was consulted by the cardiology in terms of amiodarone intoxication. On examination, asymmetric TON was also detected in the right eye. We applied a combination of WJ-MSC and rEMS to the left eye and rEMS only to the right eye. We found a dramatic improvement in both eyes. Since methanol also disrupts axpolasmic flow, we detected central and centrocecal scotoma, while amiodarone only disrupts ion channels, we detected peripheral concentric scotoma. Significant improvement was also observed in the eye that was treated only with rEMS. This situation supports our hypothesis that rEMS acts by regulating the ion channel balance [24]. Sildenafil and carbon dioxide causes ischemic and hypoxic changes in the optic nerve. They can disrupt ATP synthesis, axoplasmic flow, and ion balance. At higher concentrations (>10%), carbon dioxide may cause convulsions, coma and death. Corbon dioxide poisoning can occur in submarines and scuba divers when scrubbers aren't functioning properly, as seen in our one case. Damages of toxins that cause hypoxia can also significantly improve with the early application of WJ-MSC and rEMS. We think that this effect is due to the fact that rEMS increases neural blood flow and the paracrine effect of WJ-MSC [39–41]. No systemic or local side effects due to WJ-MSC and/or rEMS applications were detected.

The study has some limitations. It has reported in the literature that the paracrine effects of WJ-MSC last for an average of 3 years. Longer follow-ups are needed to determine how long the effects will continue in our cases and whether additional applications will be needed. Determining how each exosome content specifically affects ganglion cells and axons is a separate topic of research. Another limitation is that the groups were small and mostly composed of methanol intoxication. Larger, multicenter studies will contribute to homogenizing the amount of poison, the duration of application, and individual characteristics. Large case series are also needed to examine the differences between treated and untreated eyes.

Conclusion

Toxic optic neuropathies are emergent pathologies that can result in acute and permanent blindness. After poisoning with toxic substances, progressive apoptosis continues in optic nerve axons and ganglion cells. After the proper first systemic intervention, the WJ-MSC and rEMS combination seems very effective in the short-term period in cases with TON. To prevent permanent blindness, a combination of WJ-MSC and rEMS application as soon as possible may increase the chance of success in currently untreatable cases.

Availability of data and materials
The datasets generated during and/or analysed during the study are available from the corresponding author on reasonable request.

Declarations

Ethics approval and consent to participate
Ethics committee approval for the umbilical cord Wharton's jelly derived mesenchymal stem cell (WJ-MSC) study was obtained from the Ankara University Faculty of Medicine Clinical Research Ethics Committee (19-1293-18) and was also approved by the Review Board of the Cell, Organ, and Tissue Transplantation Department within the Turkish Ministry of Health (56733164/203 E.1925). Ethics committee approval for the transcranial electromagnetic stimulation study was obtained from the Ankara University Faculty of Medicine Clinical Research Ethics Committee (17-1177-18) as well as and Review Board of the Drug and Medical Device Department within the Turkish Ministry of Health (2018-136). The study was performed in accordance with the tenets of the 2013 Declaration of Helsinki. Written informed consent was obtained from the patients prior to enrollment. Authorship—All named authors meet the International Committee of Medical Journal Editors (ICMJE) criteria for authorship for this article, take responsibility for the integrity of the work as a whole, and have given their approval for this version to be published. Medical Writing Assistance—Medical writing and editorial assistance was provided by Ali Hariri

Author details
[1]Department of Ophthalmology, Faculty of Medicine, Ankara University, Ankara, Turkey. [2]Ankara University Technopolis, Bioretina Eye Clinic, Neorama Ofis 55-56 Yaşam Cad. No 13/A, Beştepe /Yenimahalle, Ankara, Turkey.

References
1. De Moraes CG. Anatomy of the visual pathways. J Glaucoma. 2013;22(5):2–7.
2. Prasad S, Galetta SL. Anatomy and physiology of the afferent visual system. Handb Clin Neurol. 2011;102:3–19.
3. Kelts EA. The basic anatomy of the optic nerve and visual system. NeuroRehabilitation. 2010;27(3):217–22.
4. Grzybowski A, Zülsdorff M, Wilhelm H, Tonagel F. Toxic optic neuropathies: an updated review. Acta Ophthalmol. 2015;93(5):402–10.
5. Altiparmak UE. Toxic optic neuropathies. Curr Opin Ophthalmol. 2013;24(6):534–9.
6. Lin HY, Liou CW, Chen SD, Hsu TY, Chuang JH, et al. Mitochondrial transfer from Wharton's jelly-derived mesenchymal stem cells to mitochondria-defective cells recaptures impaired mitochondrial function. Mitochondrion. 2015;22:31–44.
7. Paliwal S, Chaudhuri R, Agrawal A, Mohanty S. Human tissue-specific MSCs demonstrate differential mitochondria transfer abilities that may determine their regenerative abilities. Stem Cell Res Ther. 2018;9(1):298.
8. Rivero JEM, Nicolás FMN, Bernal DG, et al. Human Wharton's jelly mesenchymal stem cells protect axotomized rat retinal ganglion cells via secretion of antiinflammatory and neurotrophic factors. Sci Rep. 2018;8:16299.
9. Ruiz FL, Romero CG, Bernal GD, et al. Mesenchymal stromal cell therapy for damaged retinal ganglion cells, is gold all that glitters? Neural Regen Res. 2019;14(11):1851–7.
10. Ji S, Lin S, Chen J, Huang X, Wei CC, Li Z, Tang S. Neuroprotection of transplanting human umbilical cord Mesenchymal stem cells in a microbead induced ocular hypertension rat model. Curr Eye Res. 2018;43(6):810–20.
11. Lefaucheur JP. Transcranial magnetic stimulation. Handb Clin Neurol. 2019;160:559–80.
12. Klomjai W, Katz R, Lackmy-Vallée A. Basic principles of transcranial magnetic stimulation (TMS) and repetitive TMS (rTMS). Ann Phys Rehabil Med. 2015;58(4):208–13.
13. Burke MJ, Fried PJ, Pascual-Leone A. Transcranial magnetic stimulation: Neurophysiological and clinical applications. Handb Clin Neurol. 2019;163:73–92.
14. Silvanto J. Transcranial magnetic stimulation and vision. Handb Clin Neurol. 2013;116:655–69.
15. Guo W, Stoklund Dittlau K, Van Den Bosch L. Axonal transport defects and neurodegeneration: molecular mechanisms and therapeutic implications. Semin Cell Dev Biol. 2020;99:133–50.
16. Korneva A, Schaub J, Jefferys J, Kimball E, Pease ME, et al. A method to quantify regional axonal transport blockade at the optic nerve head after short term intraocular pressure elevation in mice. Exp Eye Res. 2020;196:108035.
17. Frühbeis C, Kuo-Elsner WP, Müller C, Barth K, Peris L, et al. Oligodendrocytes support axonal transport and maintenance via exosome secretion. PLoS Biol. 2020;18(12):e3000621.
18. Krämer-Albers EM. Extracellular vesicles in the oligodendrocyte microenvironment. Neurosci Lett. 2020;725:134–915.
19. Giblin JP, Comes N, Strauss O, Gasull X. Ion channels in the eye: involvement in ocular pathologies. Adv Protein Chem Struct Biol. 2016;104:157–231.
20. Grzybowski A, Kanclerz P. Progressive chronic retinal axonal loss following acute methanol-induced optic neuropathy: four-year prospective cohort study. Am J Ophthalmol. 2018;195:246–7.
21. Pomeranz HD, Kruger J. Case of bilateral sequential nonarteritic ishemic optic neuropathy after rechallenge with sildenafil: comment. J Neuroophthalmol. 2018;38(1):124.
22. Özmert E, Arslan U. Management of retinitis pigmentosa by Wharton's jelly derived mesenchymal stem cells: preliminary clinical results. Stem Cell Res Ther. 2020;11(1):25.
23. Özmert E, Arslan U. Management of retinitis pigmentosa by Wharton's jelly-derived mesenchymal stem cells: prospective analysis of 1-year results. Stem Cell Res Ther. 2020;11(1):353.
24. Younis HS, Shawer M, Palacio K, Gukasyan HJ, Stevens GJ, Evering W. An assessment of the ocular safety of inactive excipients following sub-Tenon injection in rabbits. J Ocul Pharmacol Ther. 2008;24(2):206–16.
25. Wysocka AM, Kot M, Sułkowski M, Badyra B, Majka M. Molecular and functional verification of Wharton's jelly mesenchymal stem cells (WJ-MSCs) Pluripotency. Int J Mol Sci. 2019;20:1807.
26. Bai L, Shao H, Wang H, Zhang Z, Su C, Dong L, Yu B, Chen X, Li X, Zhang X. Effects of mesenchymal stem cell-derived exosomes on experimental autoimmune uveitis. Sci Rep. 2017;7(1):4323.
27. Rani S, Ryan AE, Griffin MD, Ritter T. Mesenchymal stem cell-derived extracellular vesicles: toward cell-free therapeutic applications. Mol Ther. 2015;23(5):812–23.
28. Mysona BA, Zhao J, Bollinger KE. Role of BDNF/ TrkB pathway in the visual system: therapeutic implications for glaucoma. Expert Rev Ophthalmol. 2017;12(1):69–81.
29. Giannos SA, Kraft ER, Zhao ZY, Merkley KH, Cai J. Photokinetic drug delivery:near infrared (NIR) induced permeation enhancement of bevacizumab, ranibizumab and aflibercept through human sclera. Pharm Res. 2018;35(6):1.
30. Demetriades AM, Deering T, Liu H, et al. Transscleral delivery of antiangiogenic proteins. J Ocul Pharmacol Ther. 2008;24(1):70–9.
31. Meng T, Kulkarni V, Simmers R, Brar V, Xu Q. Therapeutic implications of nanomedicine for ocular drug delivery. Drug Discov Today. 2019. https://doi.org/10.1016/j.drudis.2019.05.00.
32. Li SK, Hao J. Transscleral passive and iontophoretic transport: theory and analysis. Expert Opin Drug Deliv. 2017;15(3):283–99.
33. Joseph RR, Tan DWN, Ramon MRM, et al. Characterization of liposomal carriers for the trans-scleral transport of ranibizumab. Sci Rep. 2017;7(1):1.
34. Pall ML. Electromagnetic fields act via activation of voltage-gated calcium channels to produce beneficial or adverse effects. J Cell Mol Med. 2013;17(8):958–65.
35. Arslan U, Özmert E. Treatment of resistant chronic central serous chorioretinopathy via platelet-rich plasma with electromagnetic stimulation. Regen Med. 2020;15(8):2001–14.
36. Özmert E, Arslan U. Management of deep retinal capillary ischemia by electromagnetic stimulation and platelet-rich plasma: preliminary clinical results. Adv Ther. 2019;36(9):2273–86.
37. Arslan U, Özmert E. Management of retinitis pigmentosa via platelet-rich plasma or combination with electromagnetic stimulation: retrospective analysis of 1-year results. Adv Ther. 2020;37(5):2390–412.
38. Danylkova NO, Pomeranz HD, Alcala SR, McLoon LK. Histological and morphometric evaluation of transient retinal and optic nerve ischemia in rat. Brain Res. 2006;1096(1):20–9.
39. Patruno A, Ferrone A, Costantini E, et al. Extremely low-frequency electromagnetic fields accelerates wound healing modulating MMP-9 and inflammatory cytokines. Cell Prolif. 2018;51(2):e12432.
40. Maziarz A, Kocan B, Bester M, et al. How electromagnetic fields can influence adult stem cells: positive and negative impacts. Stem Cell Res Ther. 2016;7:54.
41. Parate D, Kadir ND, Celik C, et al. Pulsed electromagnetic fields potentiate the paracrine function of mesenchymal stem cells. Stem Cell Res Ther. 2020;11:46.

Publisher's Note
Springer Nature remains neutral with regard to jurisdictional claims in published maps and institutional affiliations.

MagnoVision™

www.**bioretina**.com.tr

BİORETİNA BİYOTEKNOLOJİ VE
BİYOMEDİKAL SAĞLIK YATIRIMLARI A.Ş.
Bahçelievler Mh. 319 Cd. E Blok No:35E/B49 Gölbaşı/ANKARA

Tel: +90 (312) 235 85 10 Gsm: +90 (530) 321 75 90

info@bioretina.com.tr